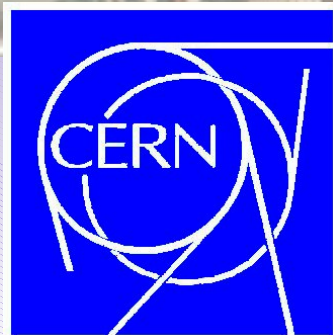
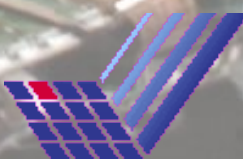


ATLAS Pixel Detector Commissioning using Cosmic Rays



Daniel Dobos
CERN – Universität Dortmund
on behalf of the ATLAS Pixel Collaboration
24.09.07

Vertex 2007 - Lake Placid, NY, USA - 23.-28. September 2007



Outline:

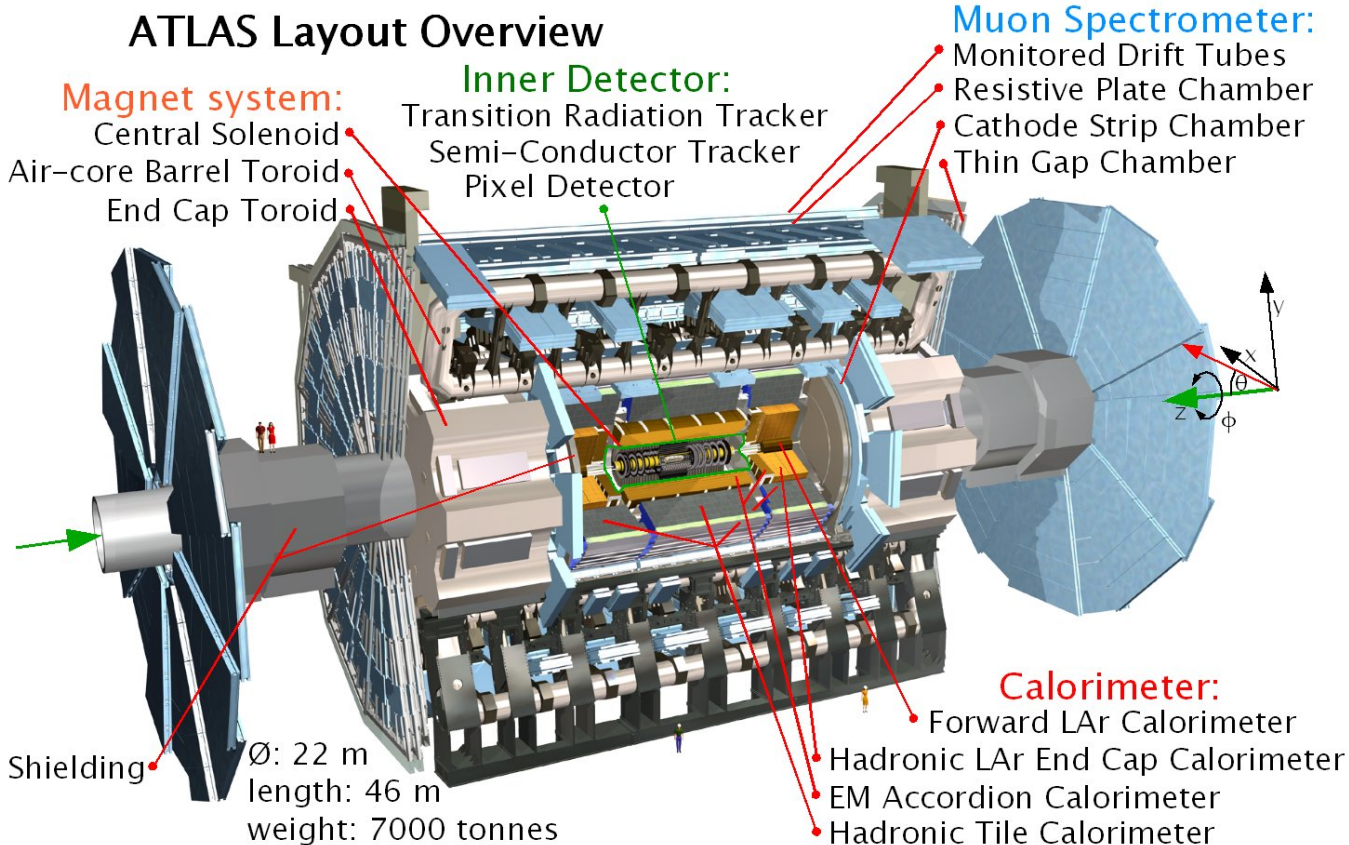
- ATLAS Pixel Detector Overview
- System Test Setup
- Optical Communication Tuning
- Detector Performance
- Cosmics Data
- Conclusions

ATLAS Pixel Detector



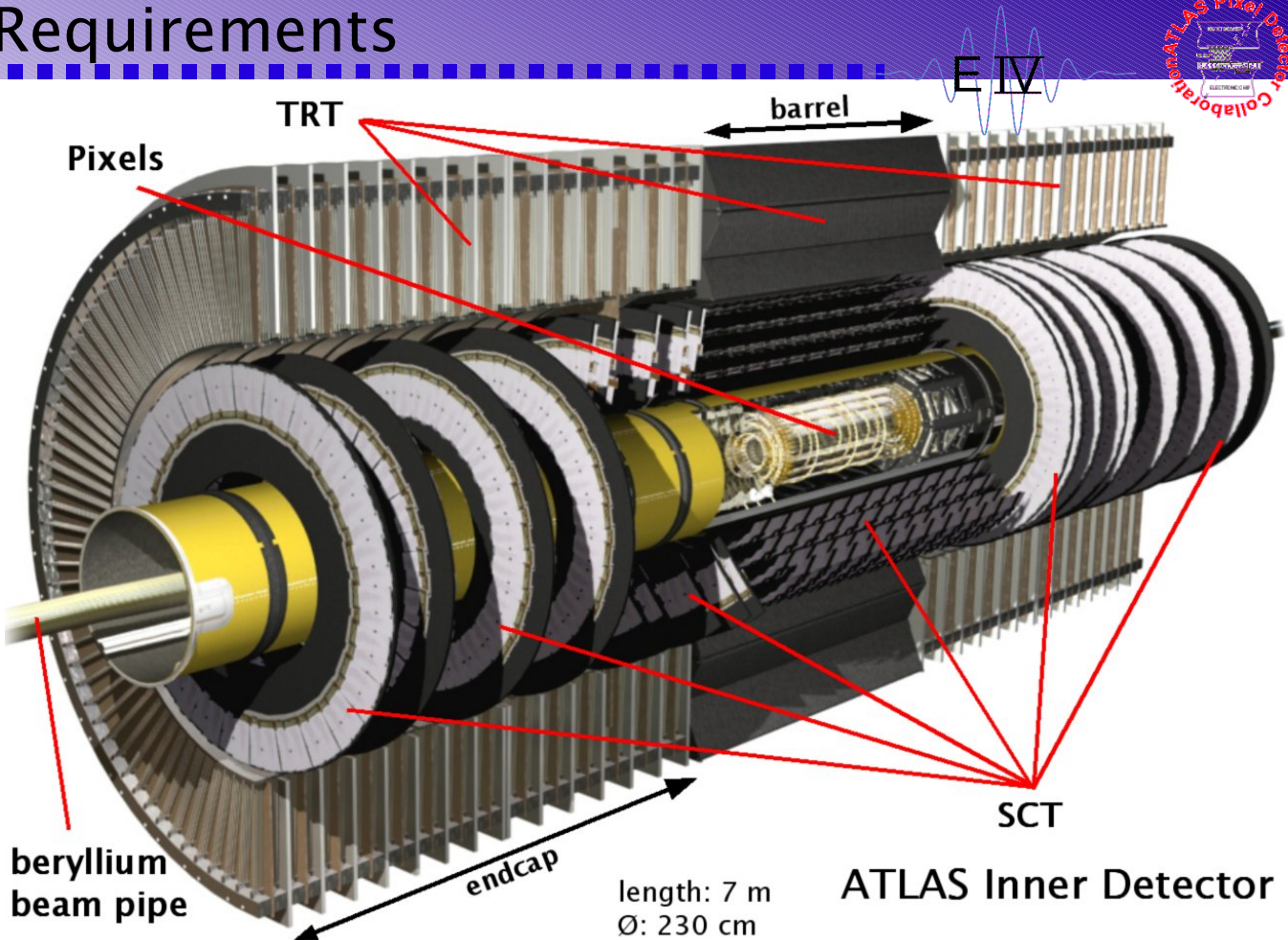
E IV

- high multiplicity tracking detector; ~ 1200 tracks per bunch crossing
 \Rightarrow high granularity (80 million channels)
- high impact parameter resolution; $\sim 12 \mu\text{m}$ vertex resolution
 \Rightarrow high granularity, low mass
- high radiation dose tolerance; $\sim 10^{15} n_{\text{eq}}/\text{cm}^2$ (NIEL) or 50 Mrad
 \Rightarrow low temp. & radiation-hard design tubes, ...)
- high time resolution; 40 MHz bunch crossing rate
 \Rightarrow fast preamplifier rise time
- high occupancy/long trigger decision; 2 μs Level1 trigger latency
 \Rightarrow buffering of hits on-detector
- low interaction length; $\sim 10\% X_0$ ($\sim 0.7\%$ per Module)
 \Rightarrow low mass (thinned readout electronics, carbon–carbon support structure, aluminum cables and cooling tubes, ...)



Pixel Detector Design Requirements

- high multiplicity tracking detector; ~ 1200 tracks per bunch crossing
 \Rightarrow high granularity (80 million channels)
- high impact parameter resolution; $\sim 12 \mu\text{m}$ vertex resolution
 \Rightarrow high granularity, low mass
- high radiation dose tolerance; $\sim 10^{15} n_{\text{eq}}/\text{cm}^2$ (NIEL) or 50 Mrad
 \Rightarrow low temp. & radiation-hard design , ...)
- high time resolution; 40 MHz bunch crossing rate
 \Rightarrow fast preamplifier rise time
- high occupancy/long trigger decision; 2 μs Level1 trigger latency
 \Rightarrow buffering of hits on-detector
- low interaction length; $\sim 10\% X_0$ ($\sim 0.7\%$ per Module)
 \Rightarrow low mass (thinned readout electronics, carbon–carbon support structure, aluminum cables and cooling tubes, ...)

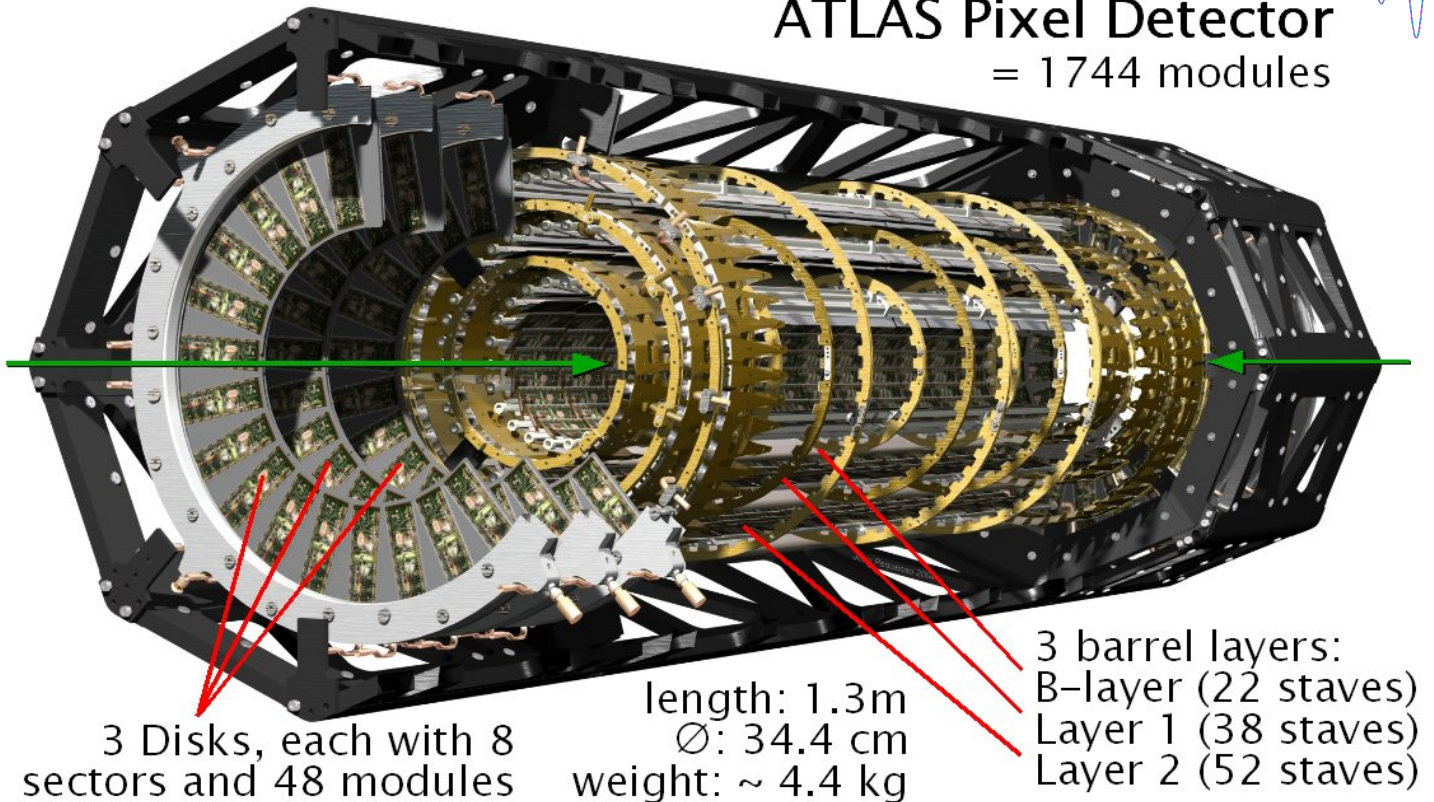


Pixel Detector Design



ATLAS Pixel Detector
= 1744 modules

E IV



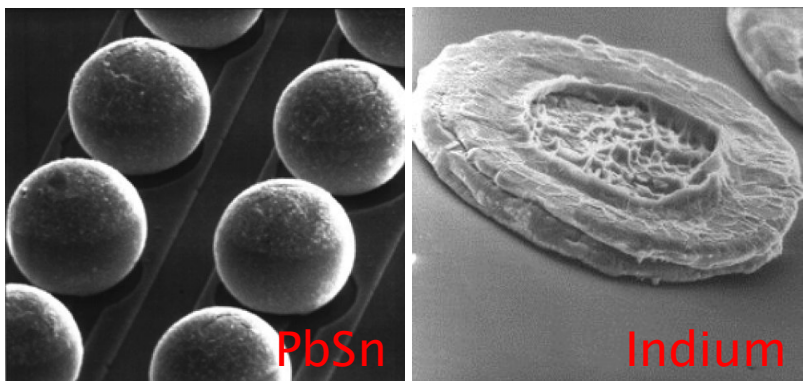
- 3 Barrel layers ($r = 5, 9, 12$ cm)
- 2 Endcaps with 3 Disks each
- 3 space points for pseudorapidity < 2.5
- 80 million channels in 1744 Pixel Modules
- 1.8 m^2 active sensor area
- $\sim -10^\circ\text{C}$ operating temperature with ~ 10 kW power load \Rightarrow evaporative C_3F_8 cooling integrated into carbon support structure

1st large scale active pixel detector (soon) in operation

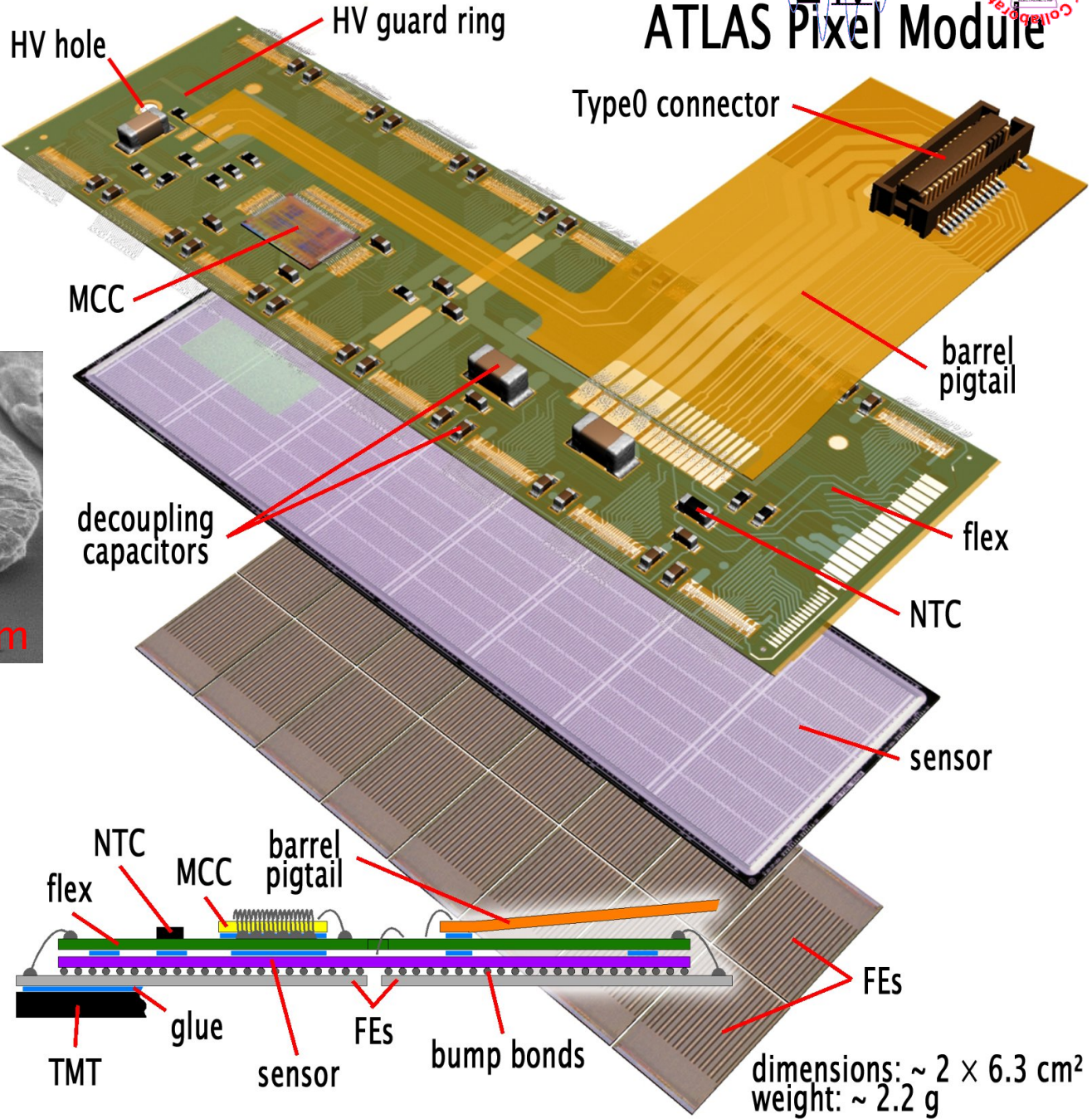
ATLAS Pixel Module



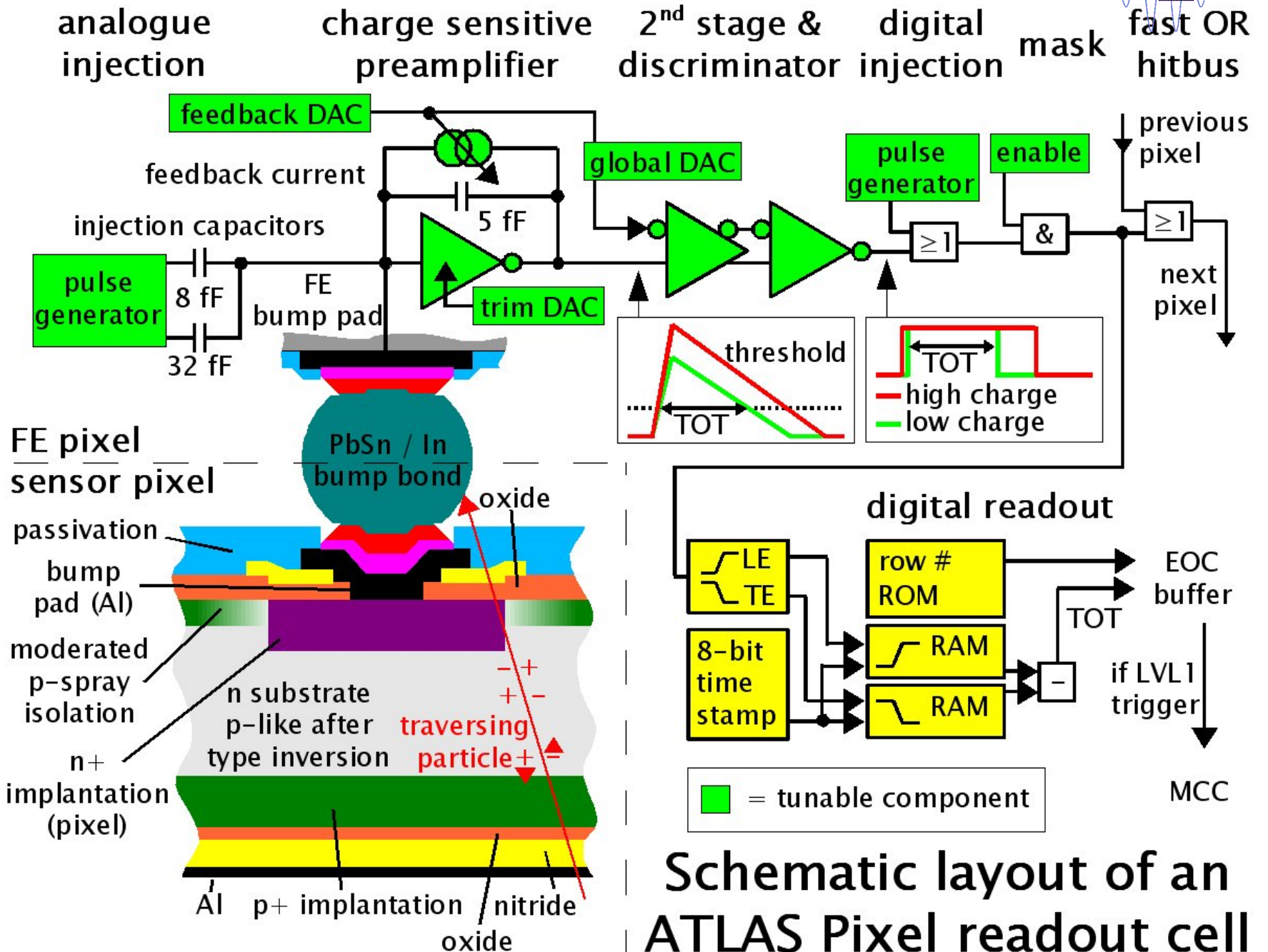
- ~ 47k pixels ($50 \times 400 \mu\text{m}$) on n^+np^+ silicon sensor
- 16 Front-End (FE) chips connected with bump bonds (flip chipping) with the Pixel sensor



- FEs connected with wire bonds to a flexible circuit board (flex: routing and passive components)
- readout of the FEs by a Module Control Chip (MCC)
⇒ module based event building



FE pixel schematic

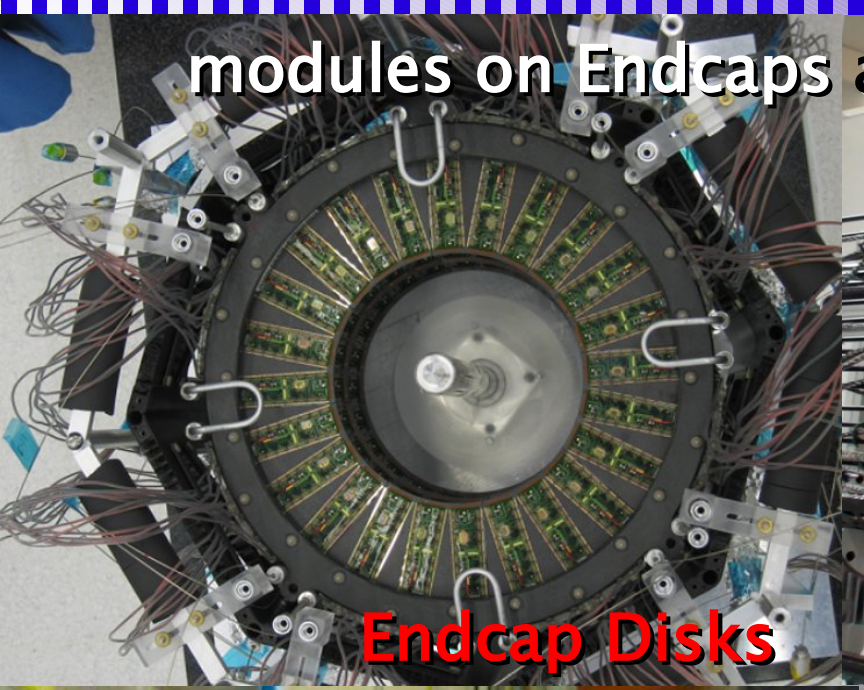


Schematic layout of an
ATLAS Pixel readout cell

Pixel Detector Integration

modules on Endcaps and Barrel are identical

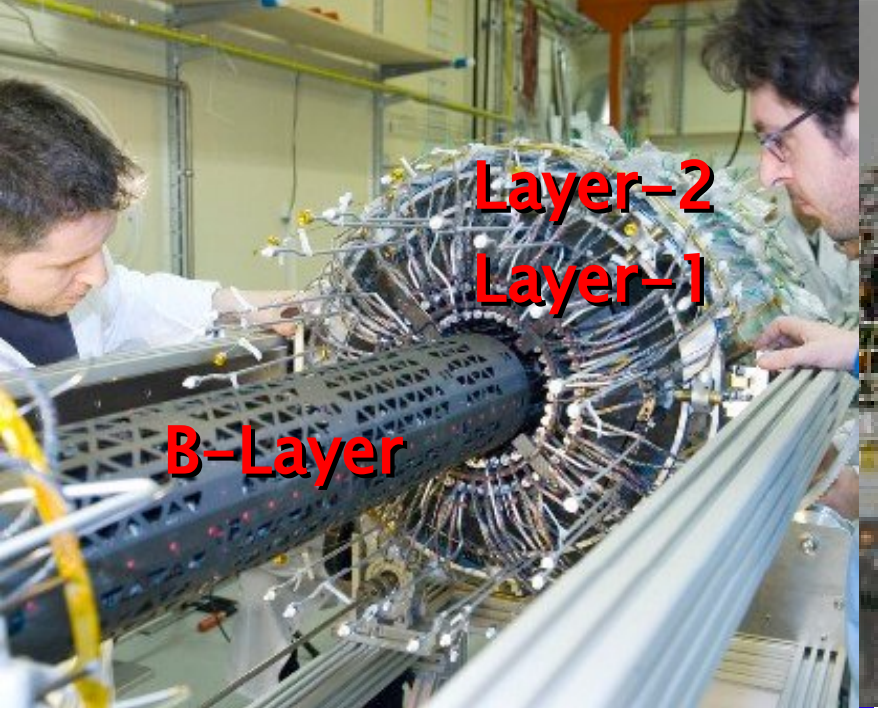
E IV



Endcap Disks

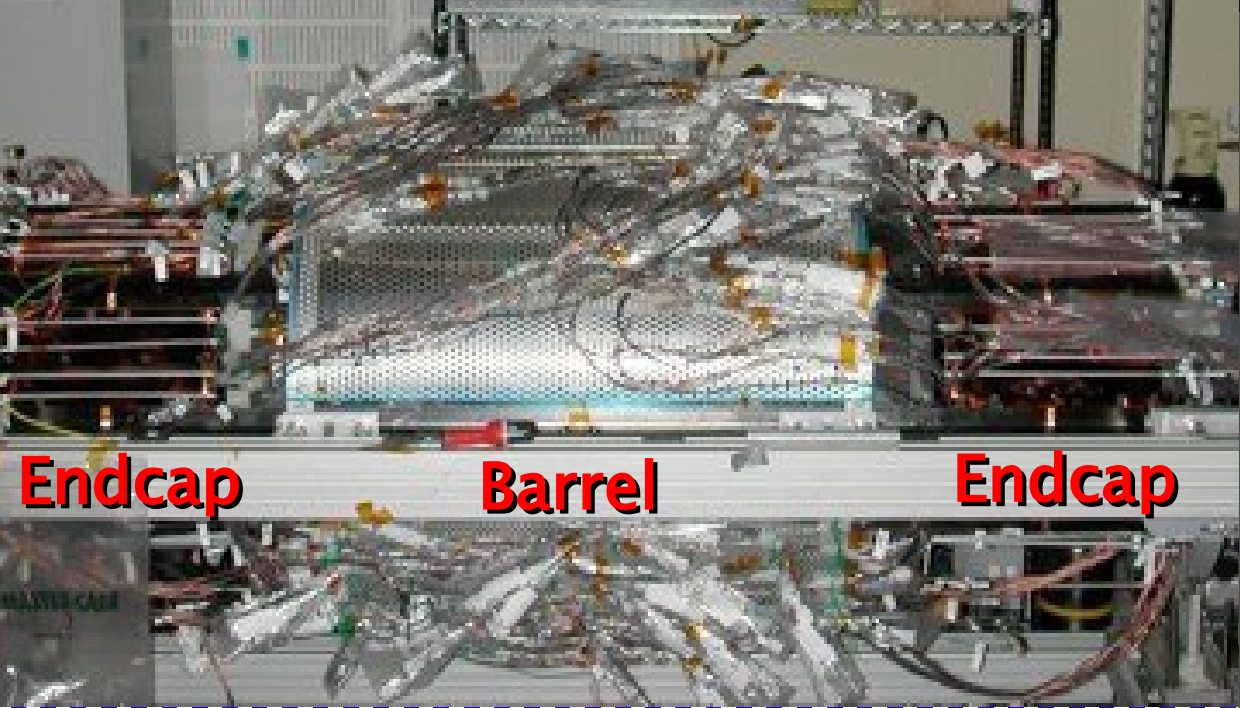


Barrel Layer Halfshell



B-Layer

Layer-2
Layer-1

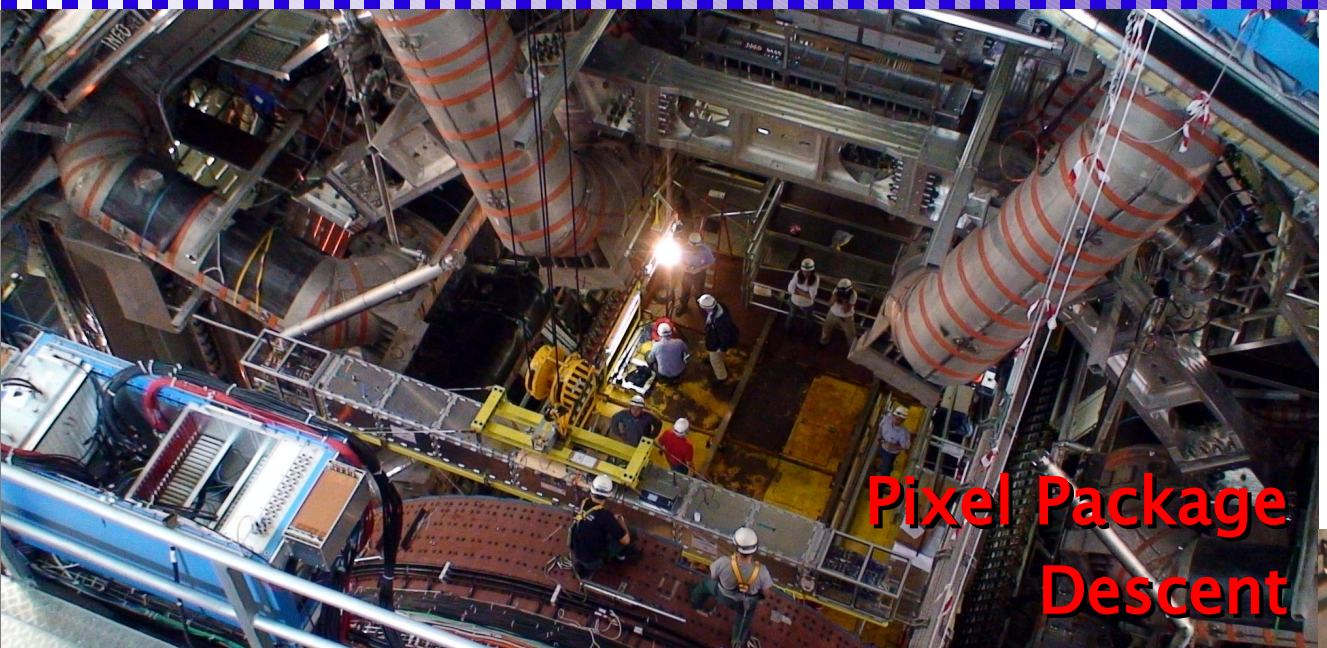


Endcap

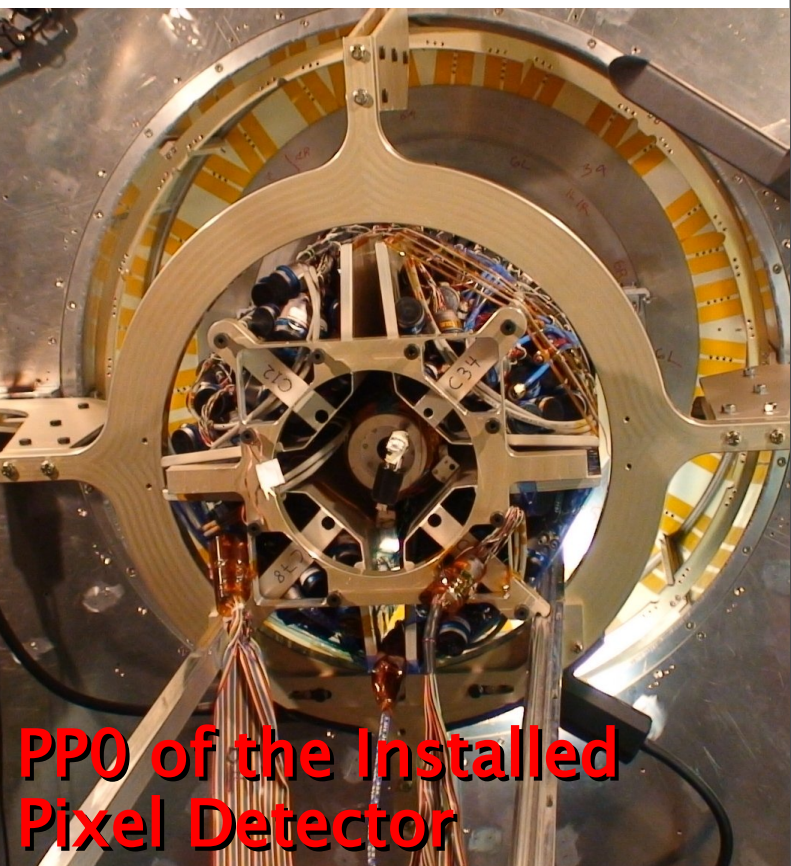
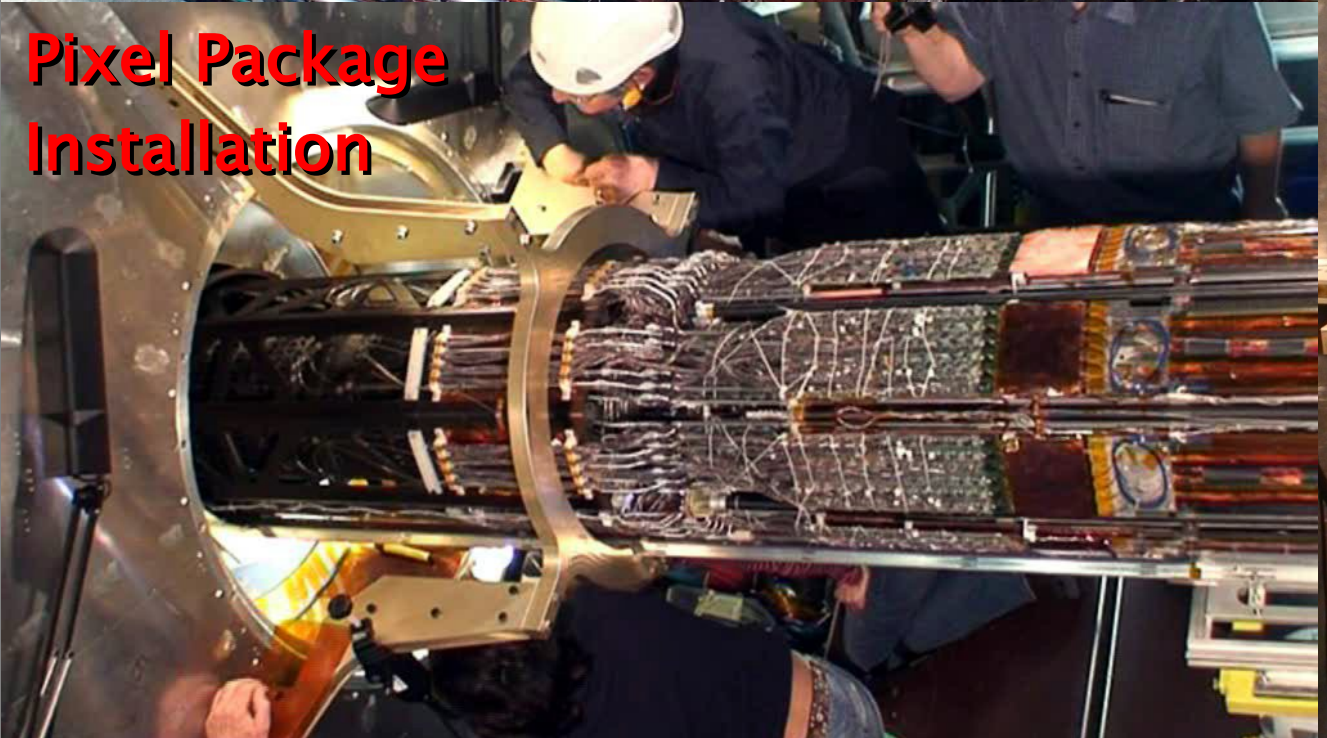
Barrel

Endcap

Pixel Detector Installation

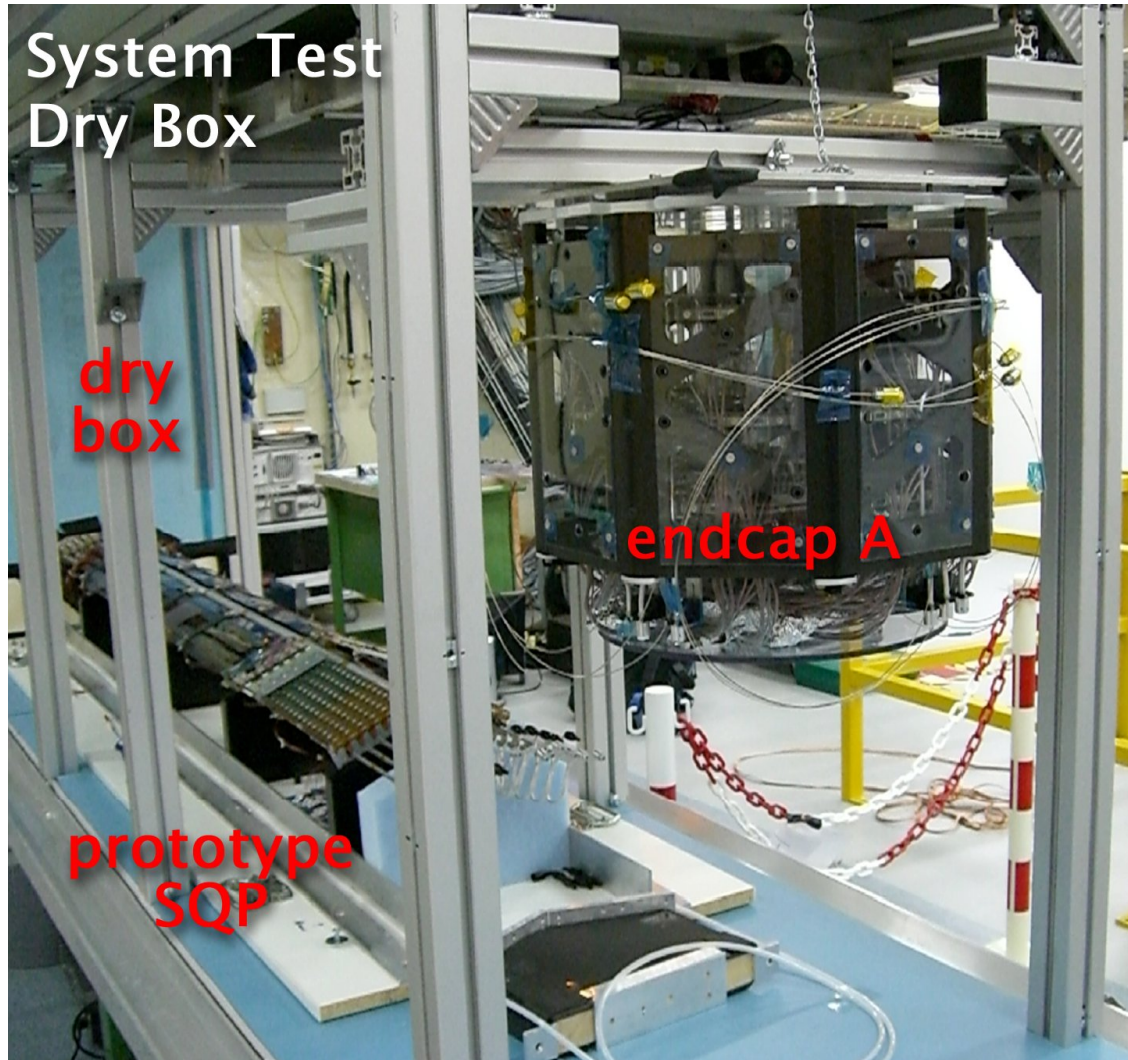


- Pixel Detector Package (detector with service quarter panels) lowered and installed in late June
- next step: cabling of service cables and fibers at PPO



- verify the performance and interaction of production detector and service components (threshold, noise, cooling, ...)
- test complete infrastructure (HW, SW, procedures) on ~10% of the entire detector (Endcap A, 144 modules, 24 optoboards) ⇒ biggest operated Pixel system so far
- realistic long term operation (shifts, 24/7, experts on-call, ...) to learn for real operation
- 'playground' for procedure and software developments (optical communication tuning, module tuning, tuning analyzes, slow control, DAQ, online monitoring, ...)
- test trigger and DAQ chain with cosmics: (noise occupancy, readout performance, tracking, alignment, ...)

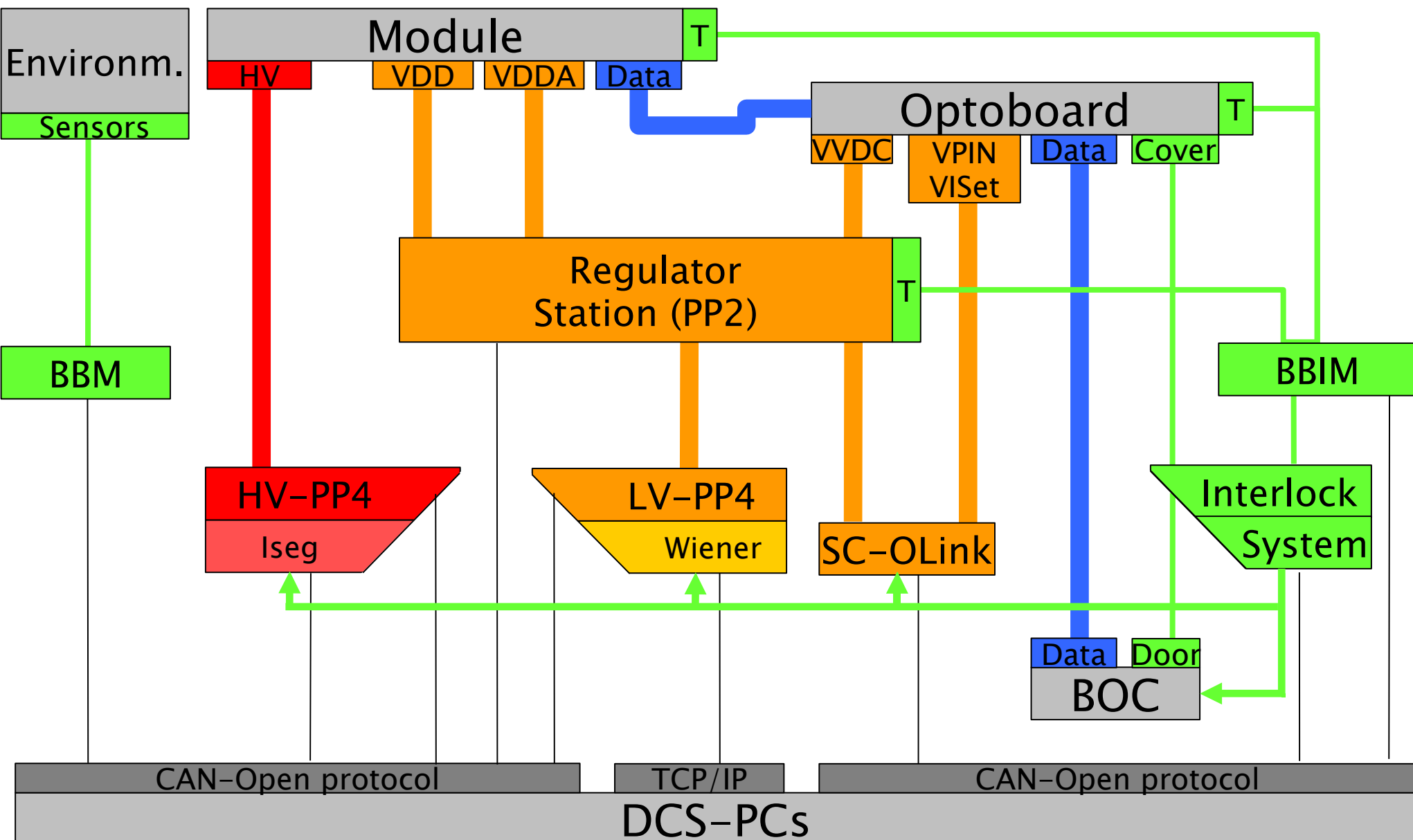
ATLAS Pixel System- and Cosmics-Test at CERN



System Test Setup



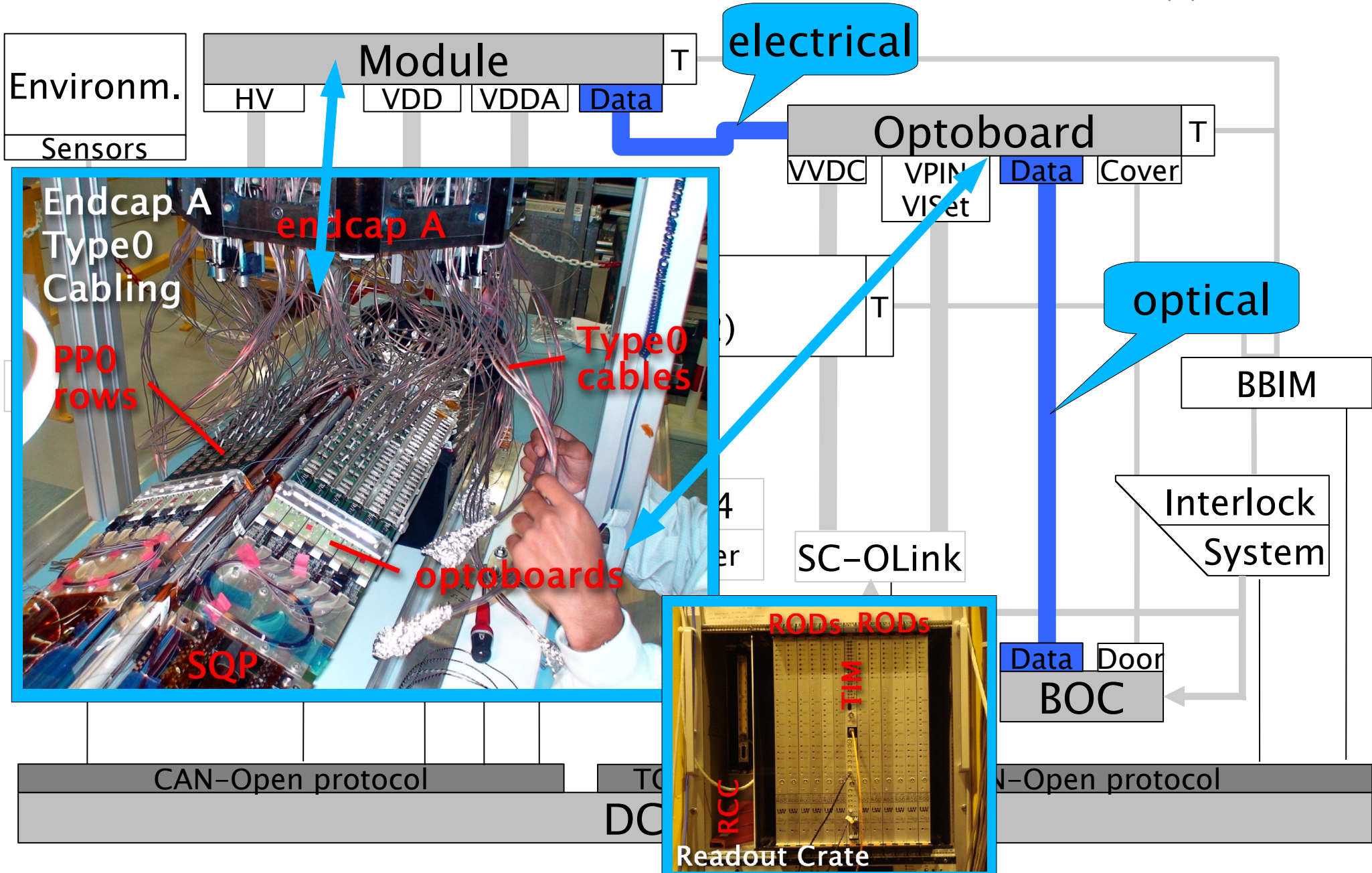
E IV



System Test Setup (Data)



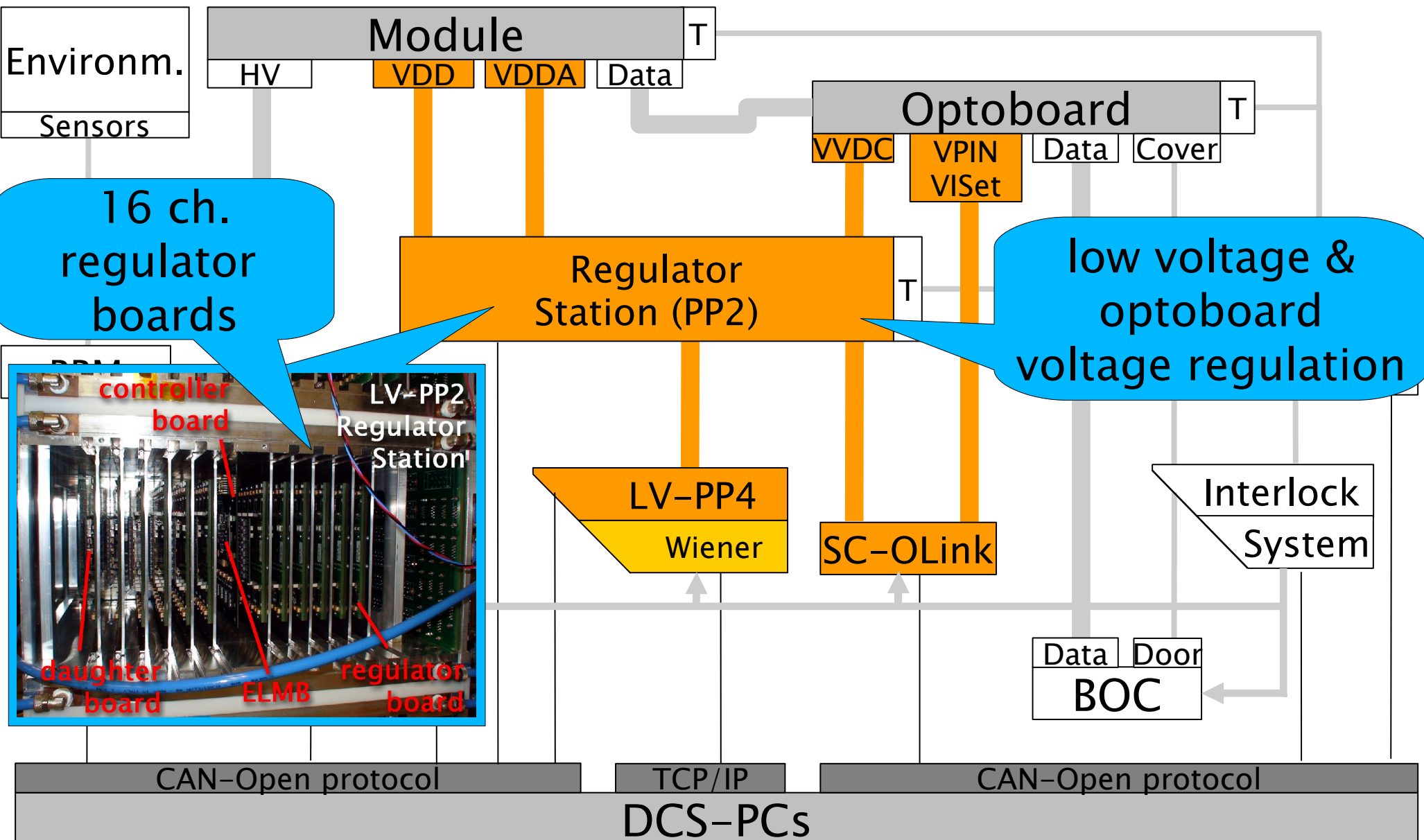
E IV



System Test Setup (Low Voltage)



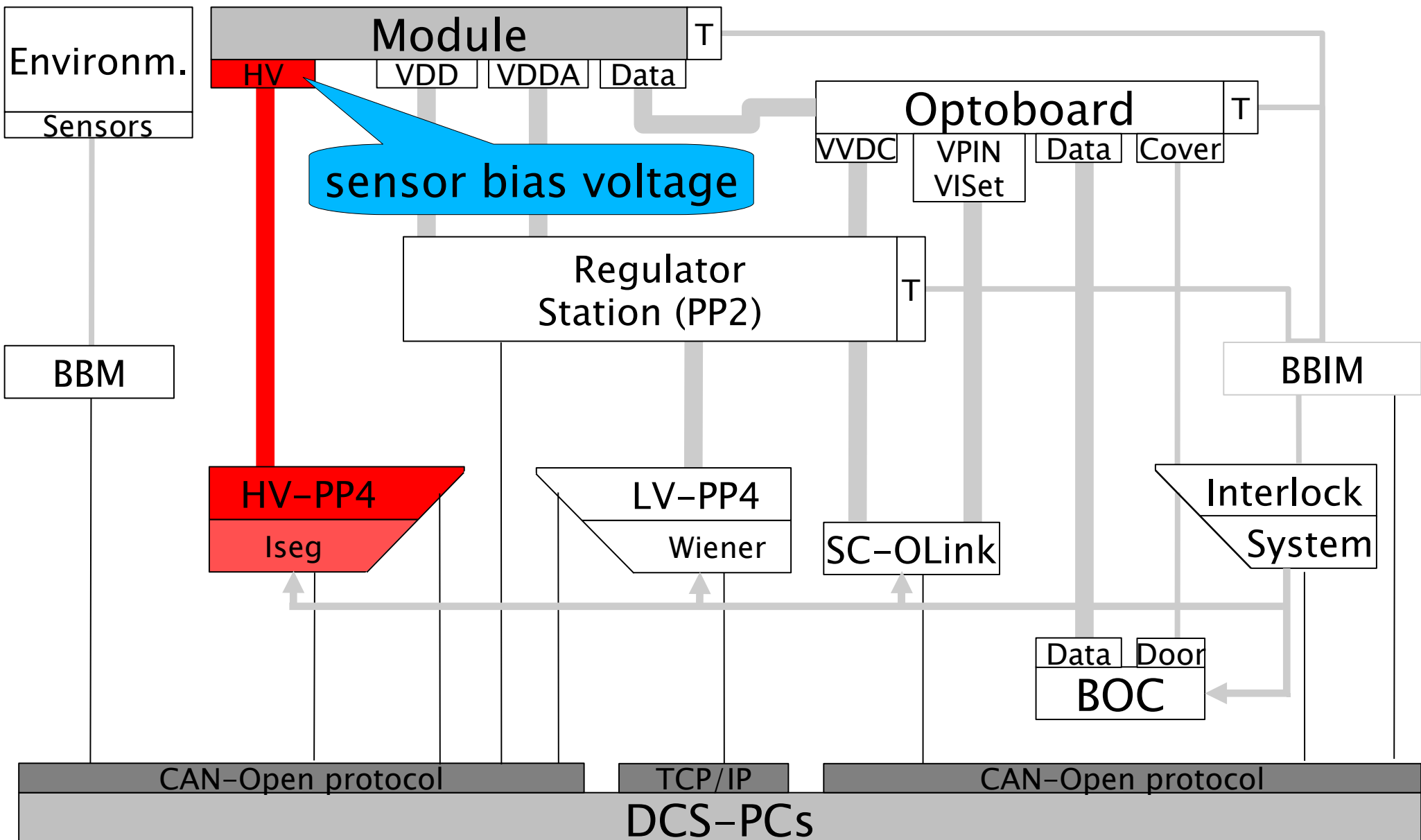
E IV



System Test Setup (High Voltage)



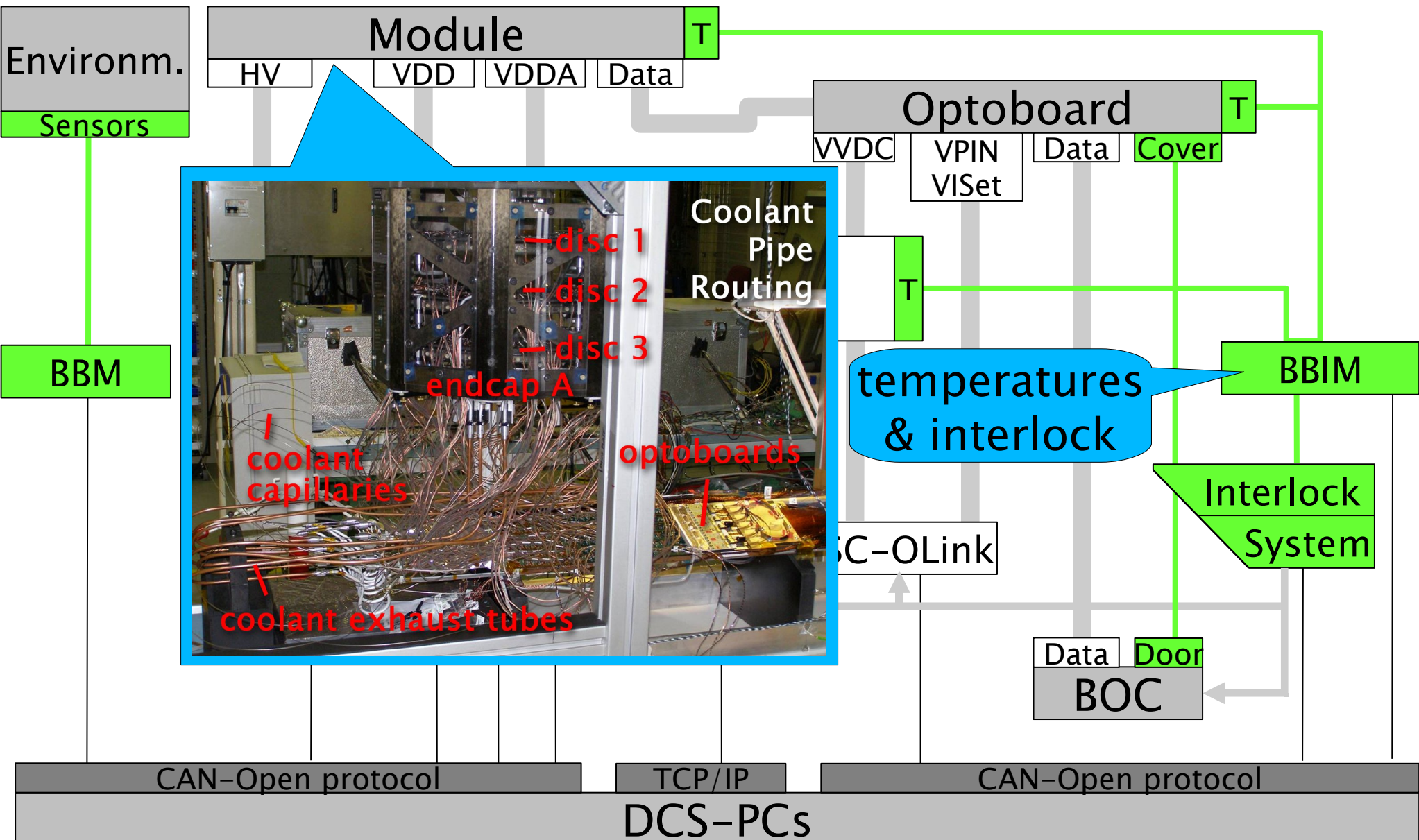
E IV



System Test Setup (Cooling & Monitoring)



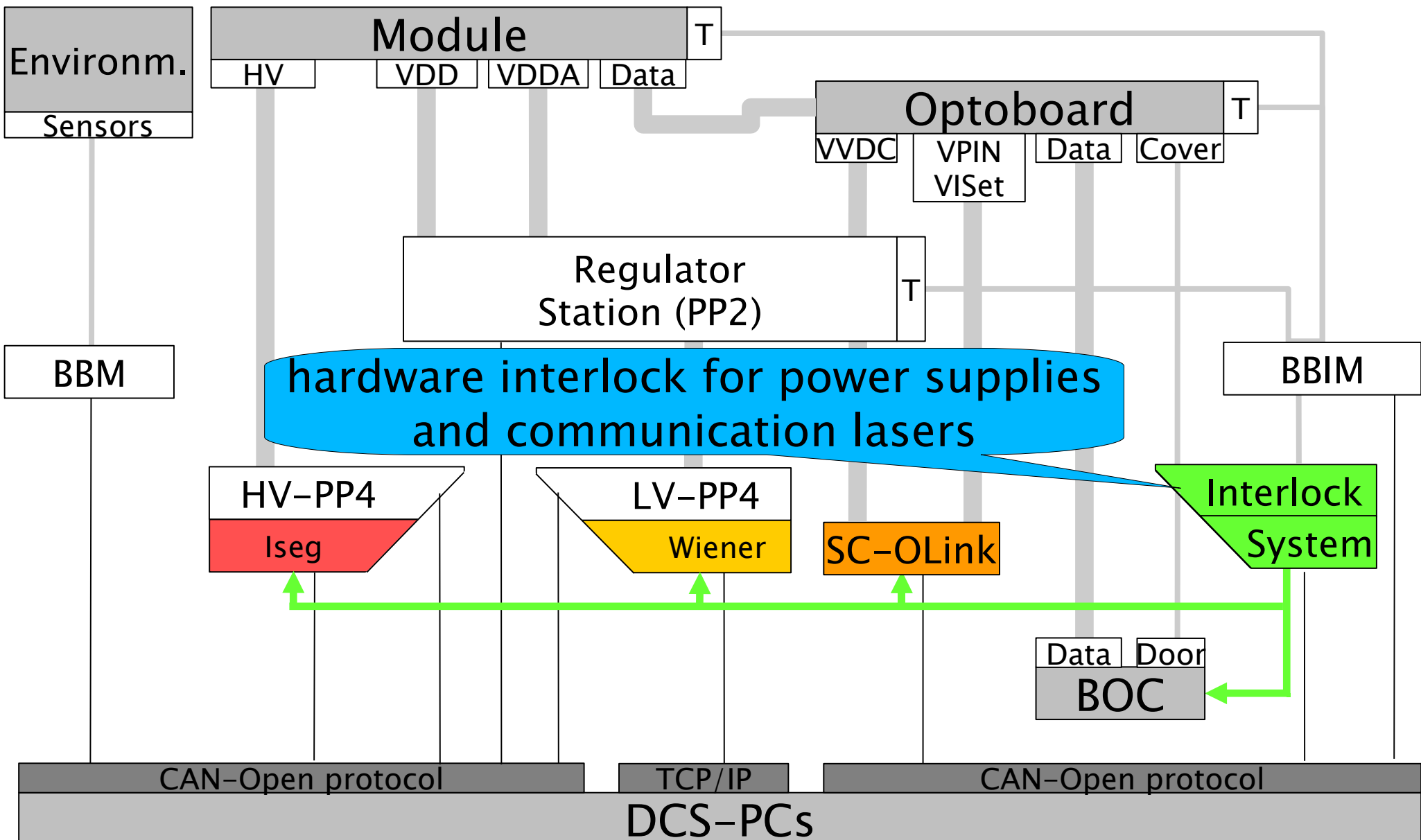
E IV



System Test Setup (Interlock)

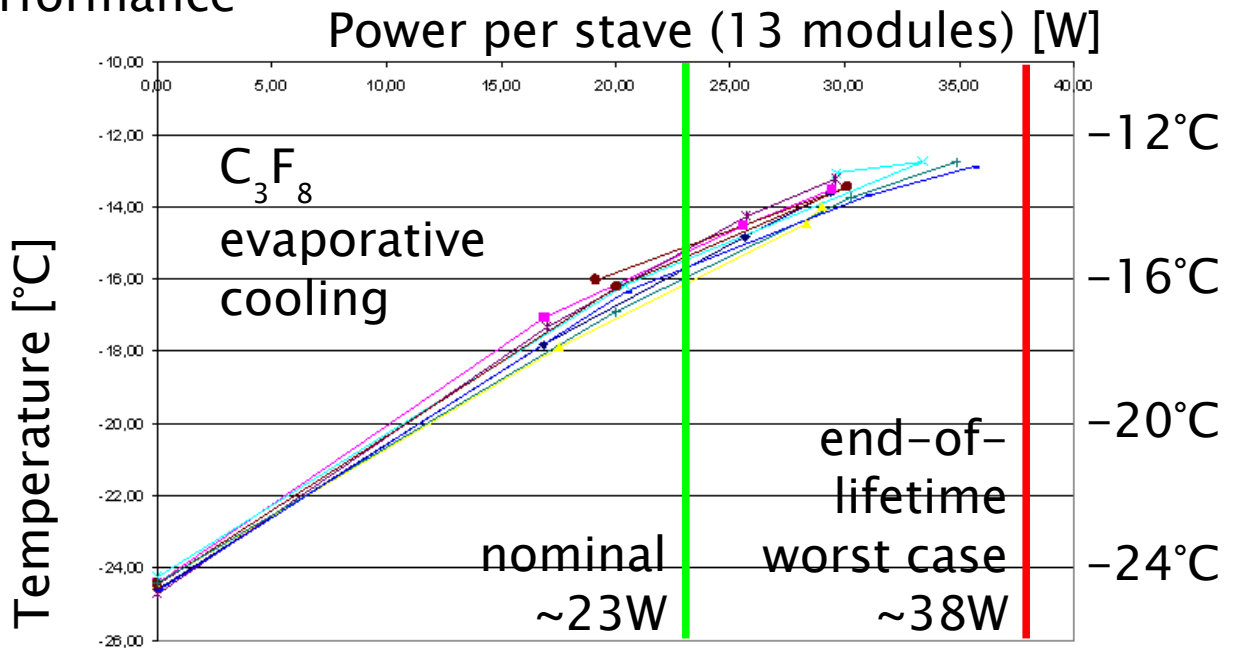


E IV



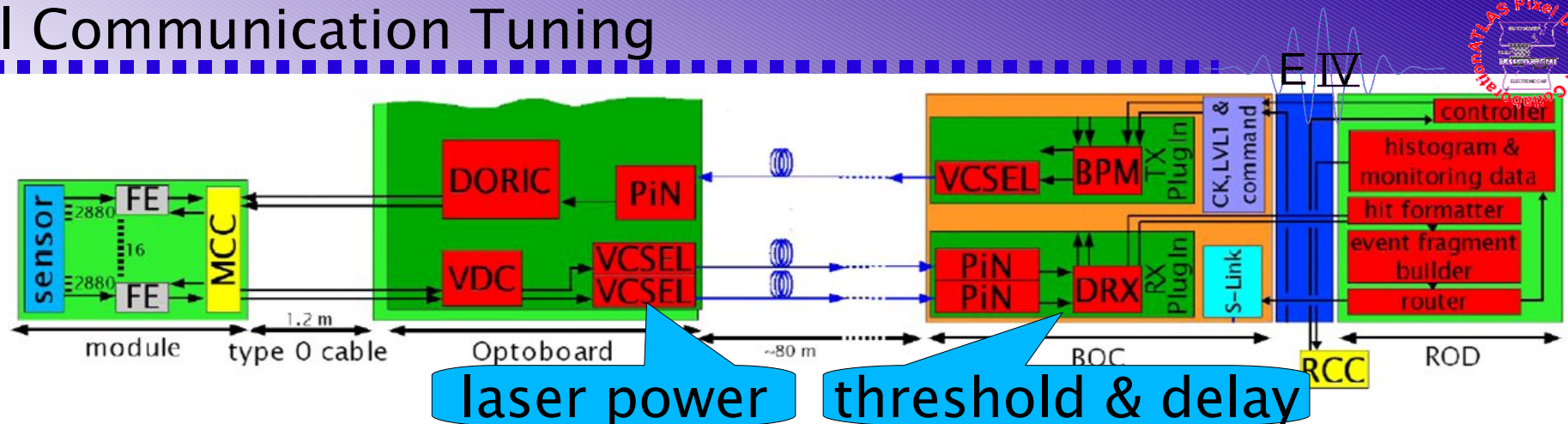
Services & Cooling

- automated service test system has been developed
- complete services chain tested including interlocks, connectivity information in the slow control software and calibration measurements
- service test system qualified for the test of the services before detector is installed in the pit
- intense development and tests in service communications and slow control software (PP2, finite state machine, detector monitoring)
- Endcap operated with evaporative C_3F_8 cooling, as will be used in the final detector with good performance

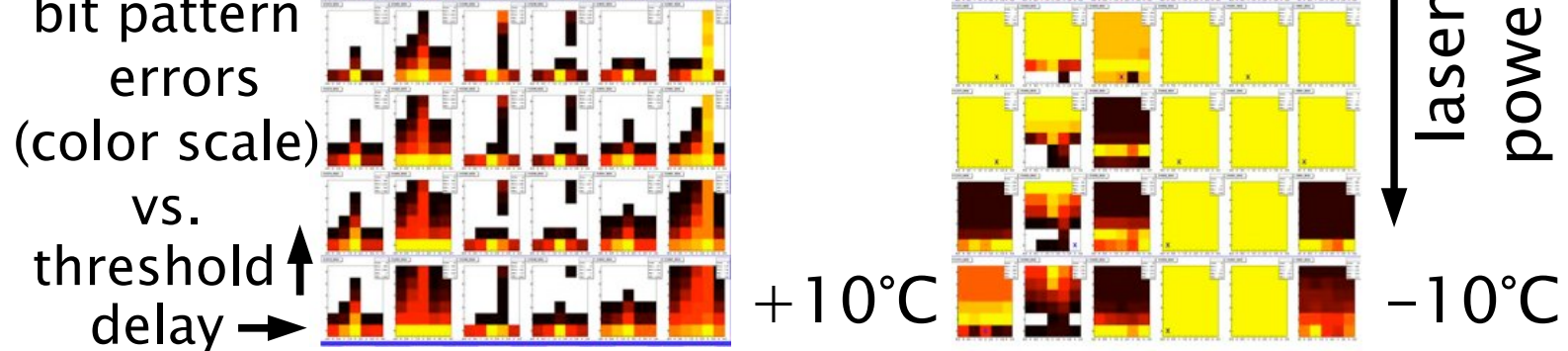


All services and cooling fulfill the requirements of the detector

Optical Communication Tuning



- several parameters need to be tuned for the optical data link between on-detector optoboards and off-detector BOC cards:
 - laser power for the optoboard (1 voltage for up to 14 channels)
 - threshold and delays at the BOC receiver side (channelwise)
- challenge: adjust optoboard laser power such that all 7 opto links have a working parameter space
- power and channel to channel light spread depends on optoboard temperature
⇒ untunable channels below 5°C



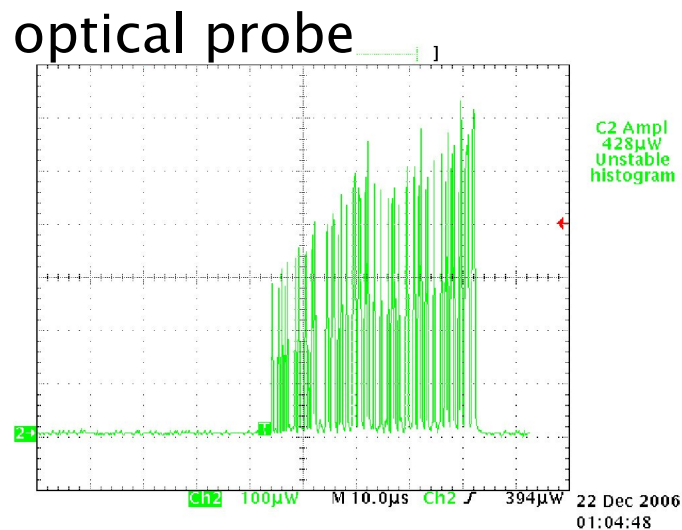
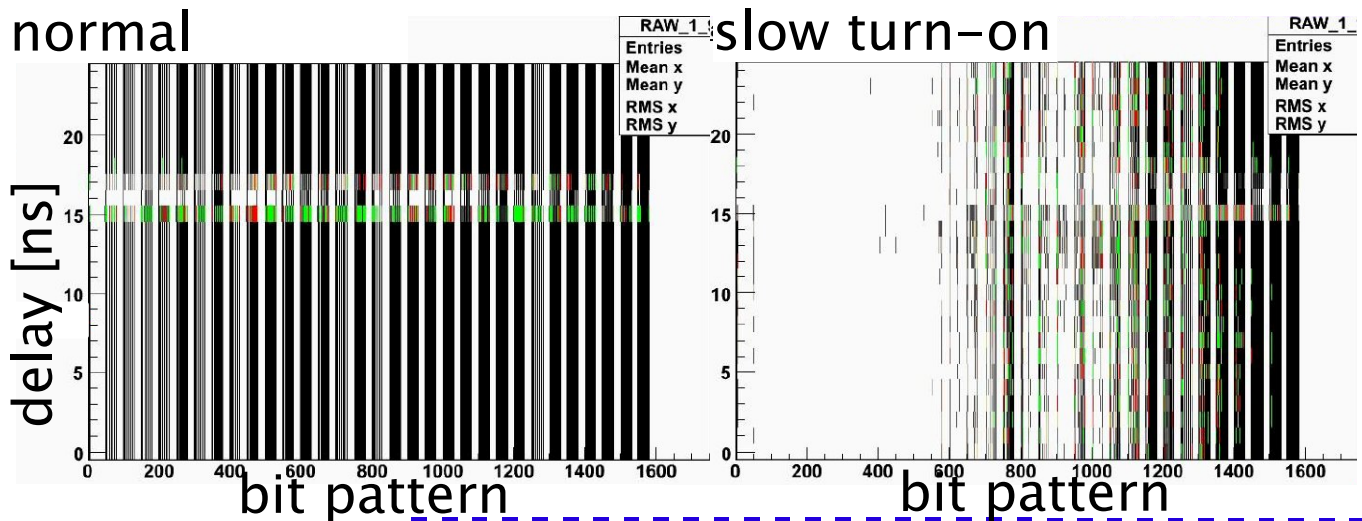
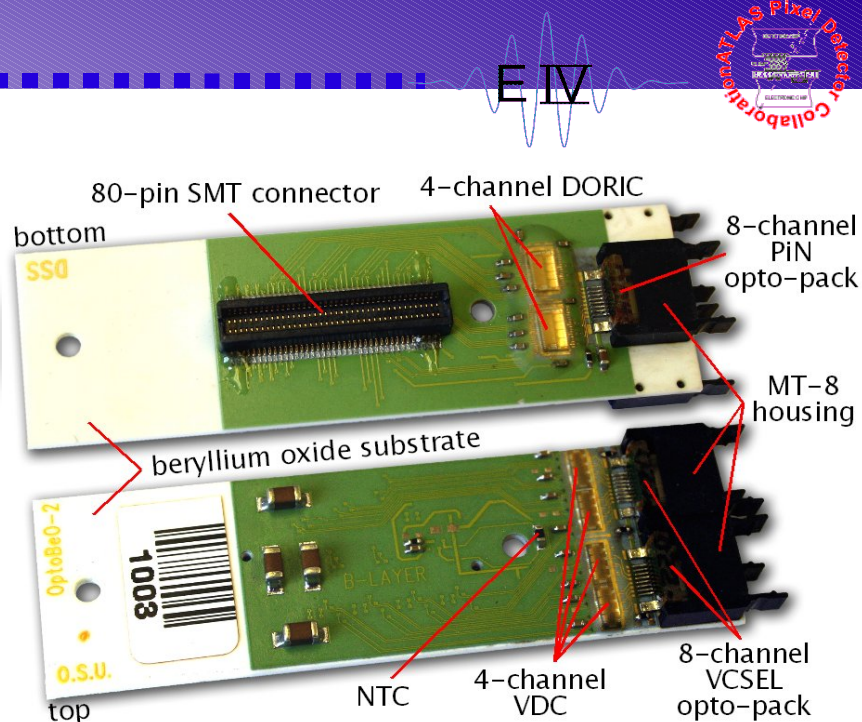
Optical Communication Tuning

- heaters have been installed on the optoboards
 ⇒ all channels behave well at ~20°C



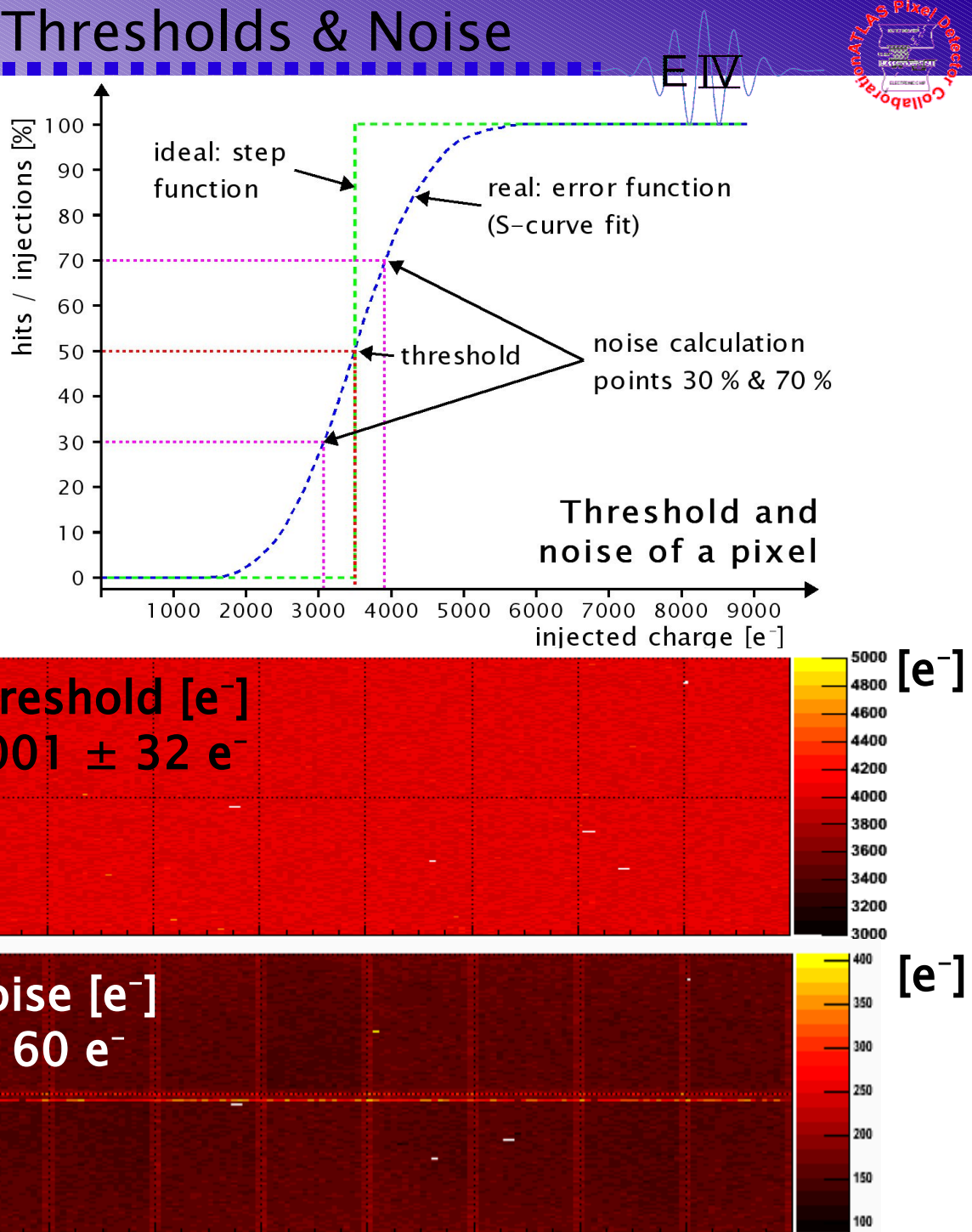
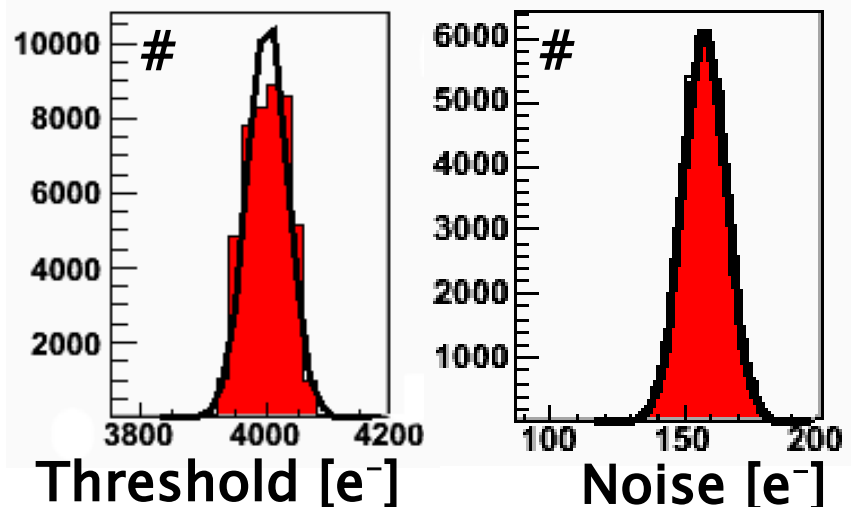
- slow turn-on of light power for few channels
 ⇒ has been addressed in the optoboard quality assurance procedure

probably most of the problems can be explained by not first-choice quality optoboards in the System Test



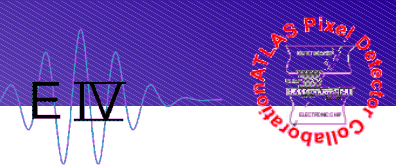
Module Tuning Performance: Thresholds & Noise

- charge injected into preamplifiers and response after discriminator measured
- nicely correlated with production data and only slightly higher ($<10e^-$)

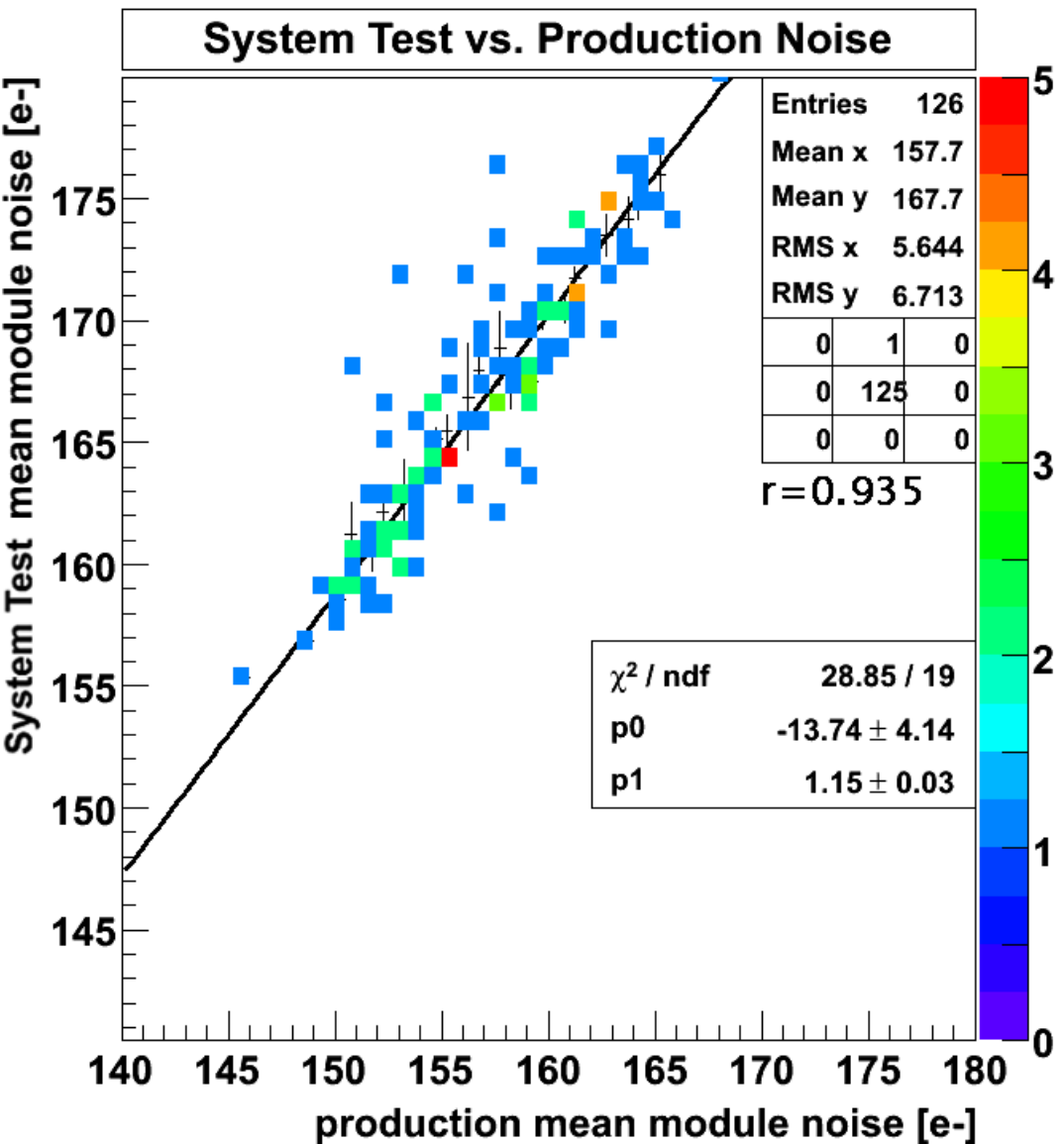
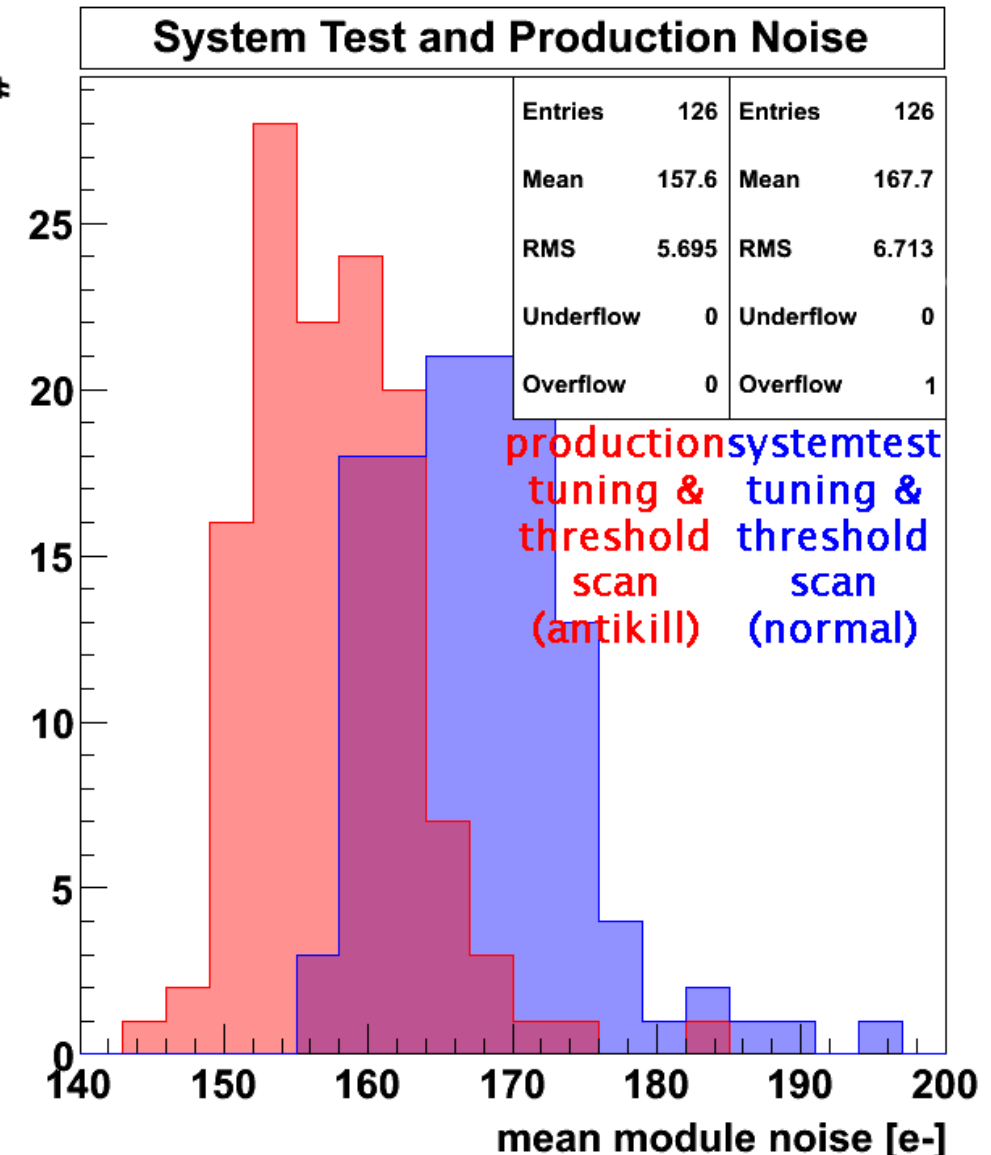


- MIP in 250 μ m silicon sensor:
mean energy loss 27 ke⁻
 \Rightarrow with charge sharing ~17 ke⁻
 \Rightarrow after life-time dose
irradiation irradiation ~ 8 ke⁻

Module Tuning Performance: Thresholds & Noise (2)



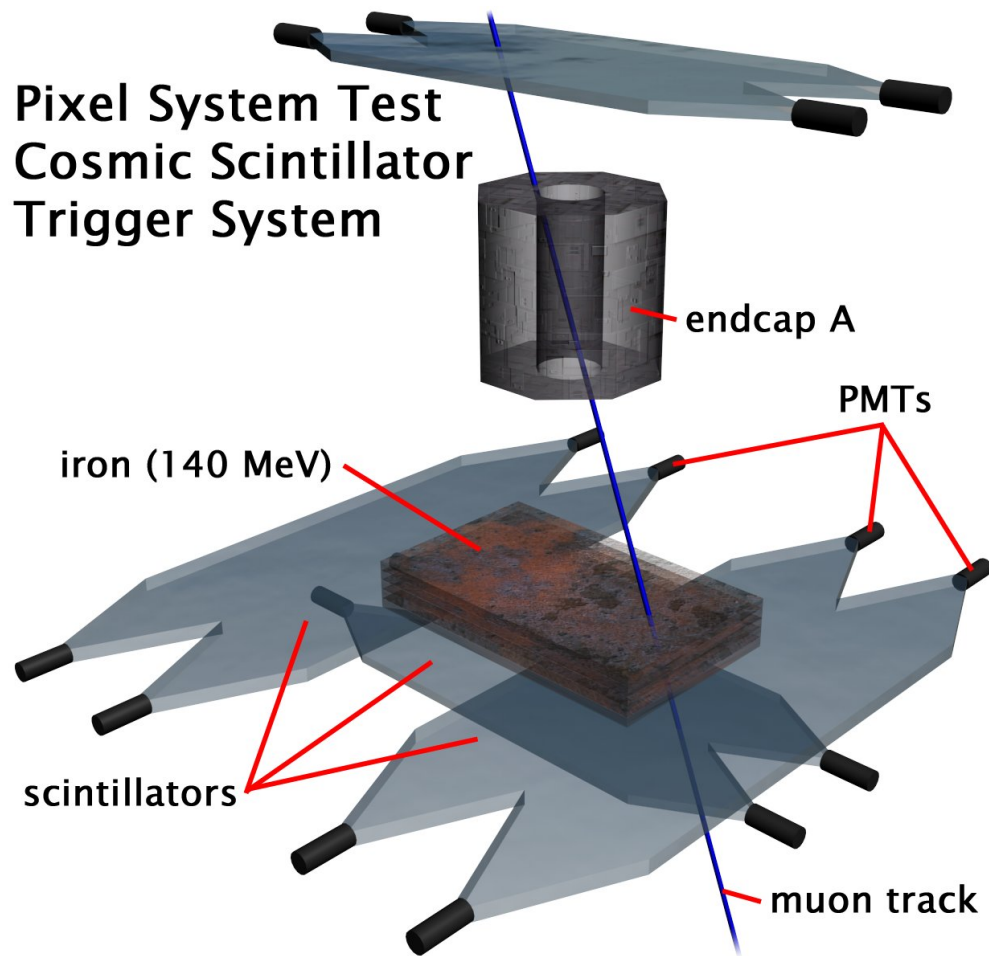
E IV



First Cosmics

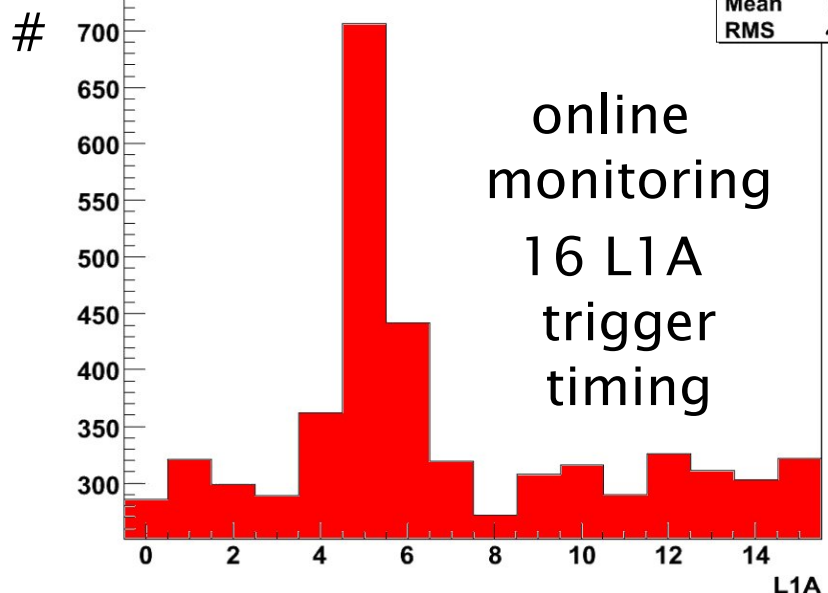


Pixel System Test Cosmic Scintillator Trigger System

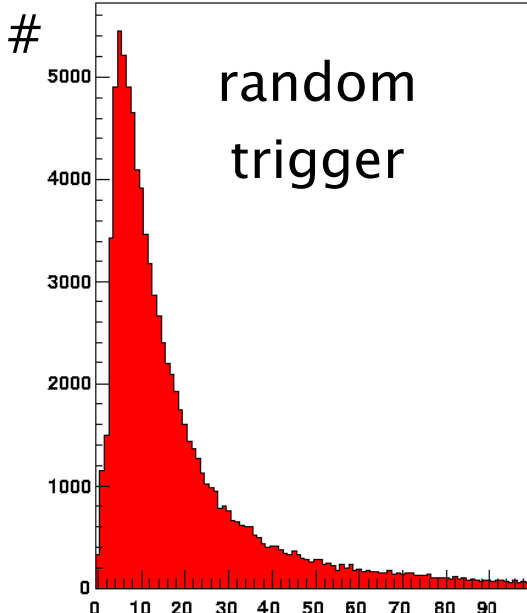


- trigger requests hit in top scintillator and any of the bottom scintillators
- hit position within 16 consecutive 'level1' triggers for cosmic triggers show clear cosmic peak above noise floor

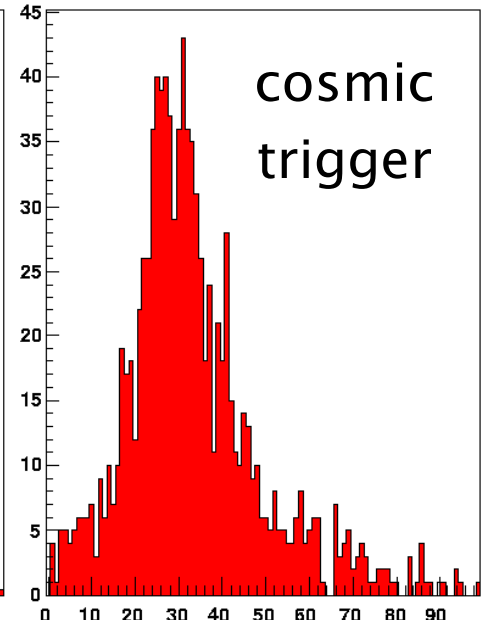
Time Alignment



online monitoring
16 L1A trigger timing



random trigger



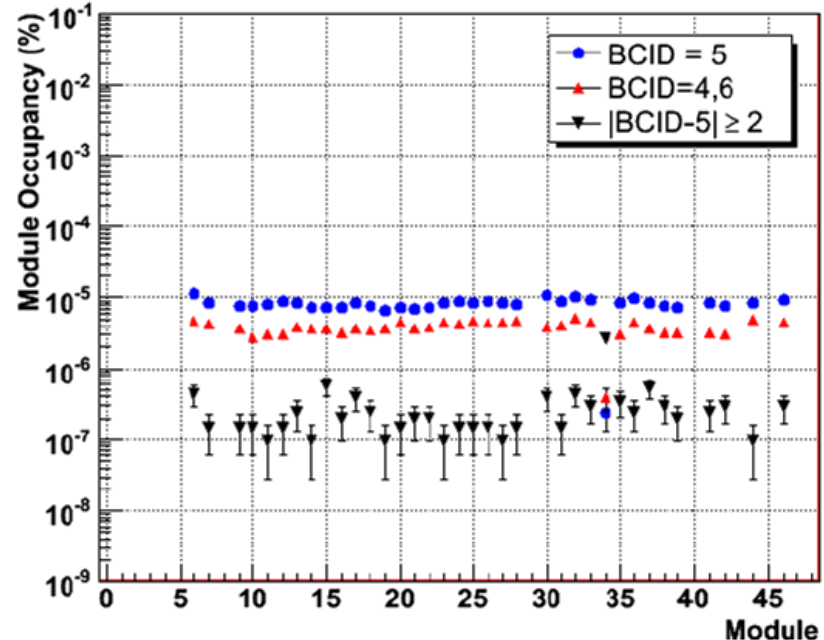
cosmic trigger

charge in time-over-threshold [25ns]

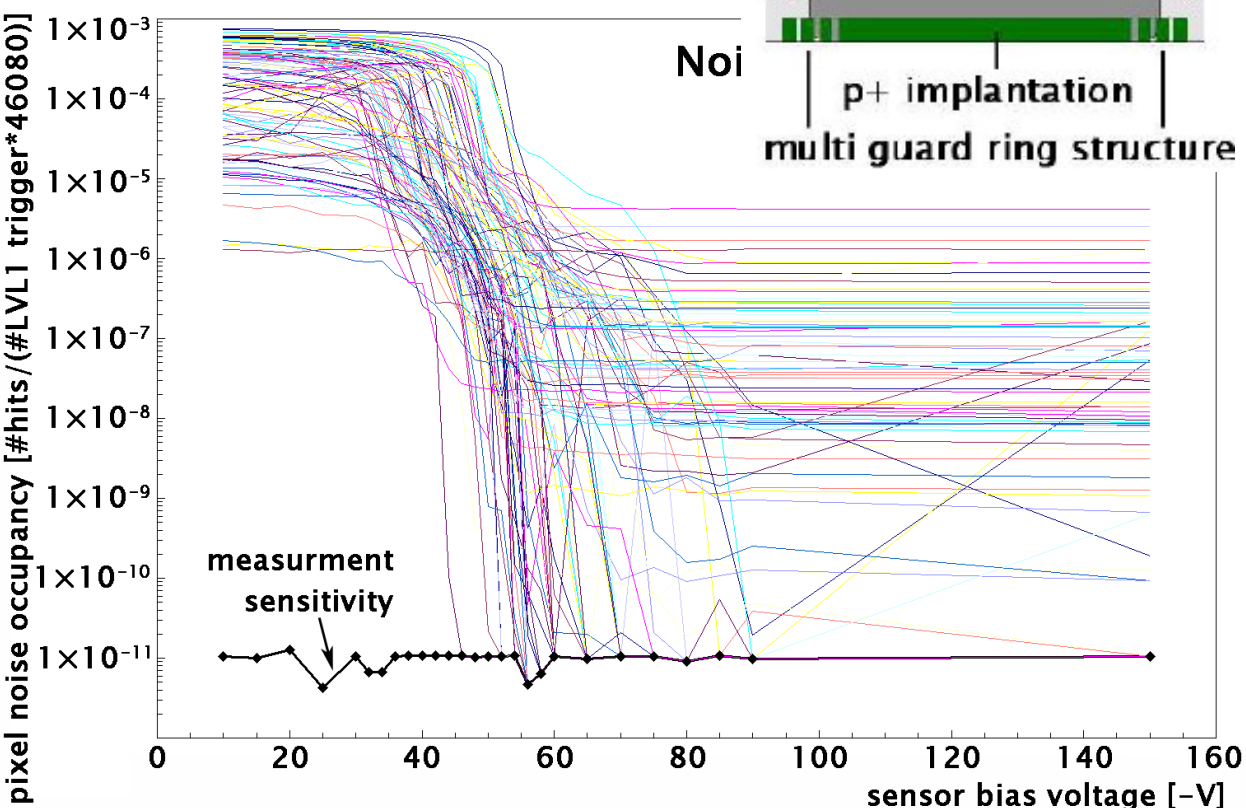
E IV

Appl_PixelGAM/SHIFT/PixelTiming		
Entries	5472	
Mean	7.305	
RMS	4.432	

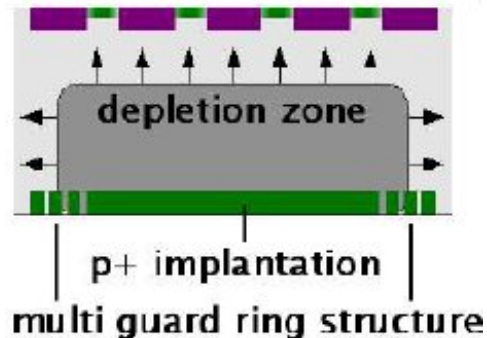
Noise Occupancy and Sensor Depletion Voltage



- noise occupancy measured with cosmic trigger
- after removal of noisy (10^{-4}) pixel noise occupancy as low as 10^{-7}
- 90% of noisy pixel identified from production measurements
- total fraction of affected pixels $>1\%$



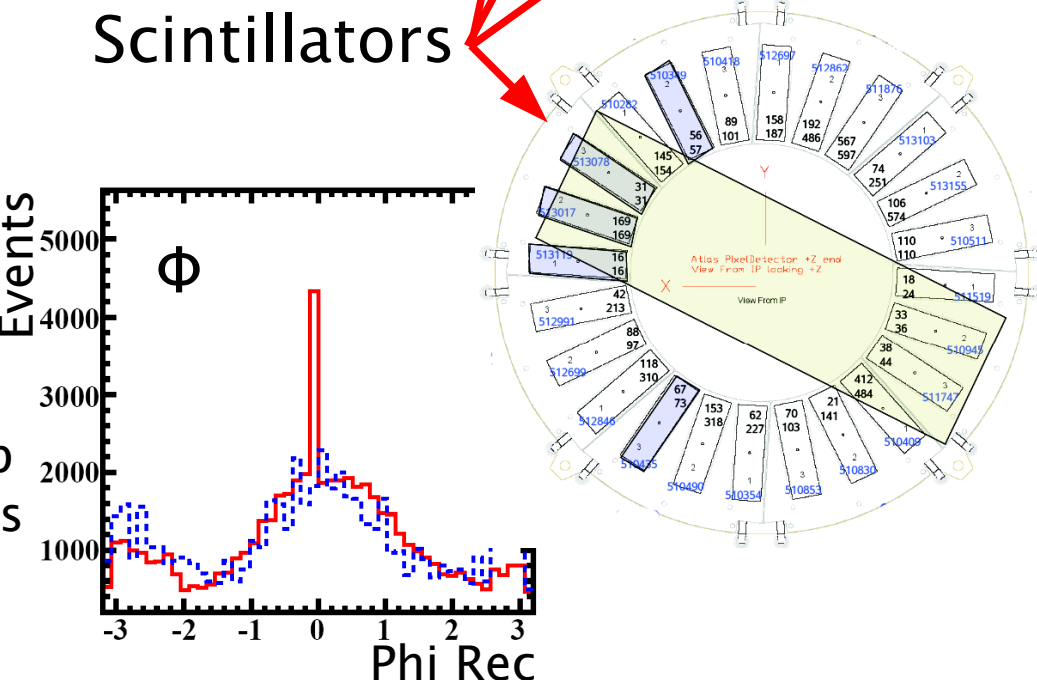
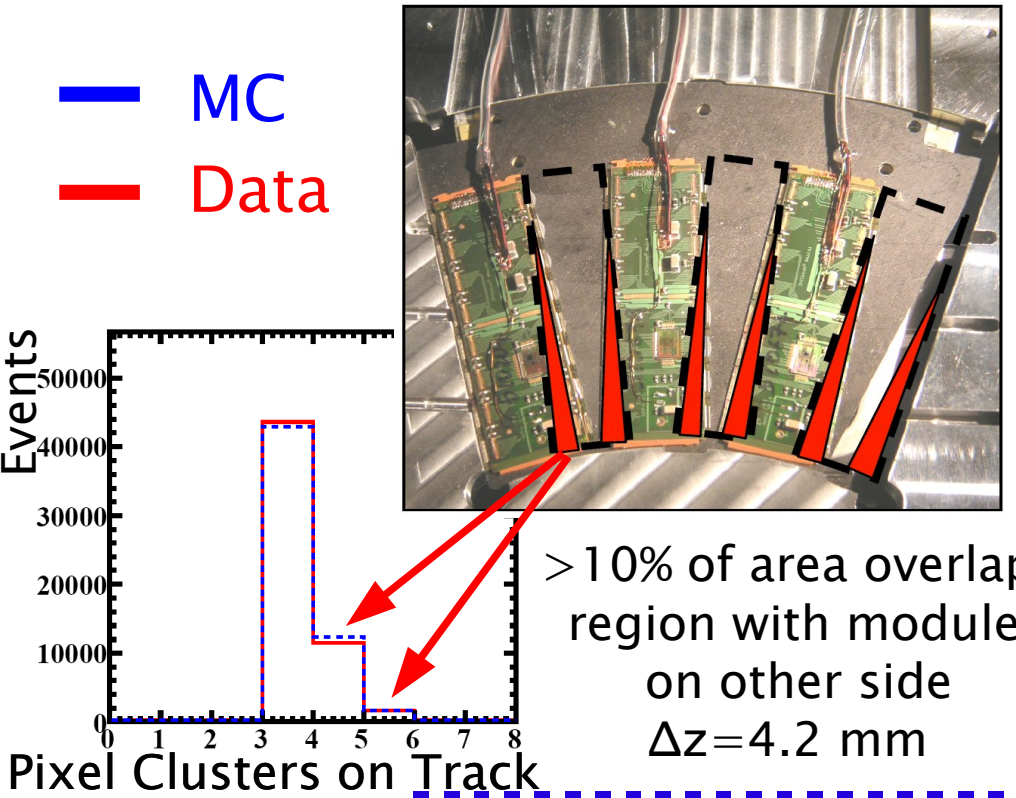
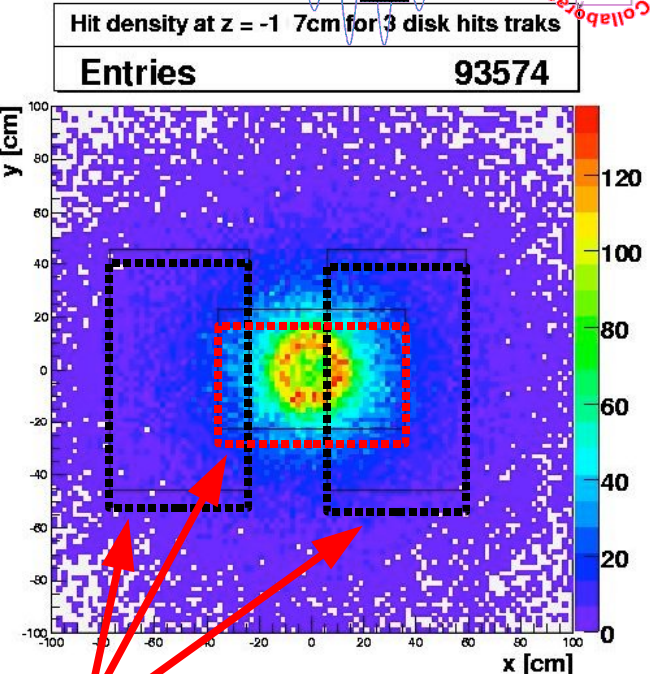
- noise occupancy with random trigger vs. sensor bias voltage measurement used to determine depletion voltage
- depletion zone grows towards pixel side \Rightarrow bias voltage below full depletion – pixel shorted \Rightarrow high capacitive load to preamplifiers \Rightarrow high noise \Rightarrow high noise occupancy



Monte Carlo vs. Data



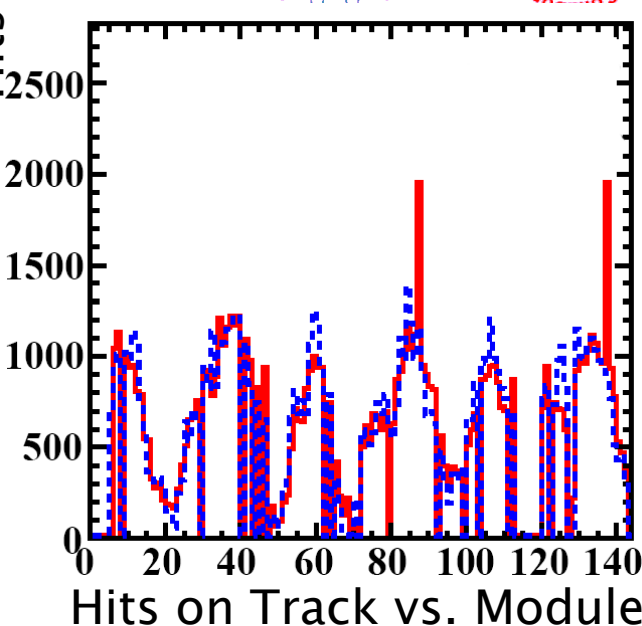
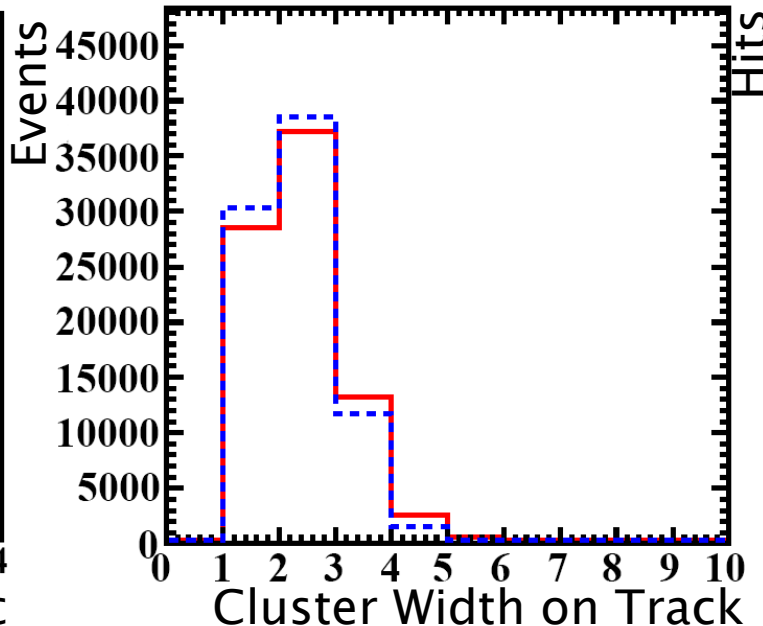
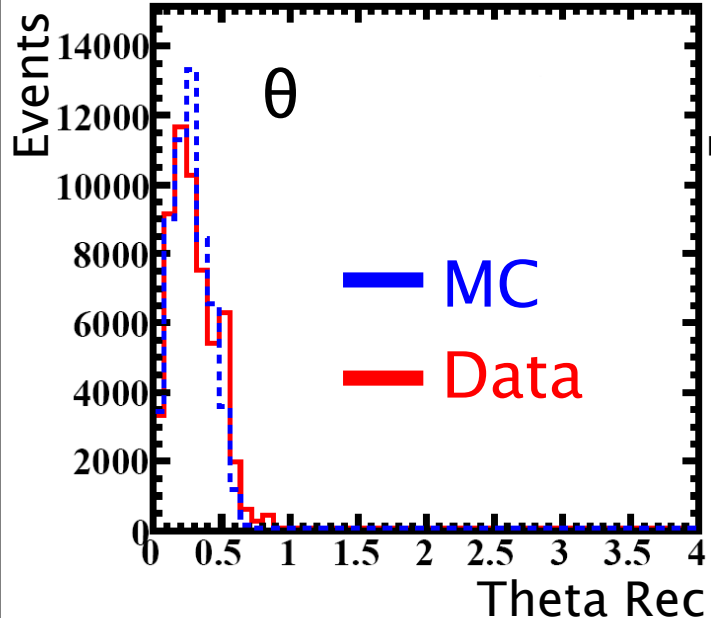
- 29 out of 144 modules disabled
- measured trigger rate 15.7 Hz vs. \sim 18 Hz full simulation rate



Monte Carlo vs. Data (2)

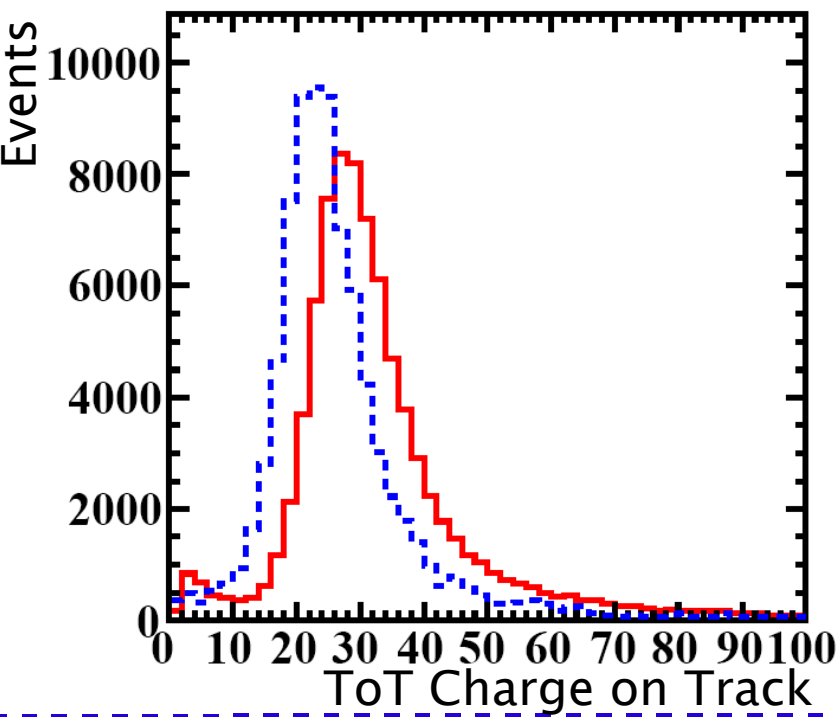


E IV



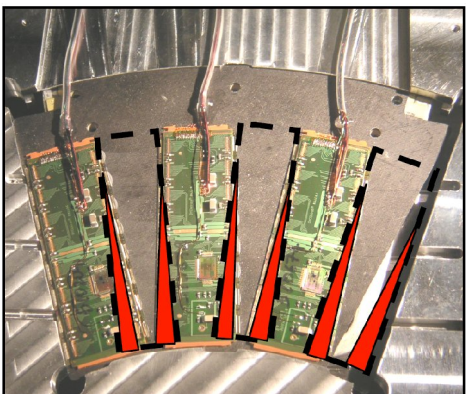
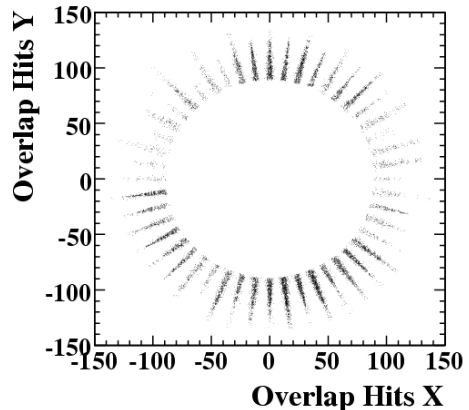
- MC tuned on cosmic data
- theta reconstruction, cluster width and hits on track vs. module agree with MC (hits on track inhomogeneous due to asymmetric scintillator, missing modules & 3 noisy pixels)
- TOT shape correct \Rightarrow TOT calibration (from production measurements) OK
 \Rightarrow shift due to wrong fit parameter C:

$$TOT = A + \frac{B}{(C + Q)}$$

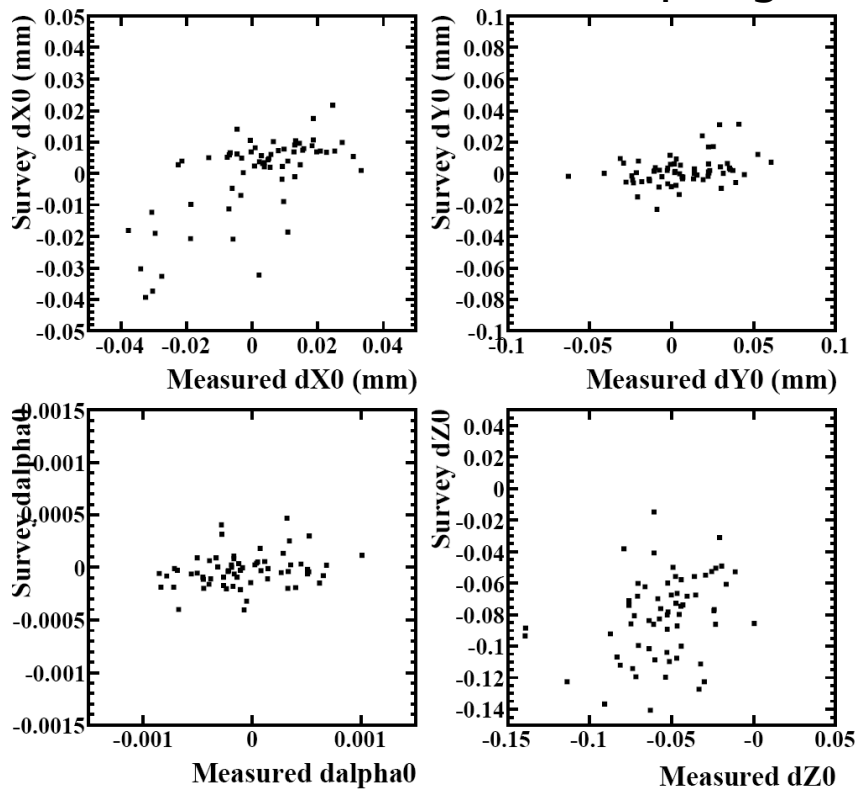


Alignment

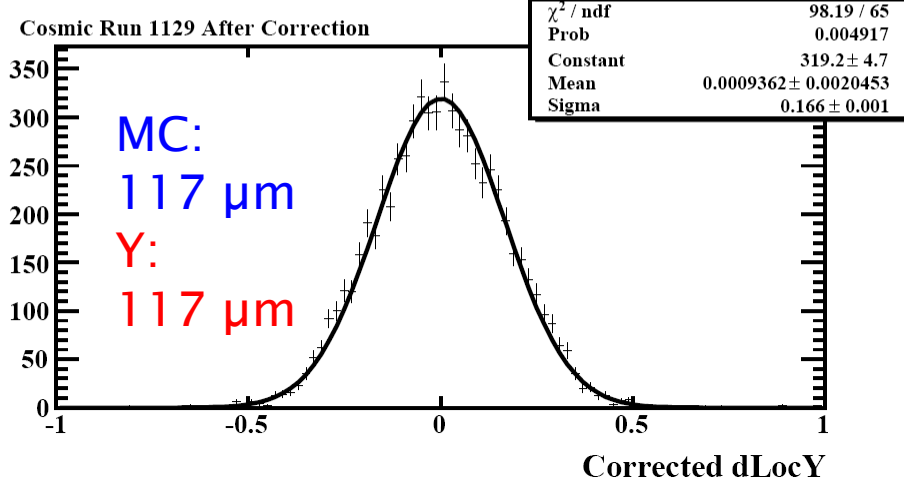
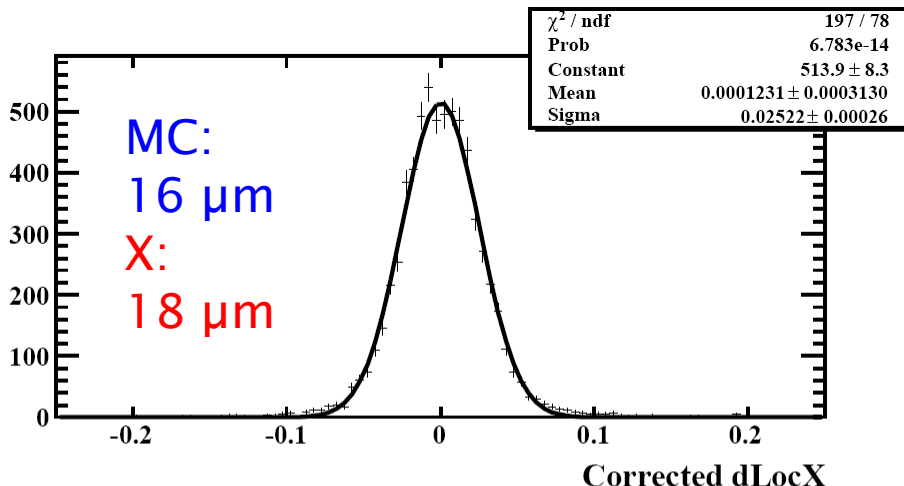
E IV



Survey vs. cosmic alignment for modules with more than 50 hits in the overlap region



- use >10% overlap region between modules on different side of a disk $\Delta z = 4.2$ mm to determine relative alignment between modules

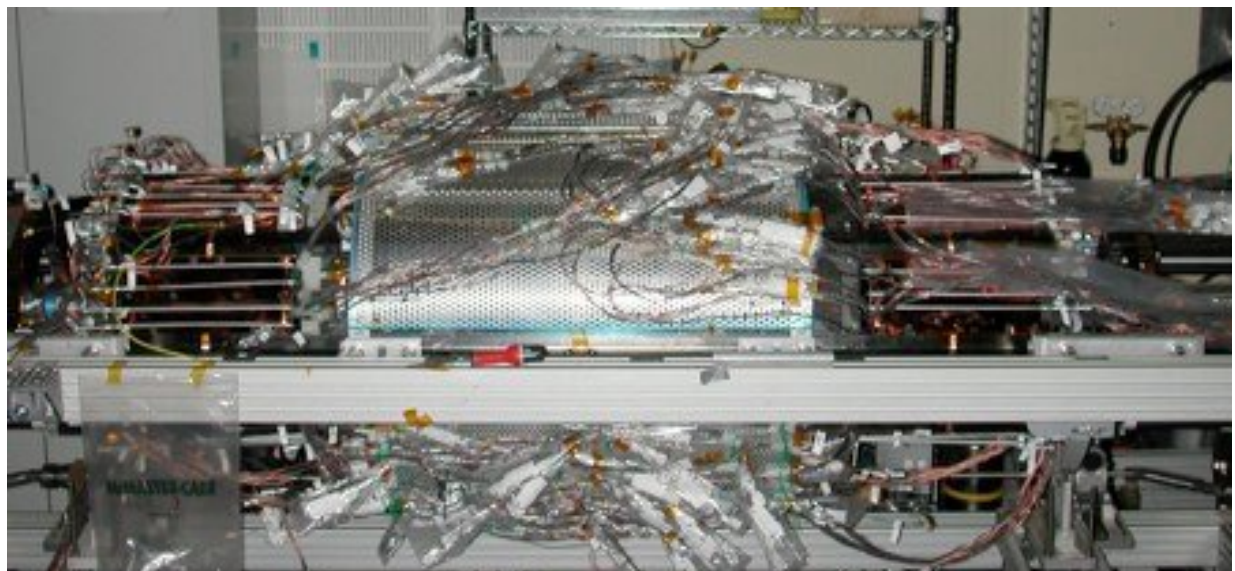


Conclusions

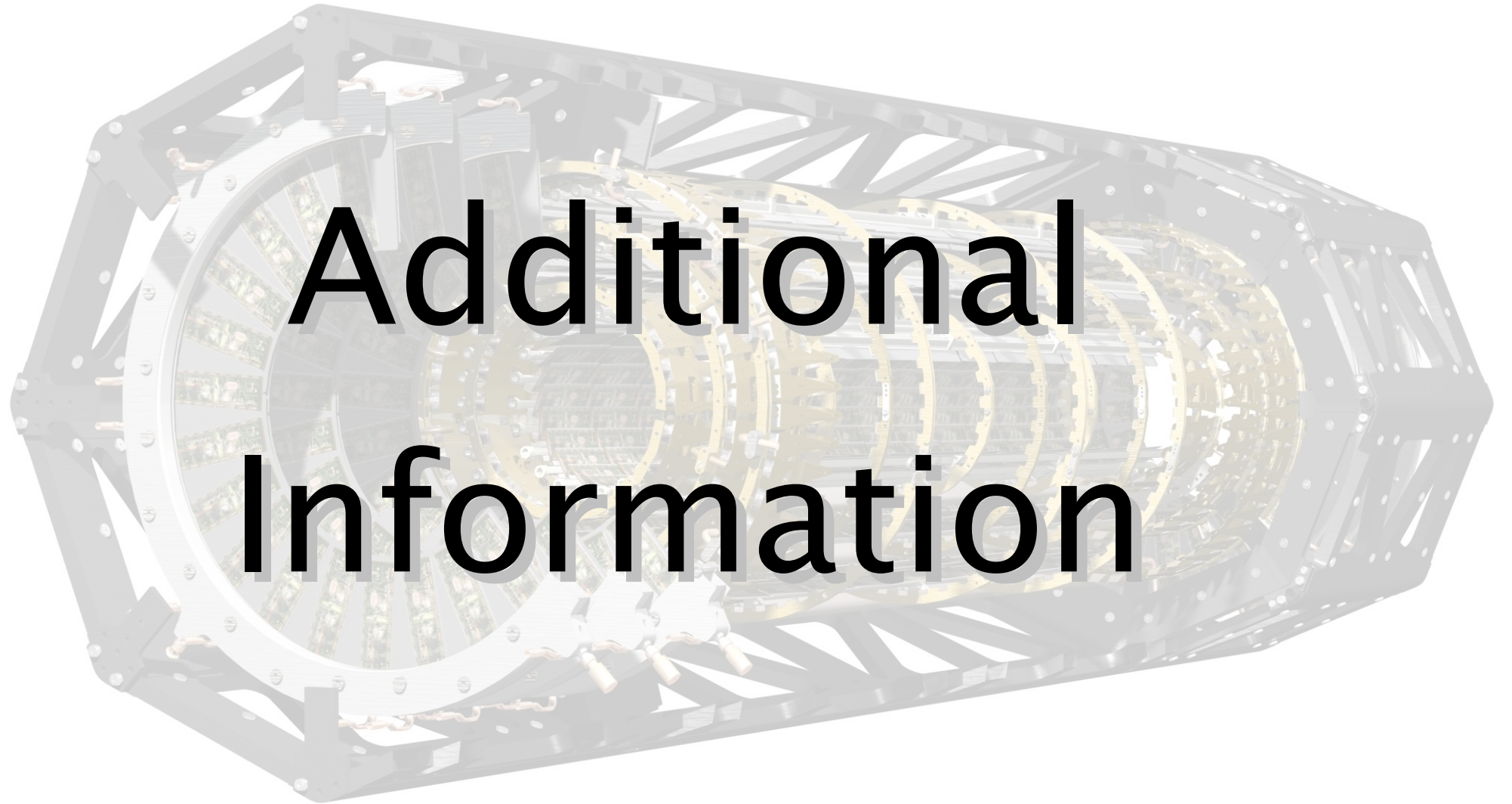
E IV



- the ~10% System Test was a success and we gained valuable experience for a successful commissioning and the operation of the detector
- various parts of the services have been validated (cooling, services, interlock system)
- huge development step was done in online and offline software driven by the System Test
- difficulties in optical communication tuning were identified in time to take necessary actions before commissioning
- expected good detector performance (threshold, noise, noise occupancy) could be verified and no system specific problems have been observed
- Monte Carlo expectations for cosmic data have been confirmed – recorded data allows us to test the entire reconstruction chain and exercise alignment and resolution studies

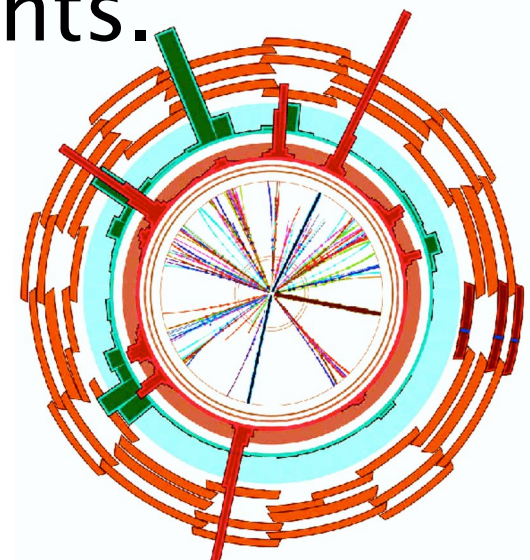
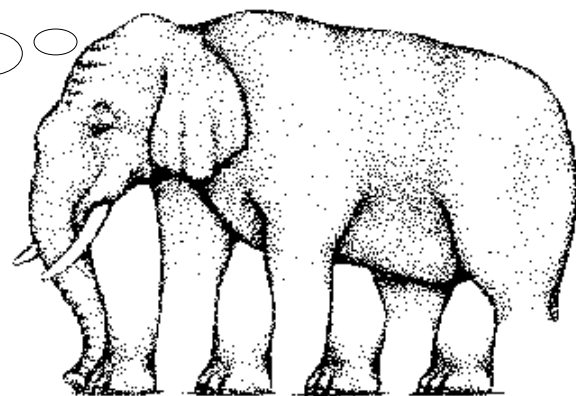


Additional Information



Tracking and Vertexing:

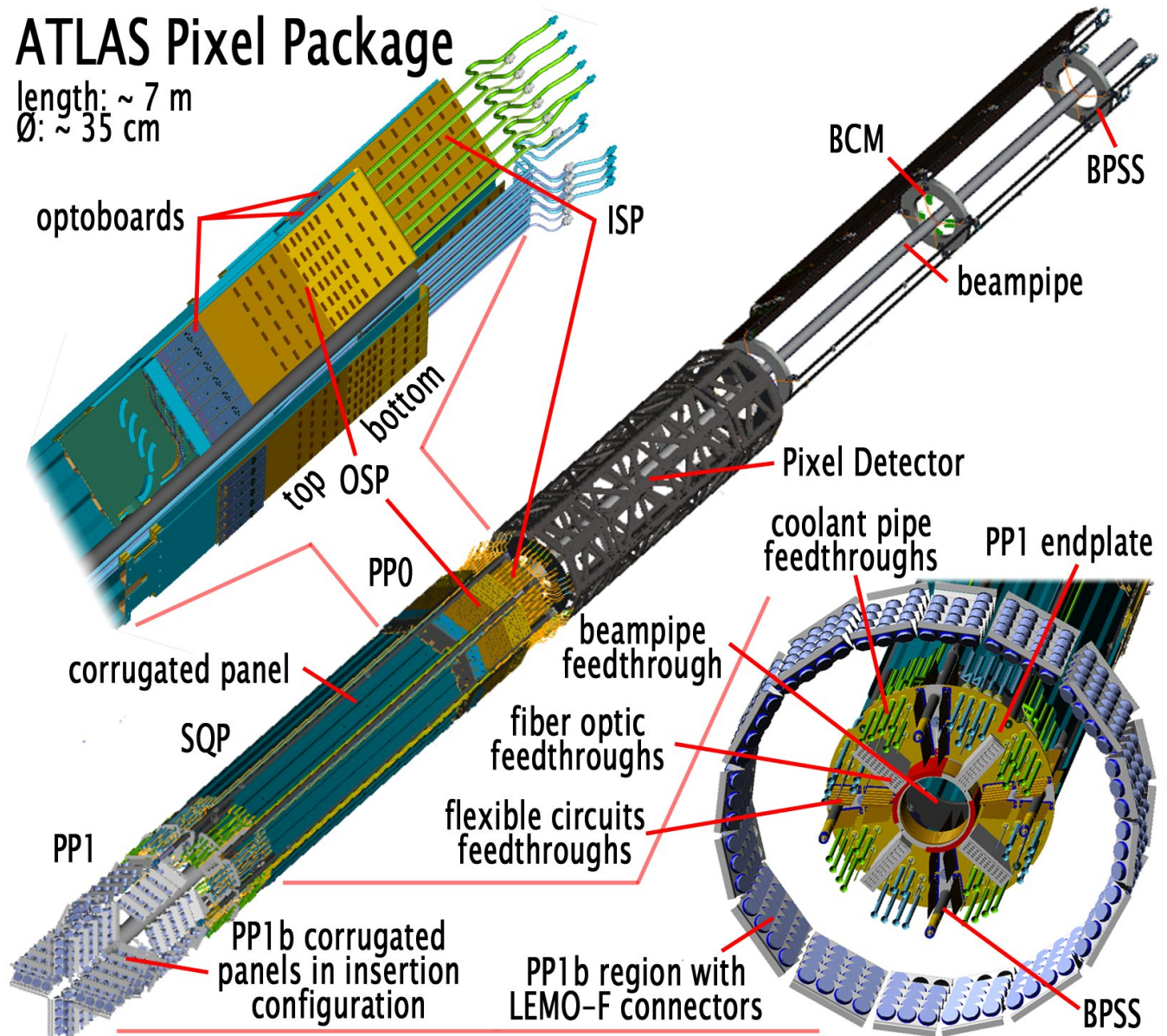
Measure sometimes (40 million times a second) many (three) ultimate precise ($\sim 12 \mu\text{m}$) space-points at zero distance ($r_{\min} \sim 5 \text{ cm}$) to the interaction point of few (1000) particle tracks with a perfect (>97% overall efficiency), radiation hard ($> 1 \cdot 10^{15} \text{ n}_{\text{MeV eq}}/\text{cm}^2$), massless ($x_0 < 10\%$) and full coverage (pseudo rapidity $< |2.5|$) detector and readout some (75k/s) selected events.



ATLAS Pixel Package

ATLAS Pixel Package

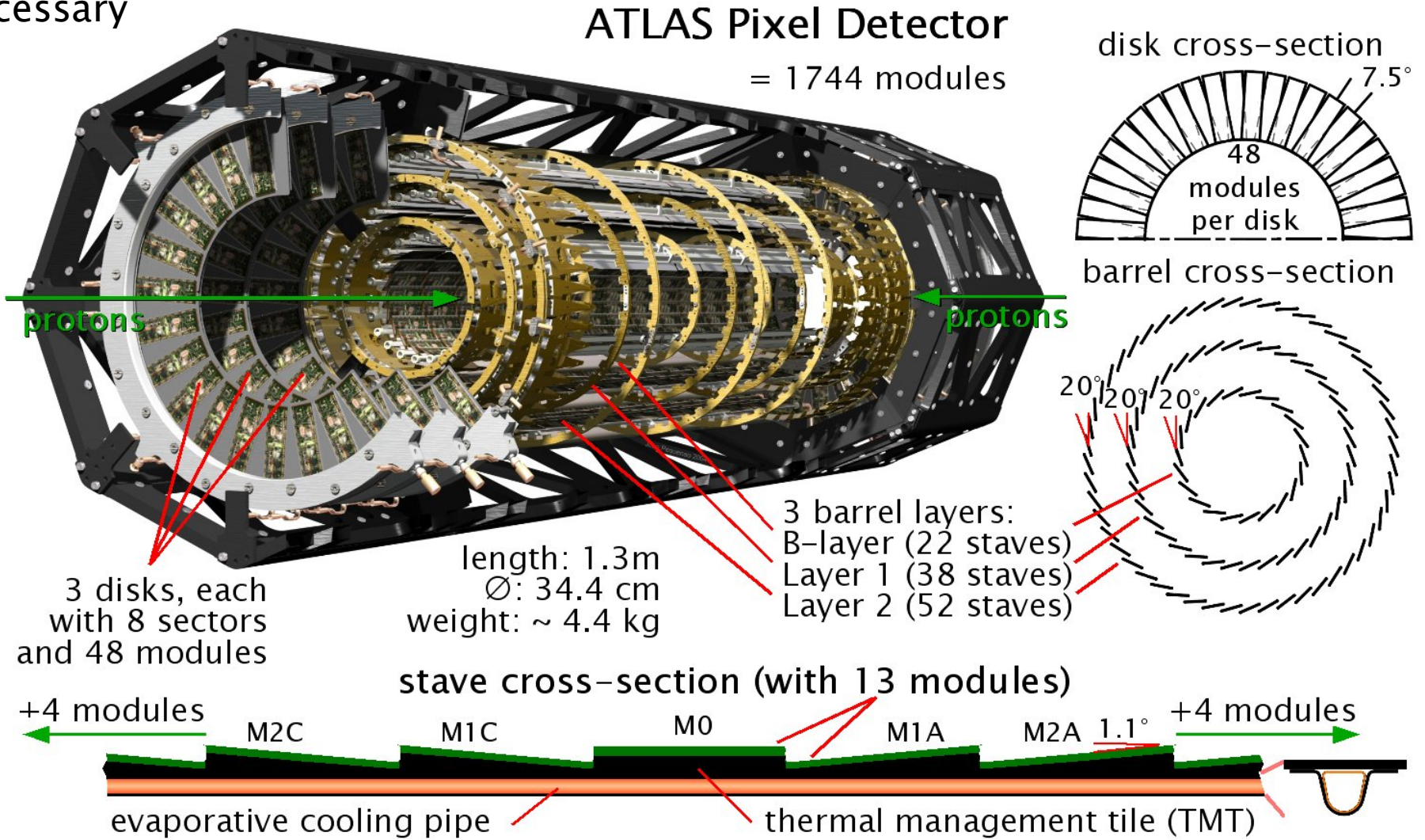
length: ~ 7 m
 \varnothing : ~ 35 cm



- beryllium beampipe integrated in the Pixel package
- active surface only in the 1.3 m long central detector section
- BeamPipe Support Structure (BPSS) connected at both ends position the beampipe in the middle of the detector and support Service Quarter Panels (SQP)
- in total eight SQPs provide all services to the detector
- cooling tubes and electrical module connections at PPO
- optoboard mounted at PPO provide optical/ electrical conversion
- all services break at PP1

ATLAS Pixel Detector

- 3-hit (3 layers and 3 disks) semiconductor detector closest to the interaction point
⇒ track resolution of $12 \mu\text{m}$ in $R\phi$ and of $100 \mu\text{m}$ in z direction ⇒ 1744 modules
- ⇒ required radiation tolerance: up to $10^{15} \text{ n}_{\text{eq}} \text{ cm}^{-2}$ (B-layer)
- overall efficiency aim: > 97 % ⇒ good charge collection even after irradiation necessary



ATLAS Pixel Sensor

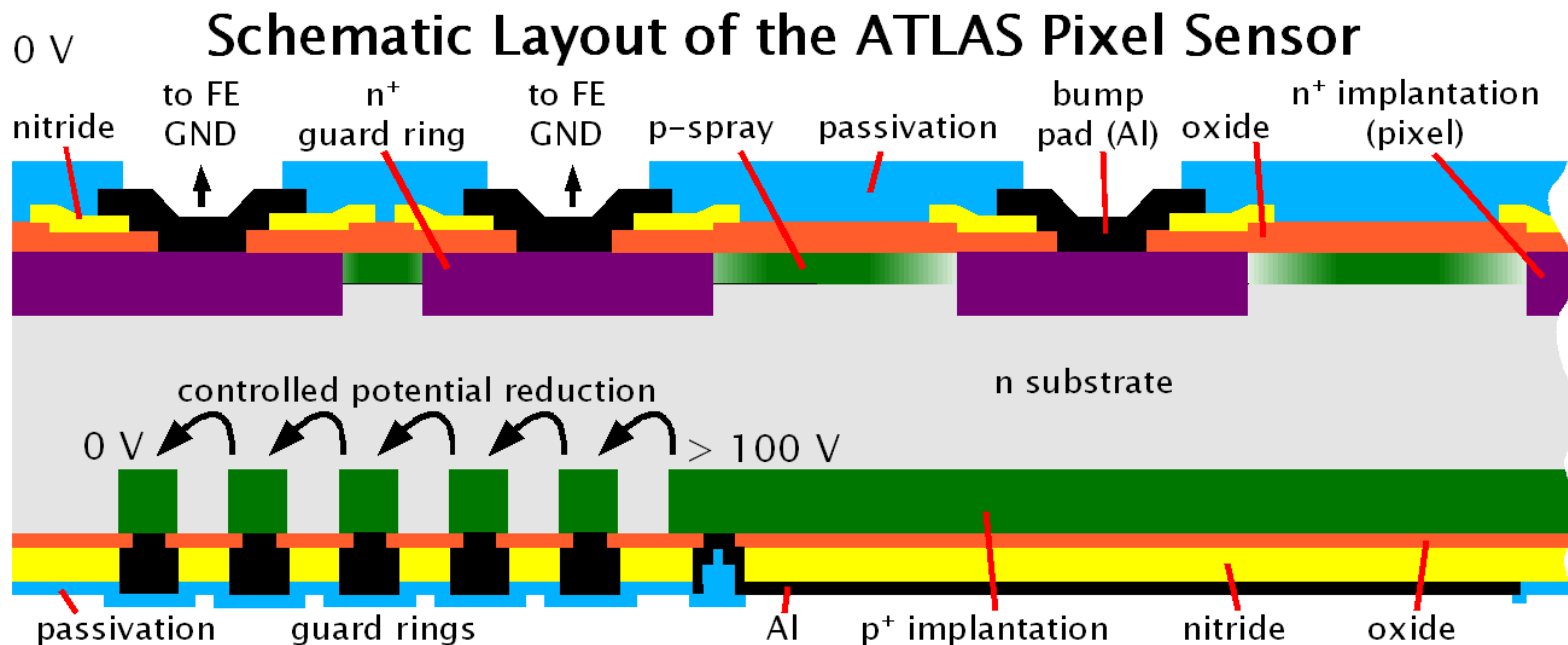
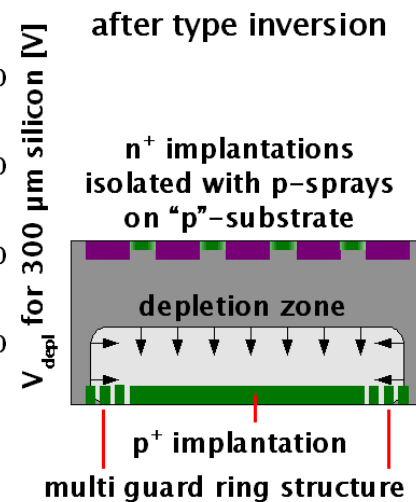
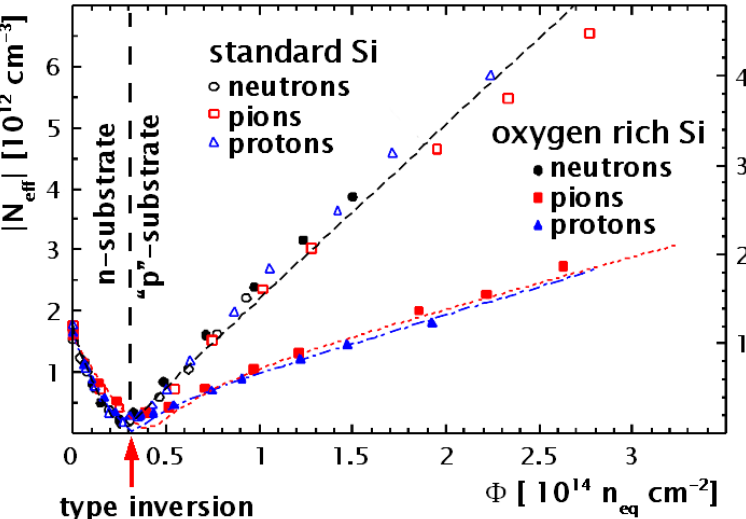
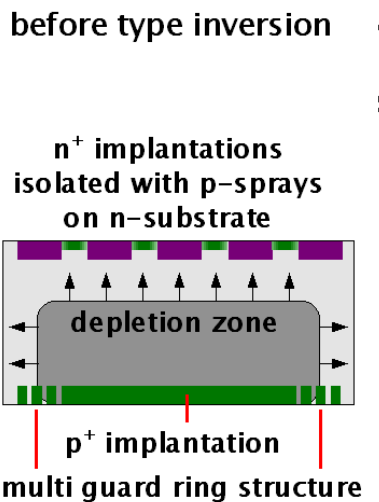


E IV

- type inversion during irradiation \Rightarrow oxygen rich Si improves radiation tolerance for pion and proton irradiation

- \Rightarrow depletion zone has to reach pixel implantations
- $\Rightarrow n^+np^+$ design
- \Rightarrow not fully depleted sensor still can detect particles

- p implantations necessary to isolate pixels
- \Rightarrow p-stop: alignment risk & high lateral maxima of electric field at bulk-oxide-p⁺ junction
- \Rightarrow p-spray: high lateral maxima of electric field at bulk-p⁺-n⁺ junction
- \Rightarrow moderated p-spray

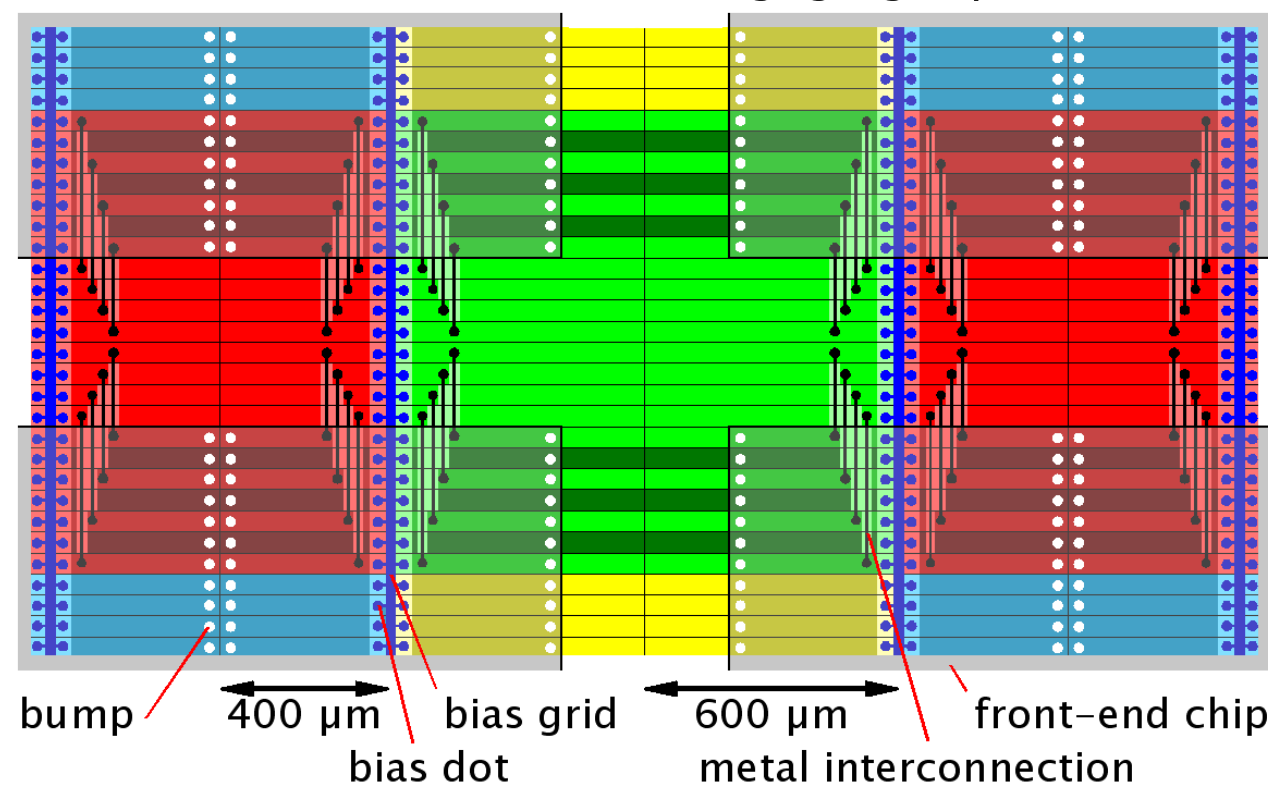


Sensor Interchip Region

E IV

ATLAS Pixel Sensor Interchip Region

- █ pixel
- █ ganged pixel
- █ inter-ganged pixel
- █ long pixel
- █ long+ganged pixel
- █ inter-long+ganged pixel



150
155
159
row
number
159
155
150

- standard **pixel** are $400 \times 50 \mu\text{m}$
- to avoid dead areas between FEs pixel are prolonged in the long direction \Rightarrow **long pixel**
- in the short pixel direction a pixel in the interchip region is connected by a metal layer to a pixel which has a connection to the FE \Rightarrow **ganged pixel**
- only every second pixel with FE connection close to the interchip region is ganged \Rightarrow allows to distinguish between interchip and FE hit for 2-pixel hits \Rightarrow higher capacitance due to metal layer for **inter-ganged pixel**
- ganged and inter-ganged pixel exist also for long pixel \Rightarrow **in total 6 pixel types**

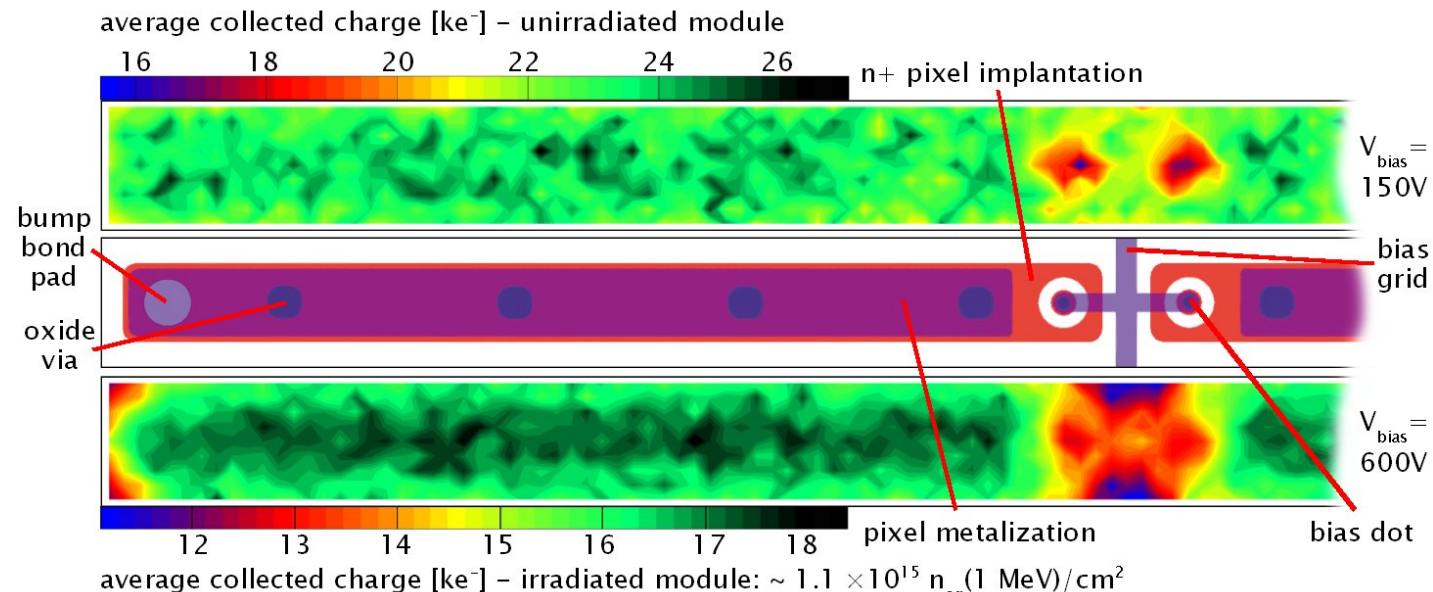
Sensor Charge Collection



E IV

- unirradiated: average collected charge homogeneous & no significant charge losses at the interfaces – but: ~ 33 % loss at bias dots caused by direct charge collection onto the bias dot and ~ 8 % between the bias dots due to indirect capacitive coupling through the p-spray to the bias grid metalization
- irradiated: not fully depleted & radiation induced trapping centers \Rightarrow 20 % lower average collected charge – increased trapping probability for charges following the bend streamlines of the electric field at the margins – high probability of charge sharing between up to 4 pixels in corners and increased indirect coupling \Rightarrow up to 33 % charge loss there

Average Charge Collection of the ATLAS Pixel Sensor



average collected charge [ke^-] – unirradiated module

16 18 20 22 24 26

n+ pixel implantation

$V_{\text{bias}} = 150\text{V}$

bump
bond
pad
oxide
via

bias
grid

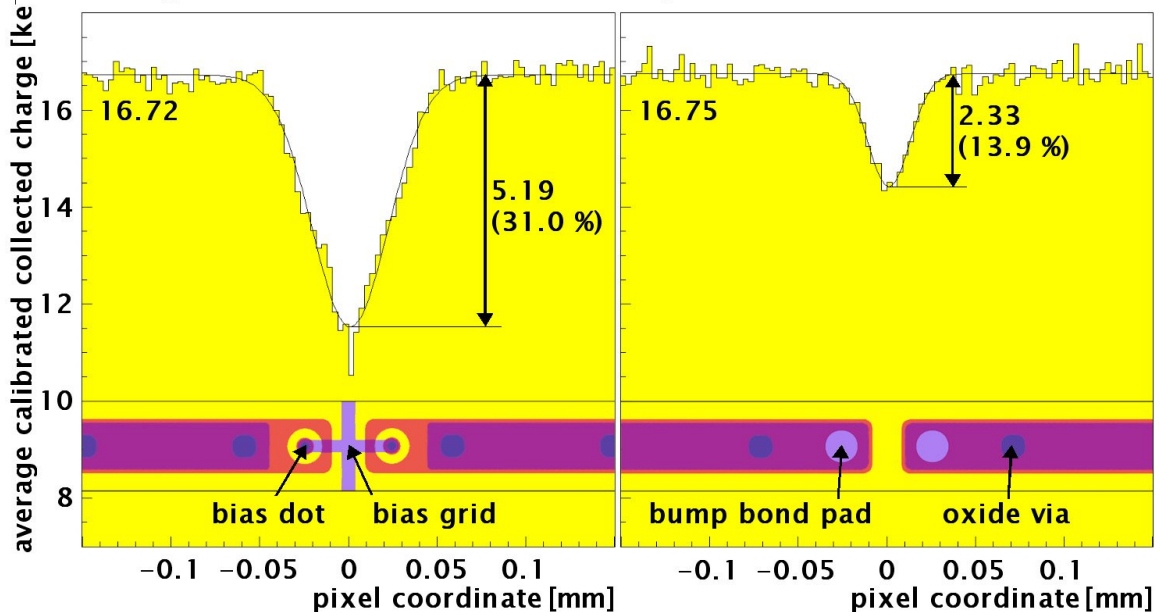
$V_{\text{bias}} = 600\text{V}$

12 13 14 15 16 17 18

pixel metalization

average collected charge [ke^-] – irradiated module: $\sim 1.1 \times 10^{15} n_{\text{eq}} (1 \text{ MeV})/\text{cm}^2$

Charge collection inefficiencies at pixel interfaces



average calibrated collected charge [ke^-]

16

14

12

10

8

-0.1 -0.05 0 0.05 0.1

pixel coordinate [mm]

-0.1 -0.05 0 0.05 0.1

pixel coordinate [mm]

bias dot bias grid

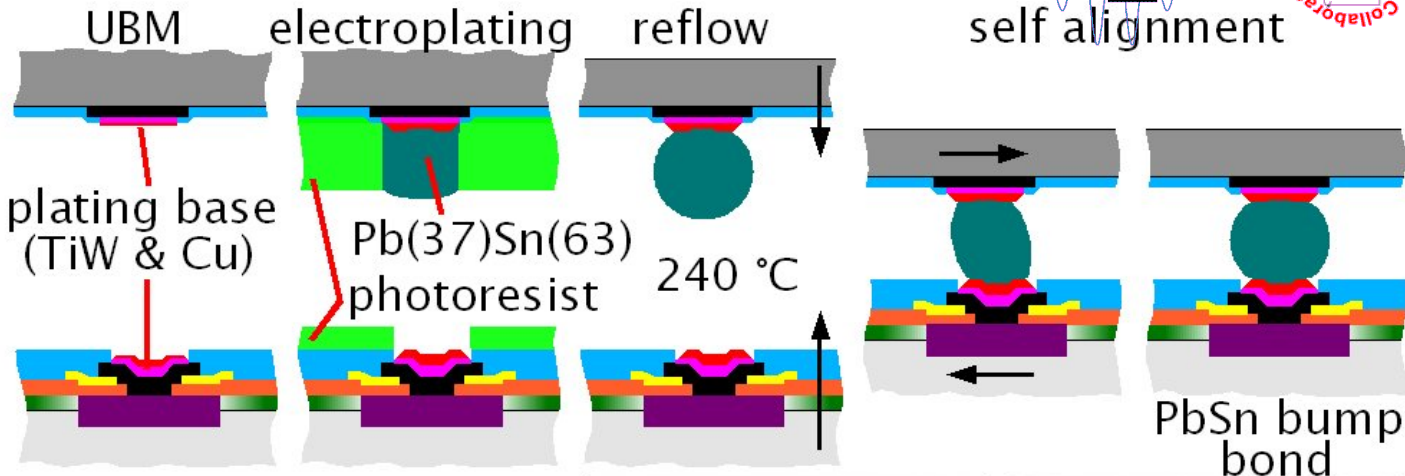
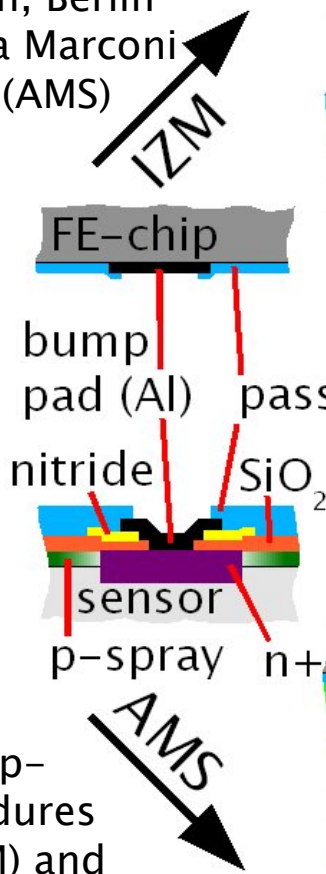
bump bond pad

oxide via

Flip-chipping at IZM and AMS

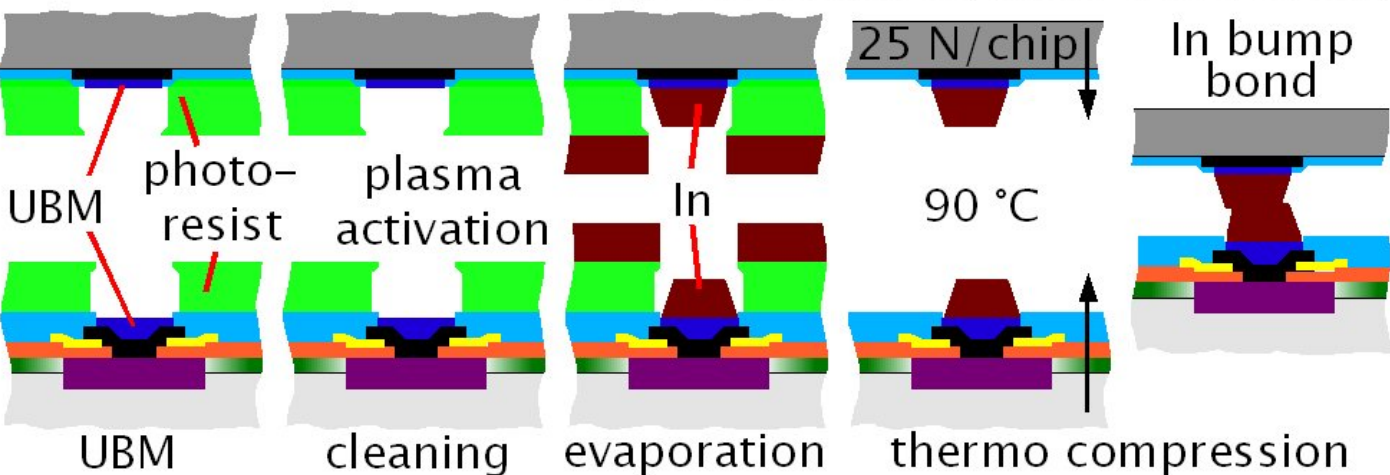


- two different vendors provide flip-chipping:
Frauenhofer Insitut für Zuverlässigkeit und Mikrointegration, Berlin (IZM) and Alenia Marconi Systems, Roma (AMS)



Bump Bonding Process at IZM & AMS

- two different flip-chipping procedures with solder (IZM) and indium (AMS) bumps and different under bump metalizations (UBM)

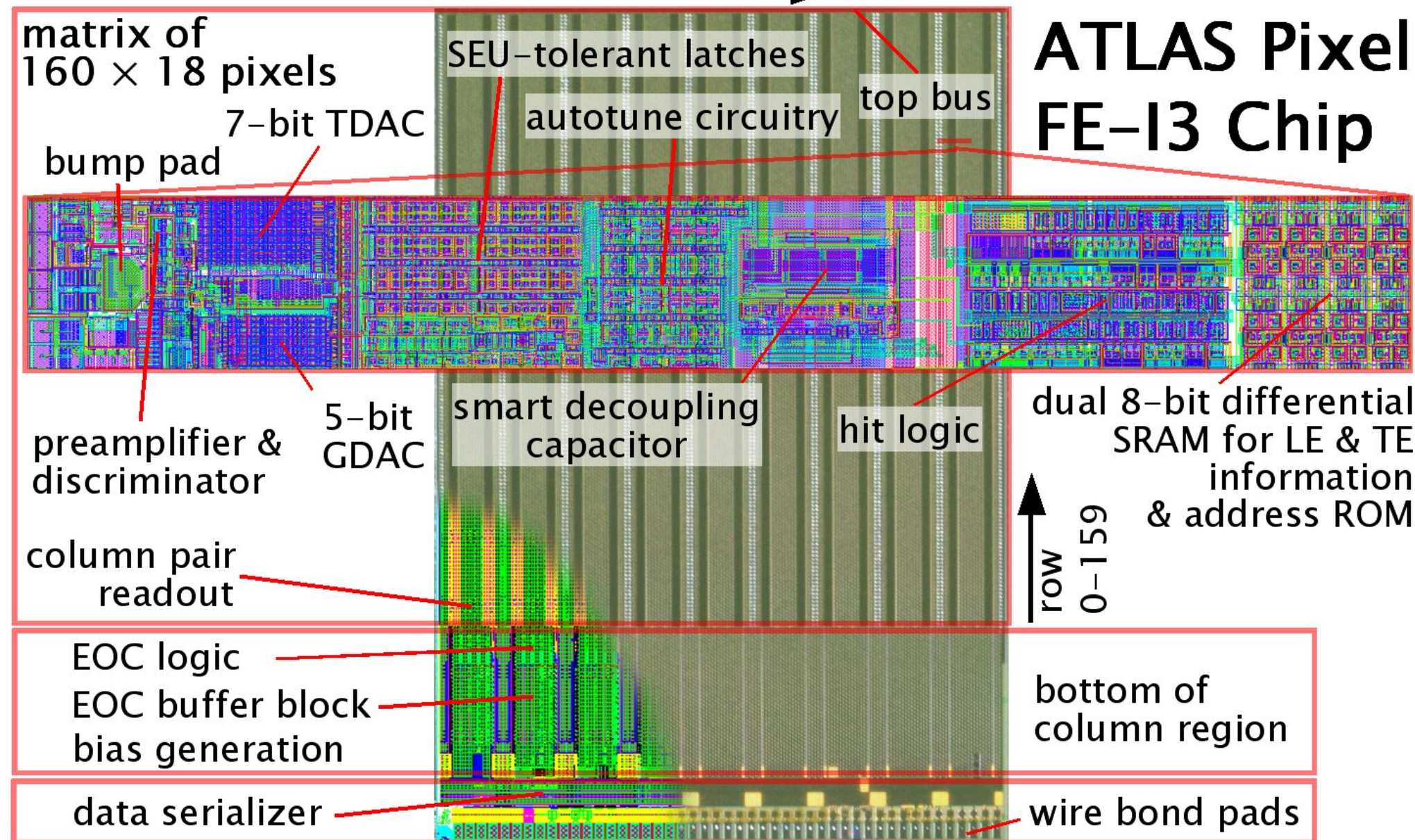


FE-I3 Readout Chip



E IV

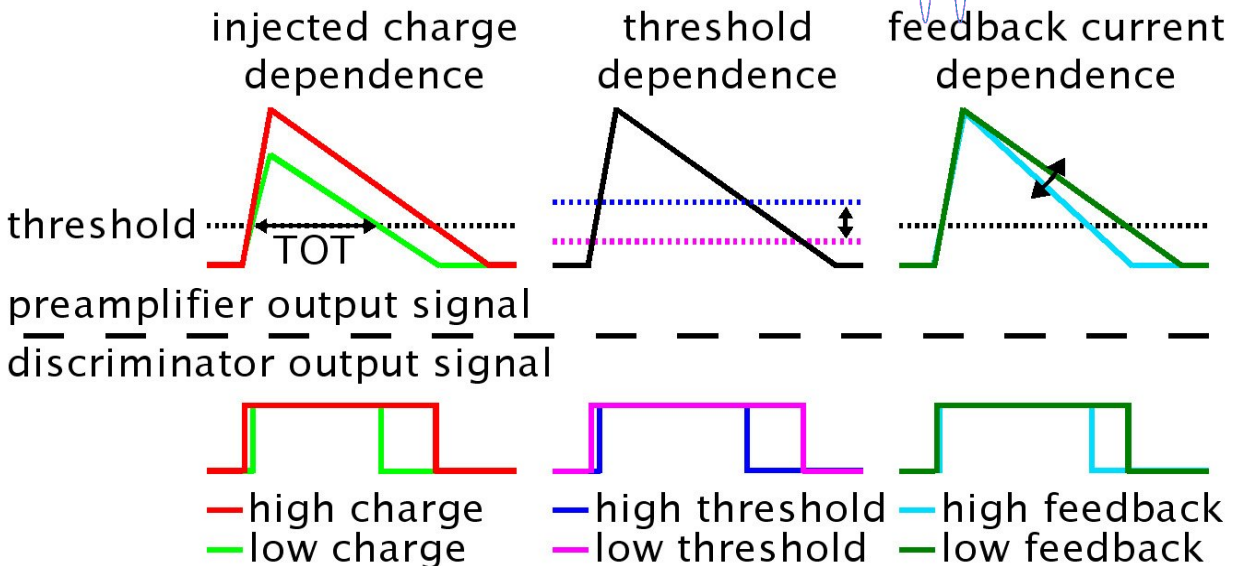
ATLAS Pixel FE-I3 Chip



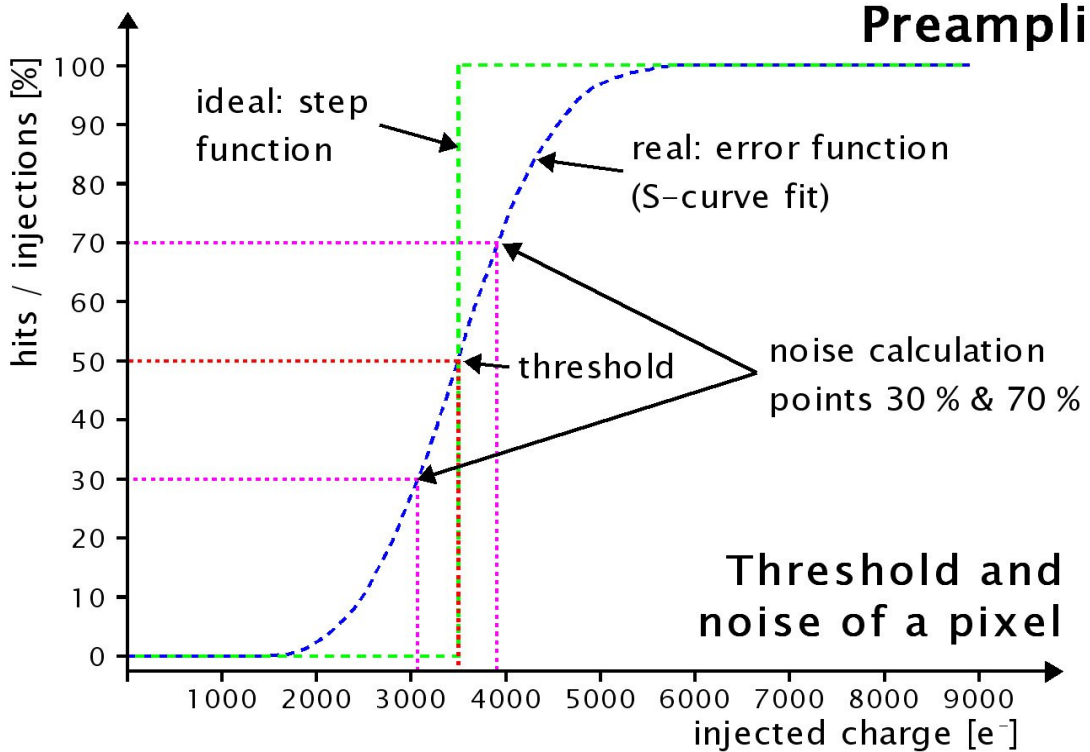
Preamplifier and discriminator signal shapes



- preamplifier output signal proportional to the collected charge; feedback current decreases signal linearity \Rightarrow discriminator used to digitalize signal \Rightarrow time over threshold (TOT) proportional to the collected charge
- each pixel can be tuned individually by changing the threshold and the feedback current



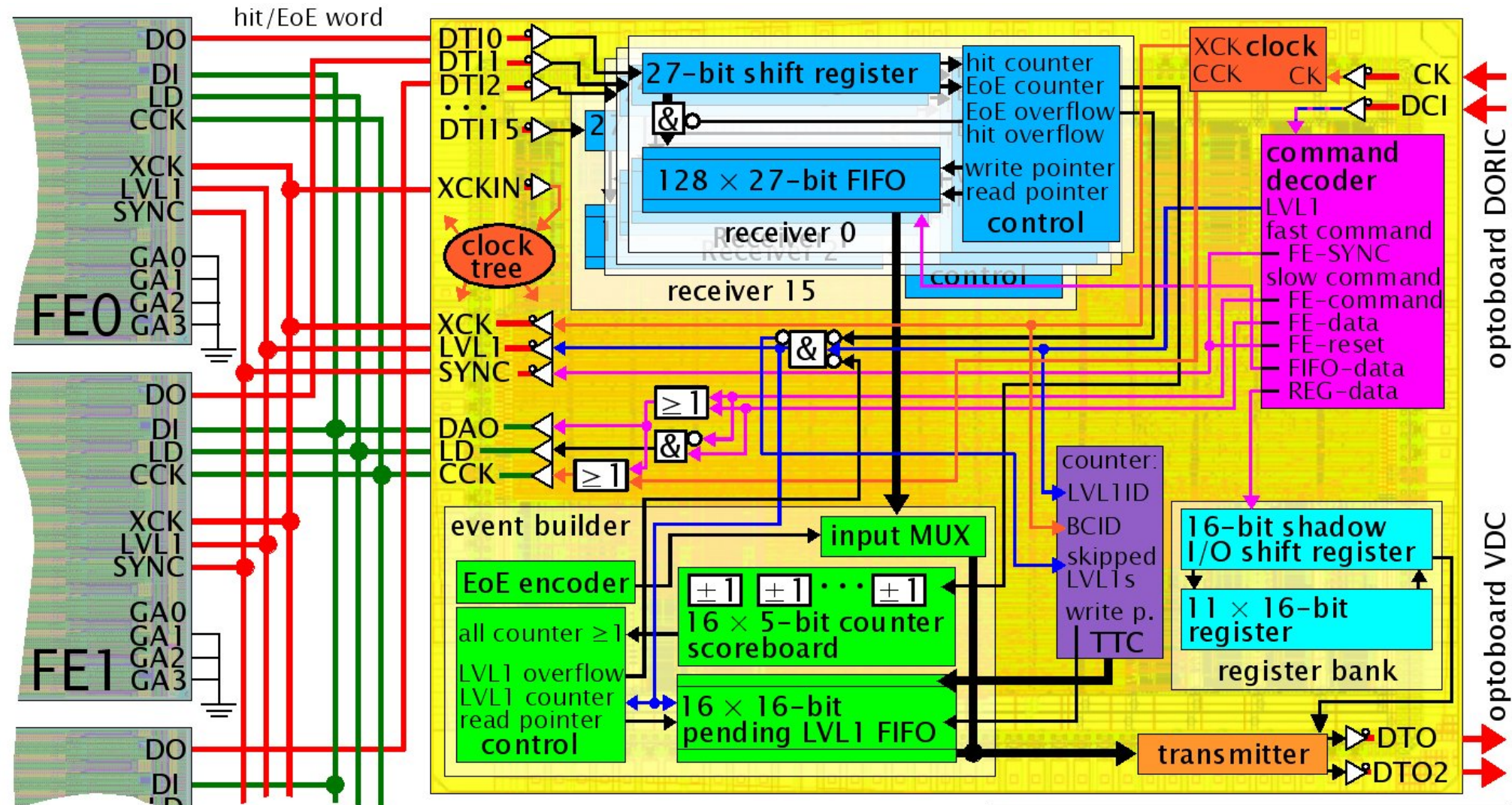
Preamplifier and discriminator signal shapes



- without noise: **step function** expected \Rightarrow all collected charges above threshold visible and collected charges below threshold are not detectable
- pixel/preamplifier noise \Rightarrow convolution of the step function and the Gaussian pixel noise distribution \Rightarrow **error function**
- \Rightarrow 50% efficiency: threshold
- \Rightarrow noise inversely proportional to the steepness of the transition from no detected hits to full efficiency

MCC Schematic

E IV

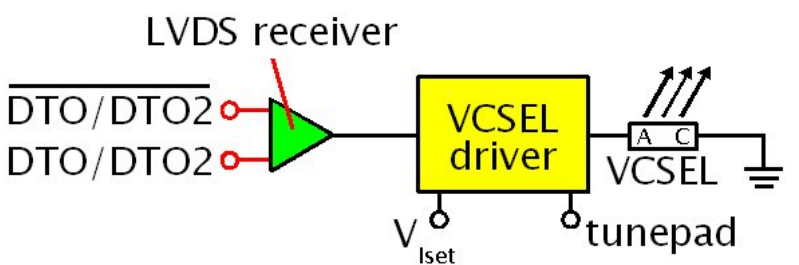
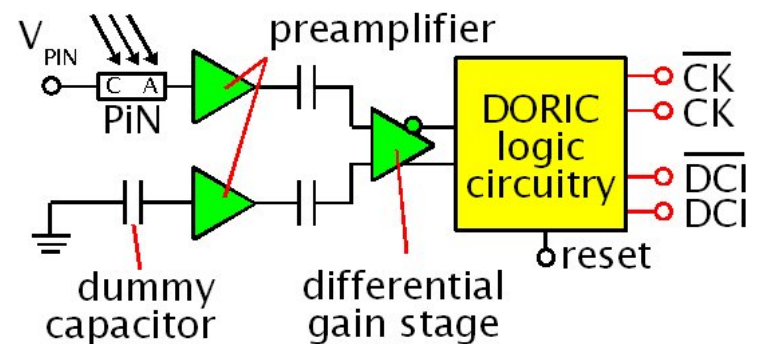
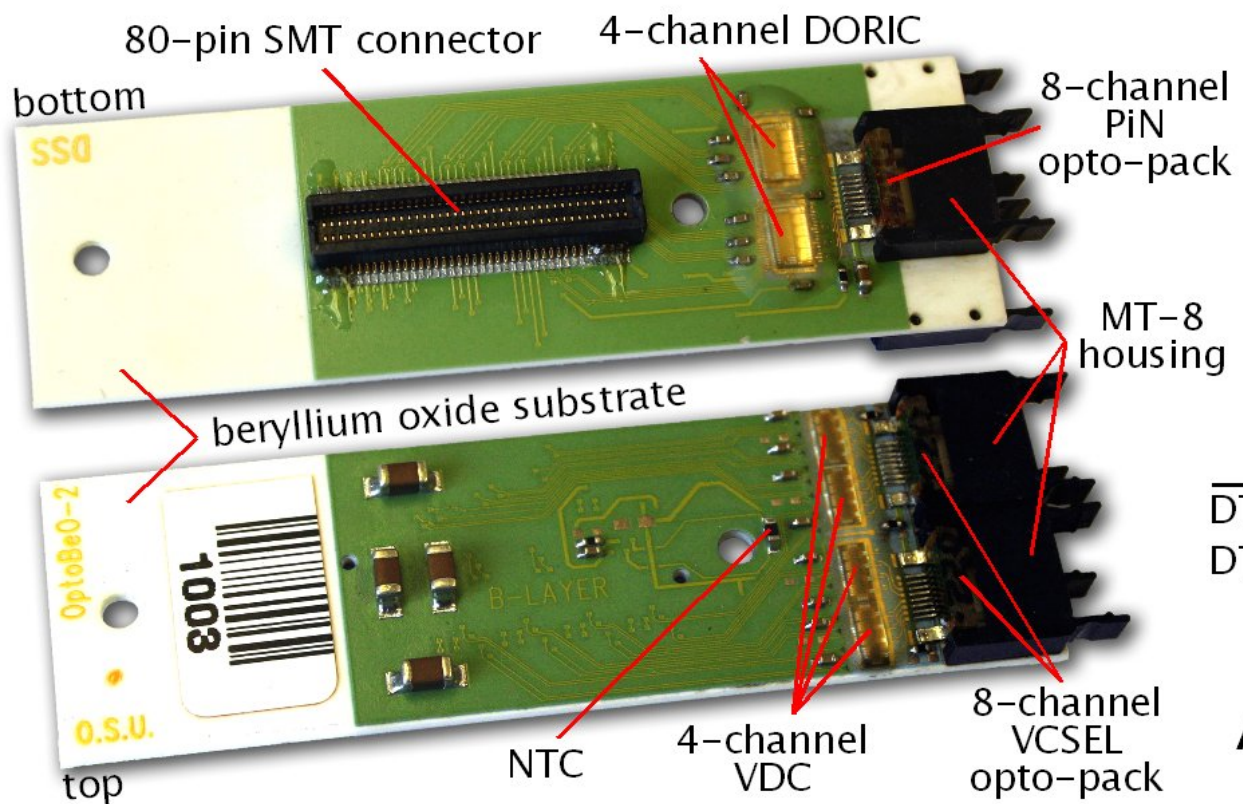
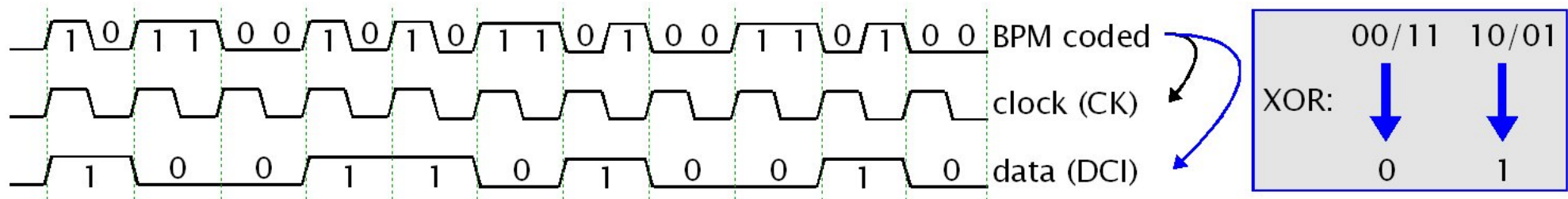


ATLAS Pixel MCC Schematic

D. Dobos CERN ATLAS Pixel Detector Commissioning using Cosmic Rays 24.09.07 38

Pixel Optoboard

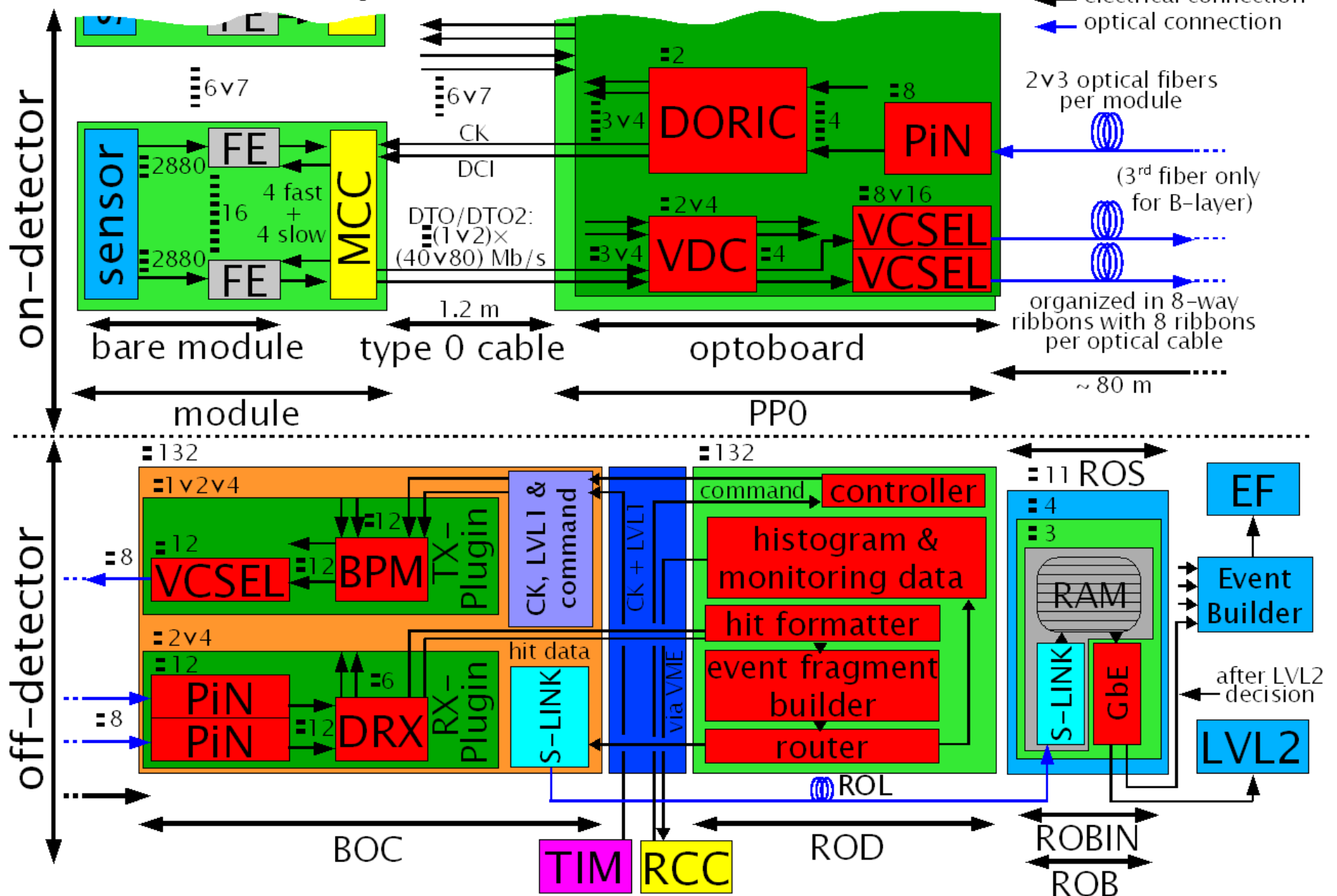
E IV



ATLAS Pixel Optoboard
dimensions: $2 \times 6.5 \text{ cm}^2$

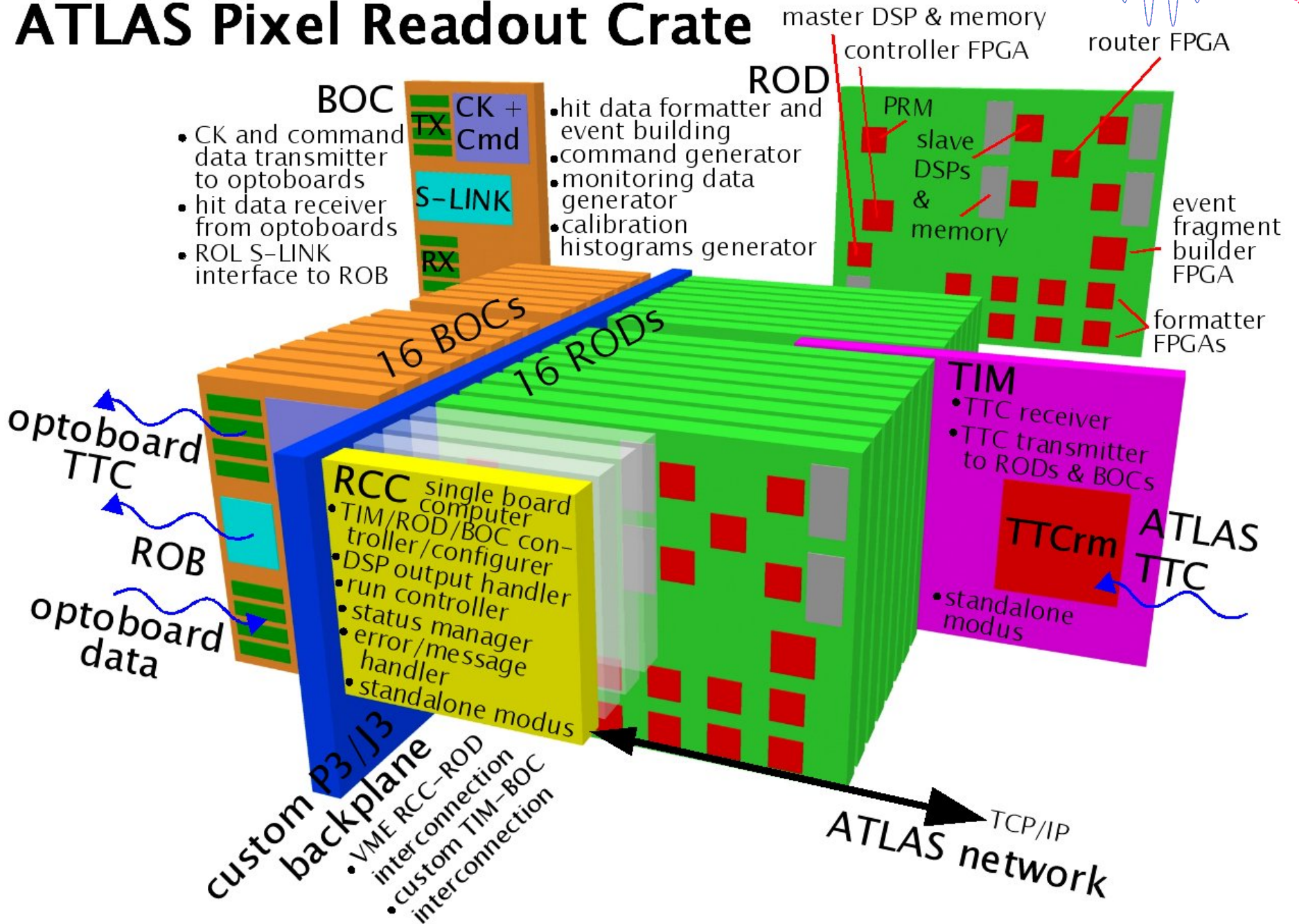
Readout Chain

ATLAS Pixel System Readout Chain



Readout Crate

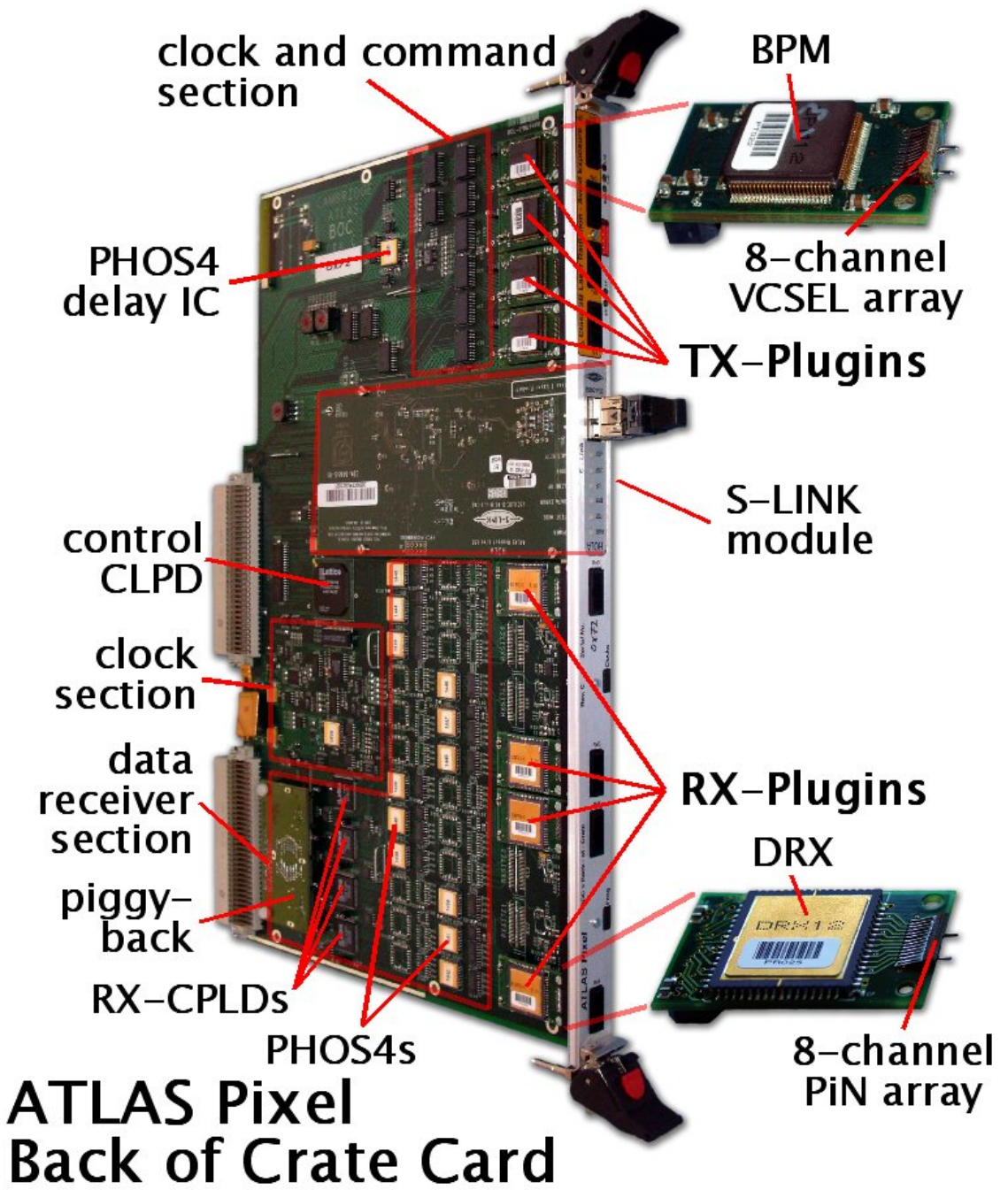
ATLAS Pixel Readout Crate



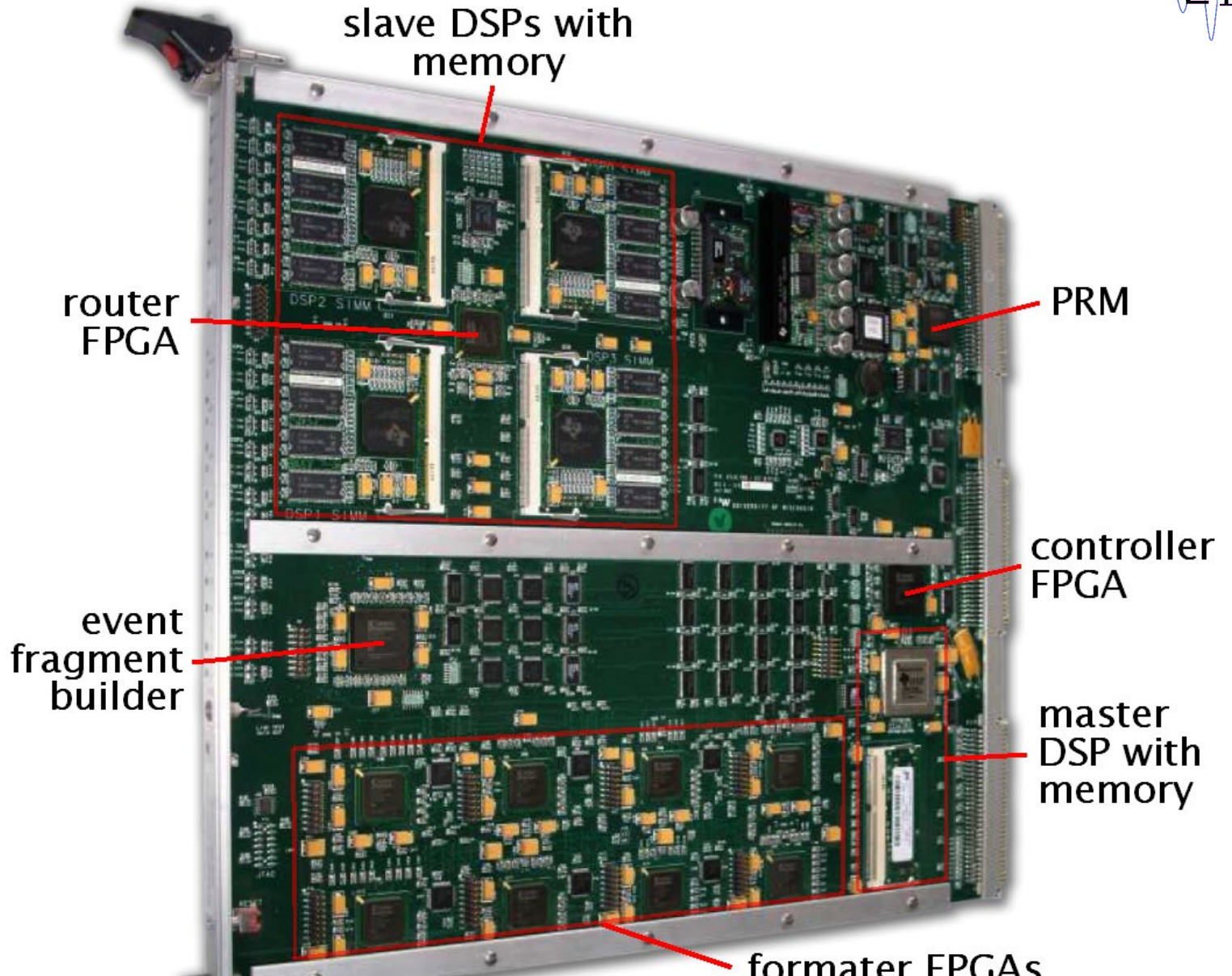
Readout Crate – BOC



E IV

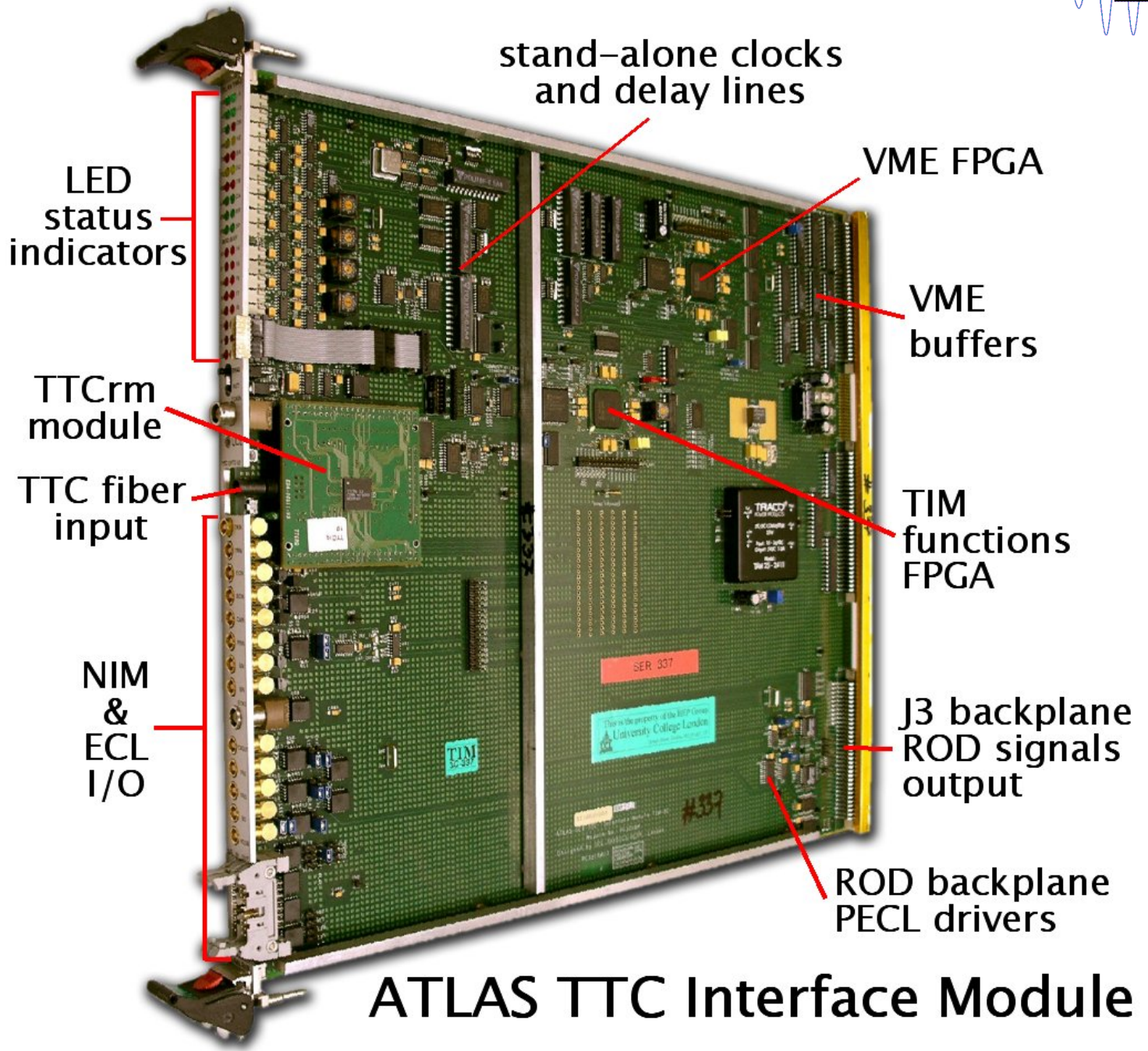


Readout Crate – ROD



ATLAS Pixel Readout Driver

Readout Crate – TIM



Optical Link Parameters

TX:

(delay-lock-loop:
determines data recovery sampling positions)

(gain stage internal feedback:
determines PiN signal discriminator thresholds)

laser current:
determines laser power of VCSEL diodes

MSR: determines VCSEL signal mark space ratios

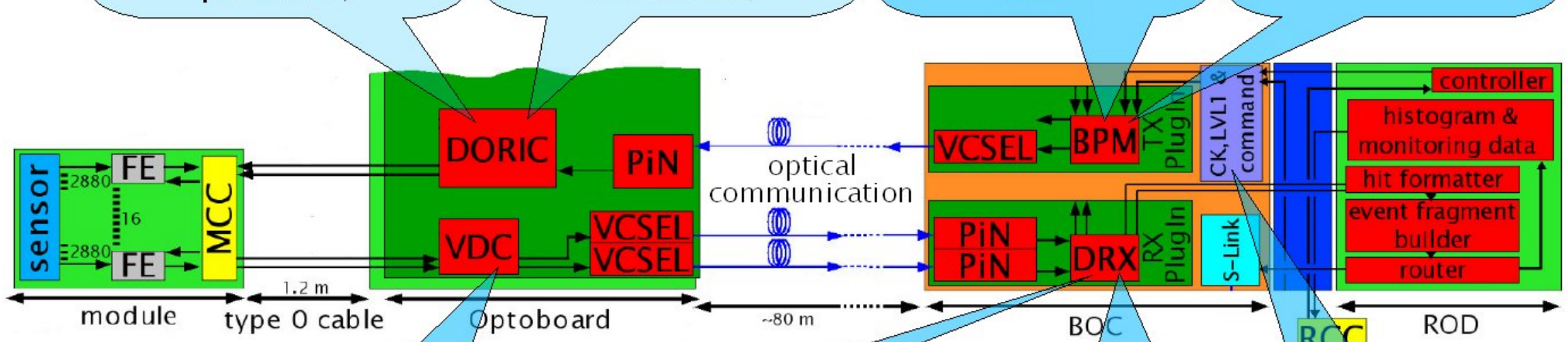
RX:

Vlset: Iset current
determines laser power of optoboard VCSEL array(s)

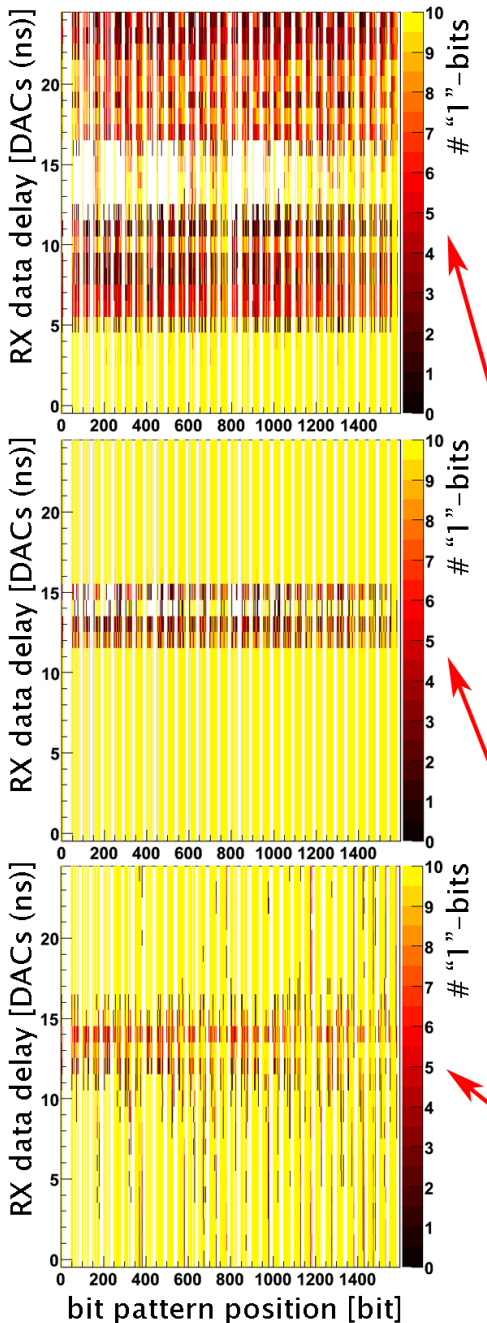
RX delay: data delay
determines first sampling positions (40 & 80 Mbit/s)

RX threshold:
determines PiN signal discriminator thresholds

V0: V-clock delay
determines second sampling positions (80 Mbit/s)



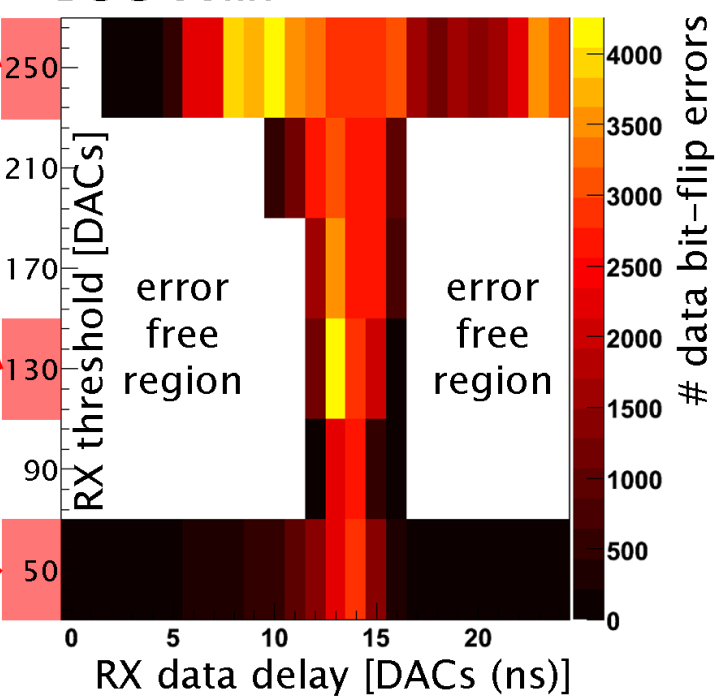
RX Threshold vs. RX Delay BOC Scan Histogram



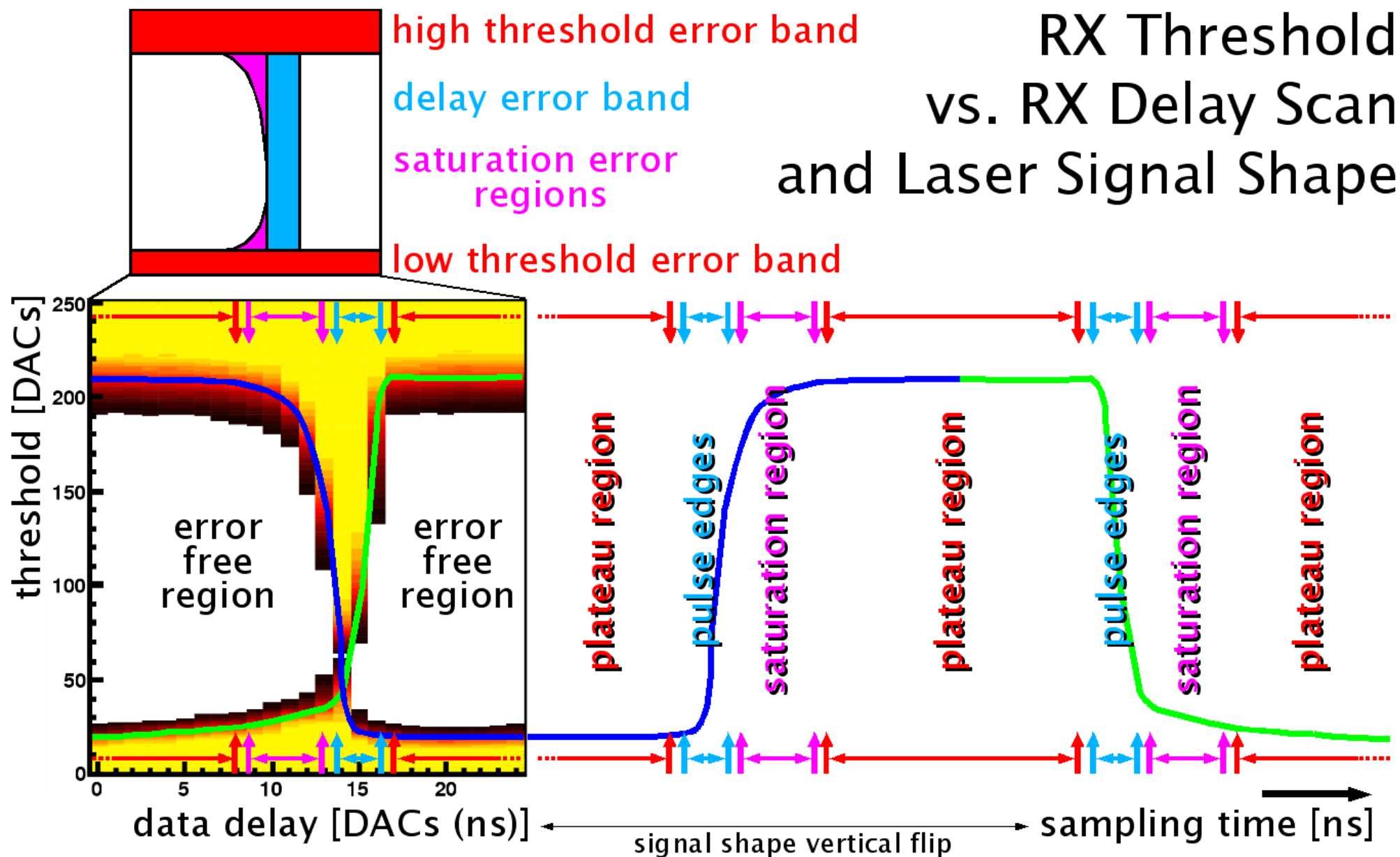
reference bit pattern



RX threshold vs. RX delay
BOC scan



RX Threshold vs. RX Delay Scan and Laser Signal Shape

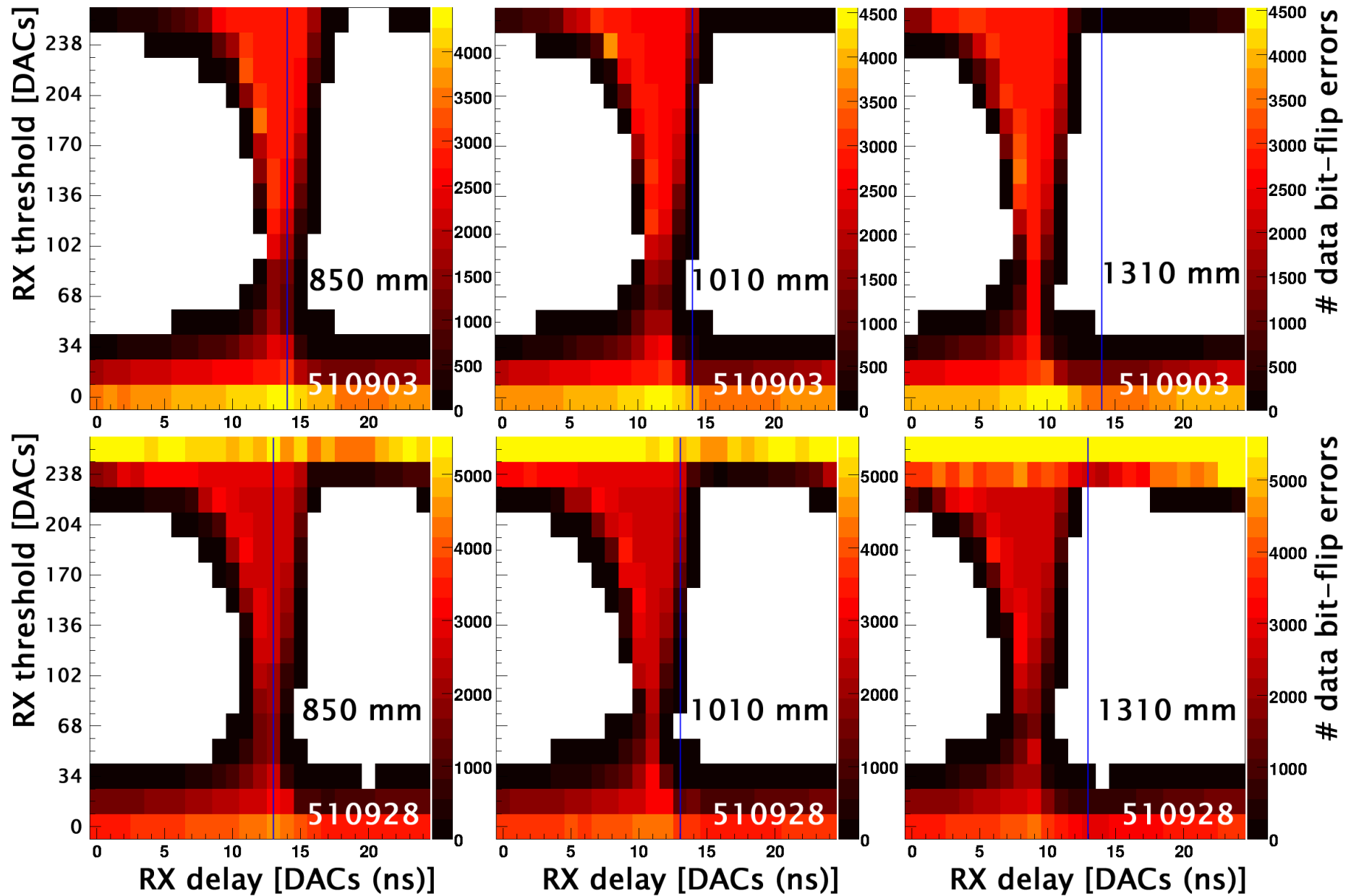


RX Delay Cable Length Dependency

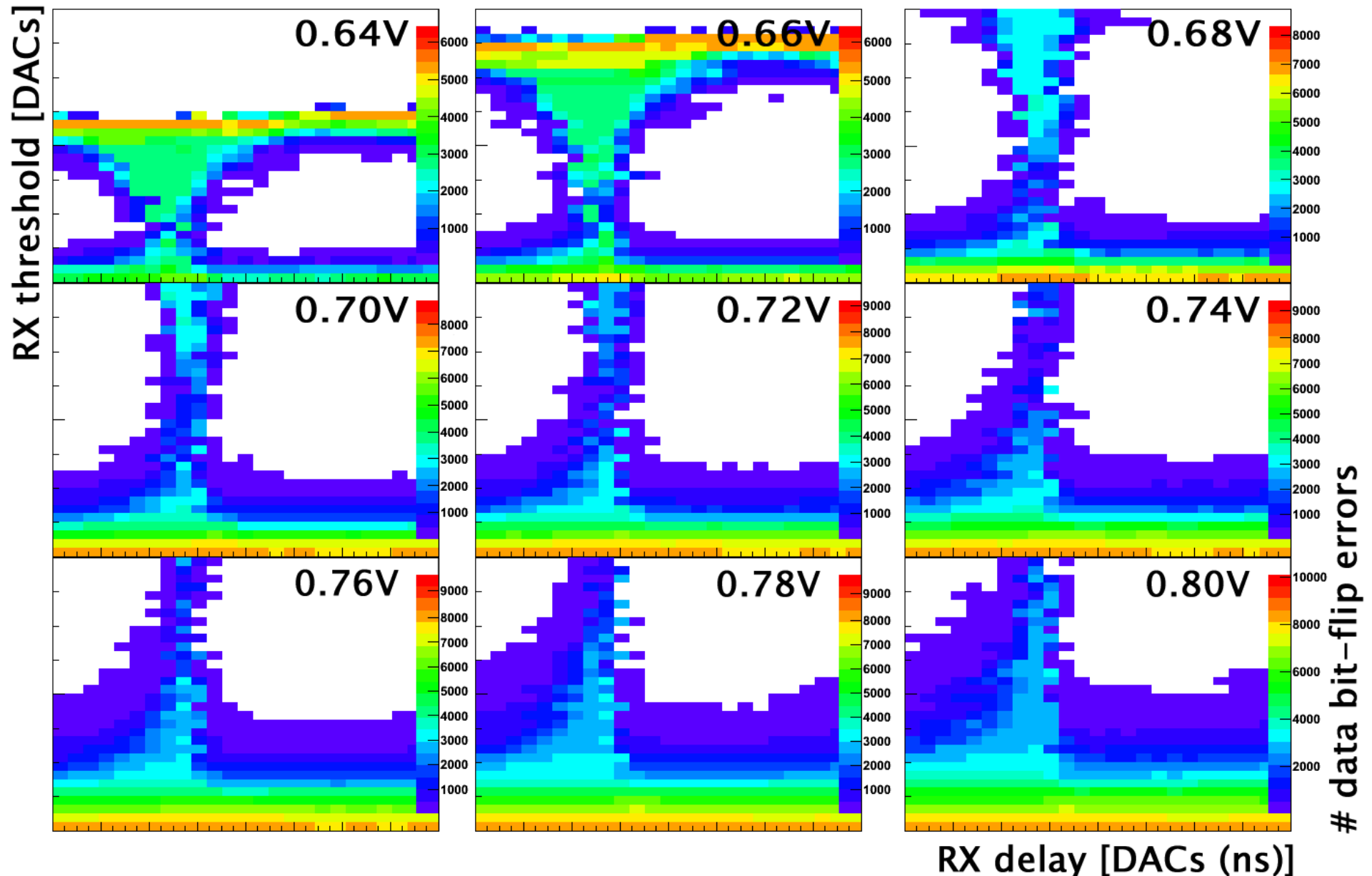


E IV

Delay Error Band Position vs. Type0 Cable Length



BOC Scans vs. Vlset

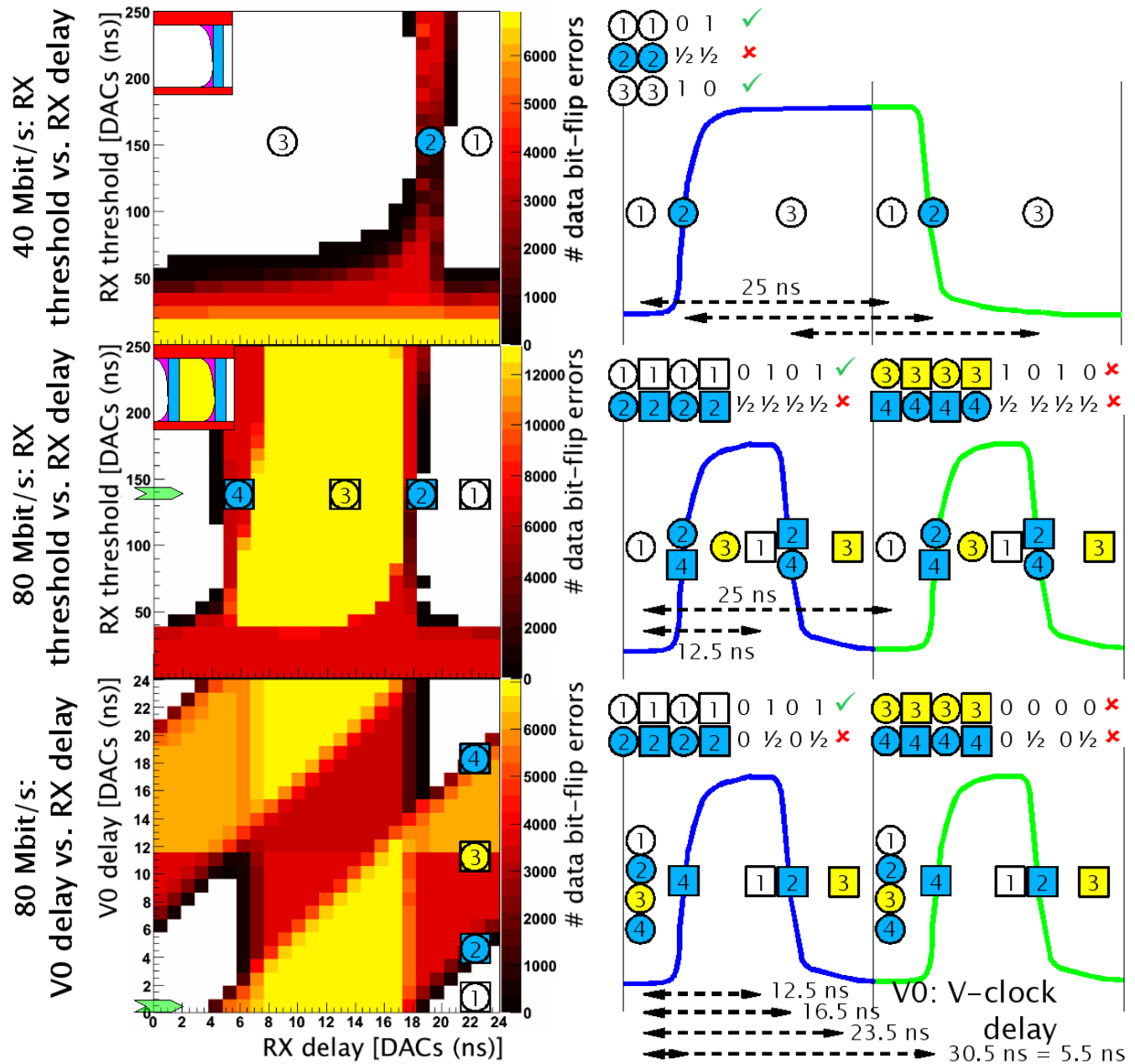


80 Mbit/s BOC Scans

80 Mbit/s BOC Scan and V0 Scan

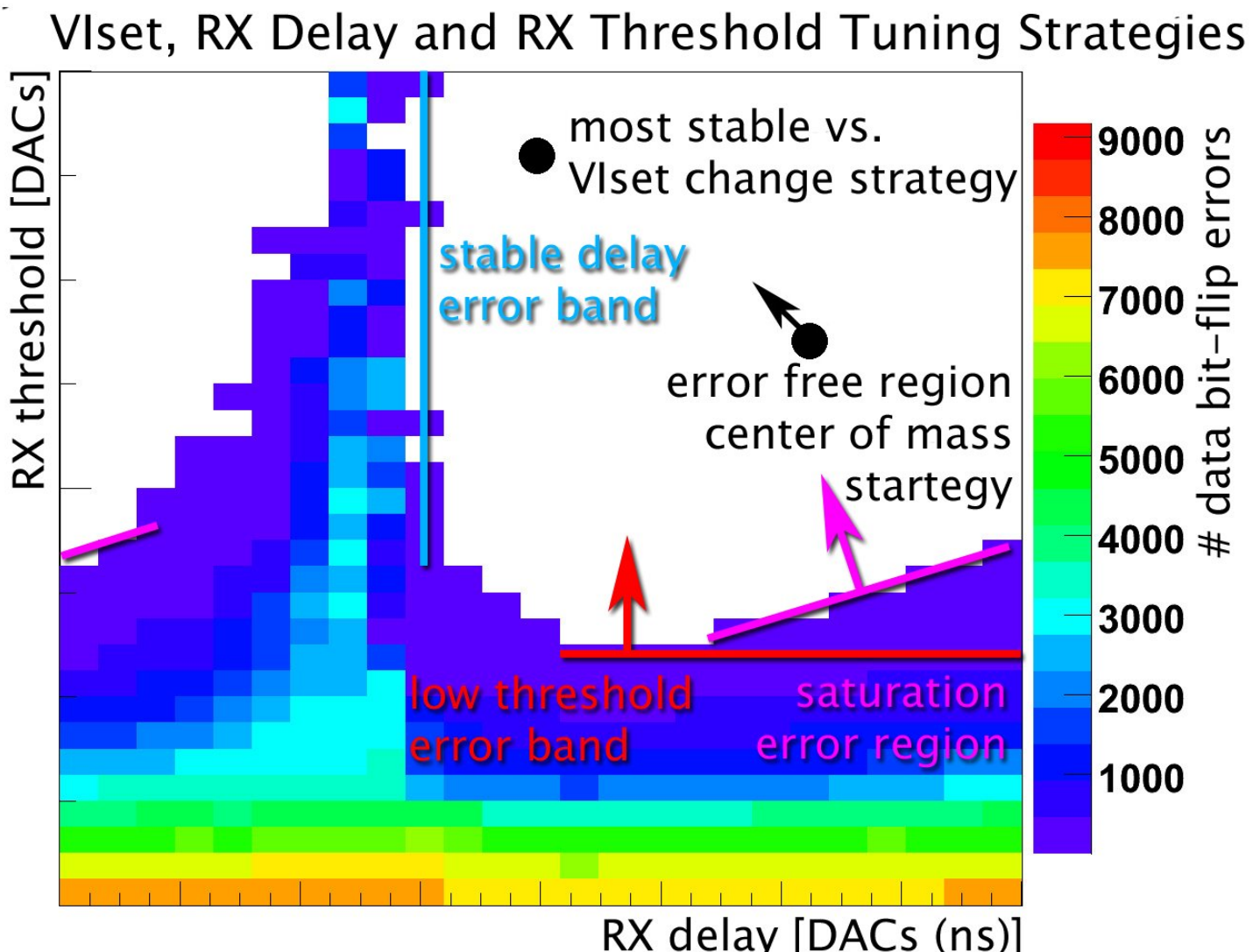
○ = B-clock sampling
 □ = V-clock sampling

E IV



Phenomenology of the good-parameter-space

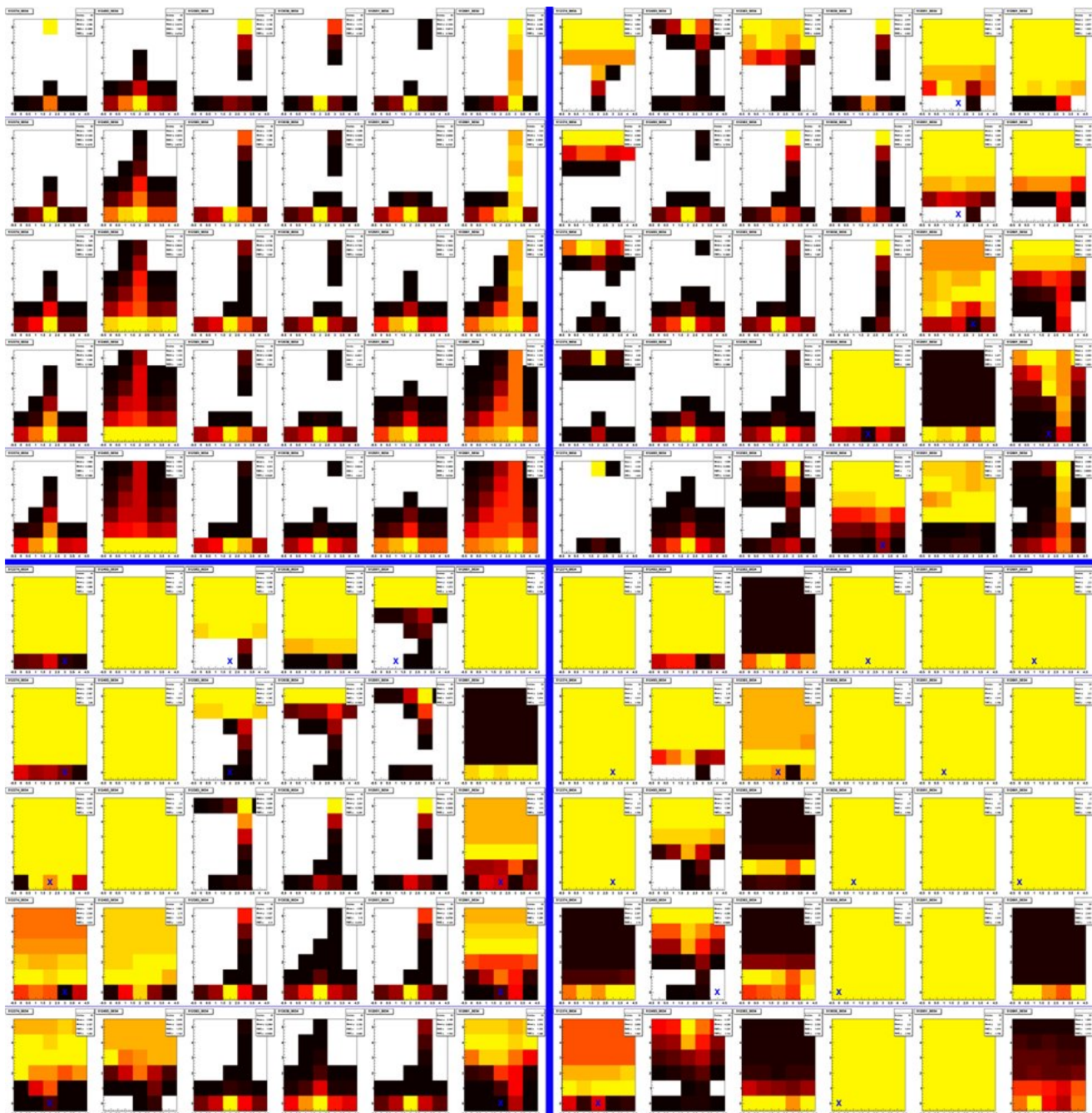
- optoboard channel dependent lower threshold band increases linearly with ViSet
- upper threshold band with much higher slope as well
- module (cable length) dependent delay-error band with threshold and ViSet stable upper and wide tailed lower edge
- good-parameter-space is reduced with increasing ViSet in upper-left direction



sector 9034 – optoboard 2029 – BAD

0.75V

11.5°C



-3.7°C

0.80V

0.85V

0.90V

0.95V

0.75V

-8.2°C

0.80V

0.85V

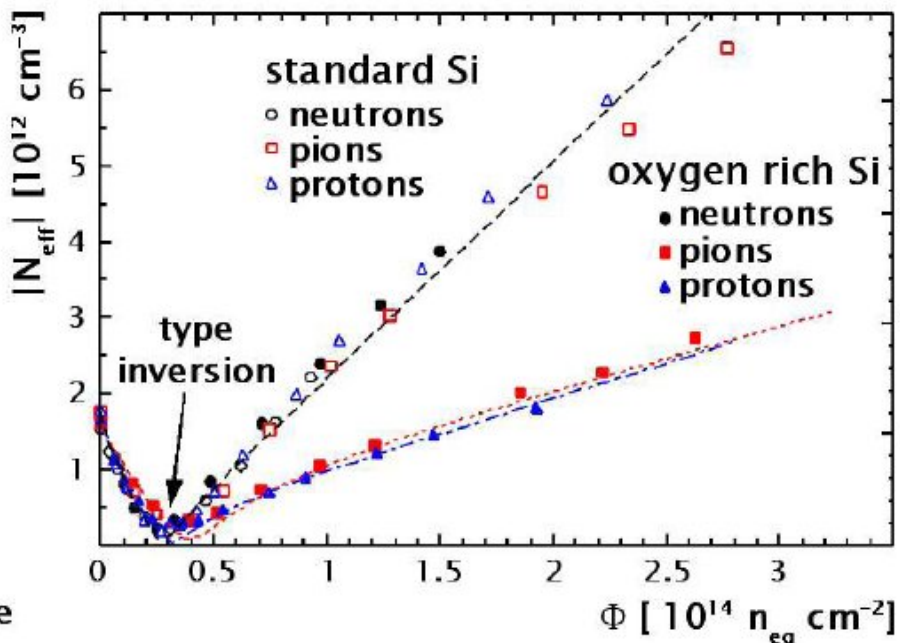
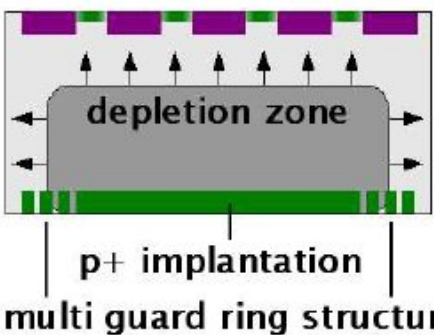
0.90V

0.95V

Noise Occupancy at the edge of the depletion voltage

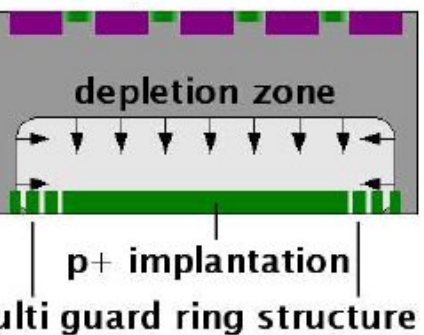
before type inversion

n^+ implantations
isolated with p -sprays
on n -substrate



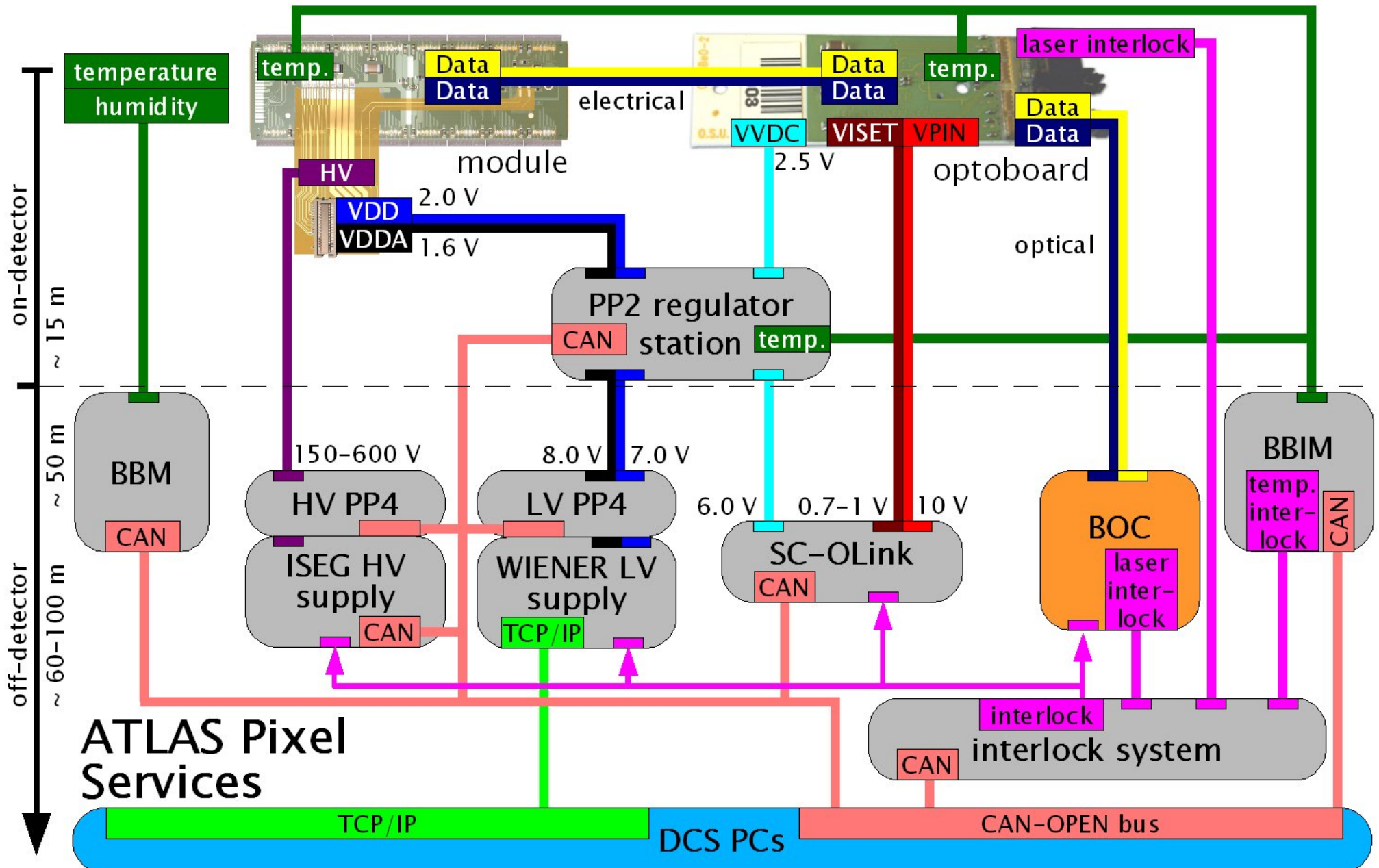
after type inversion

n^+ implantations
isolated with p -sprays
on "p"-substrate



- after type inversion depletion zone grows from pixel (n^+) to p^+ side
- before type inversion depletion zone grows towards pixel implantations
- 'under depleted' => all pixel short-circuited => high capacitive load to FE preamplifiers => high noise => high noise occupancy

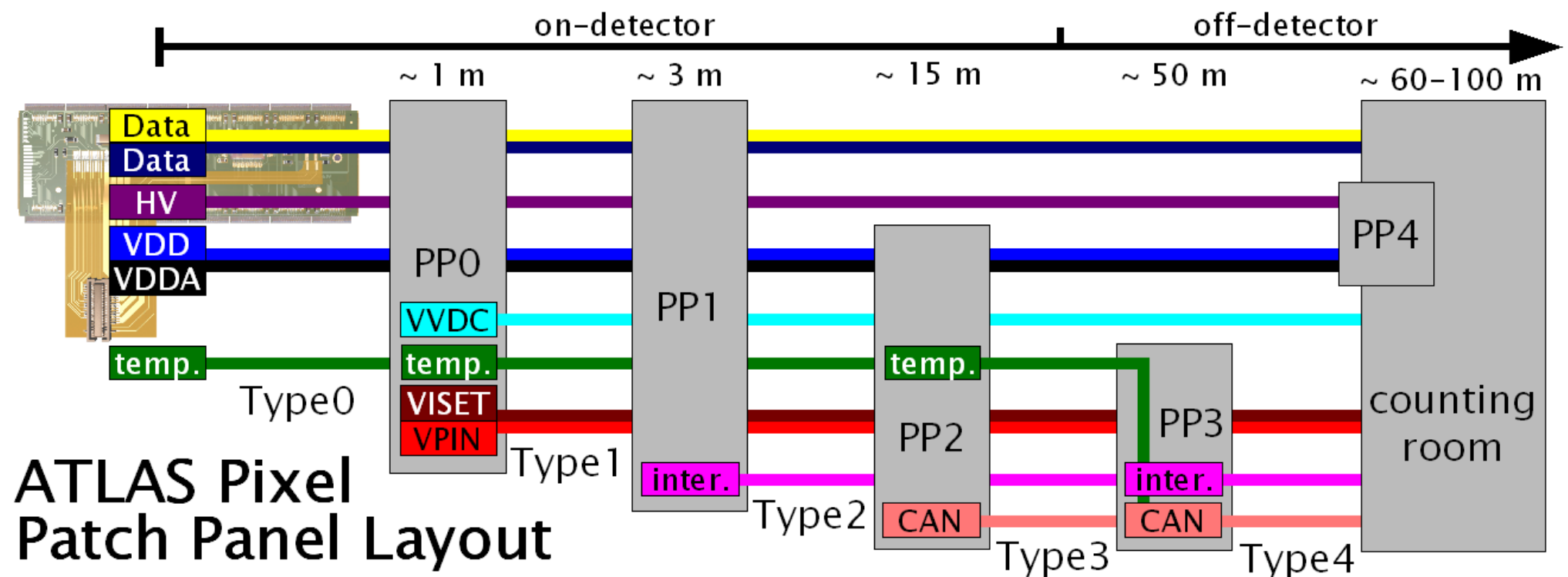
Pixel Services



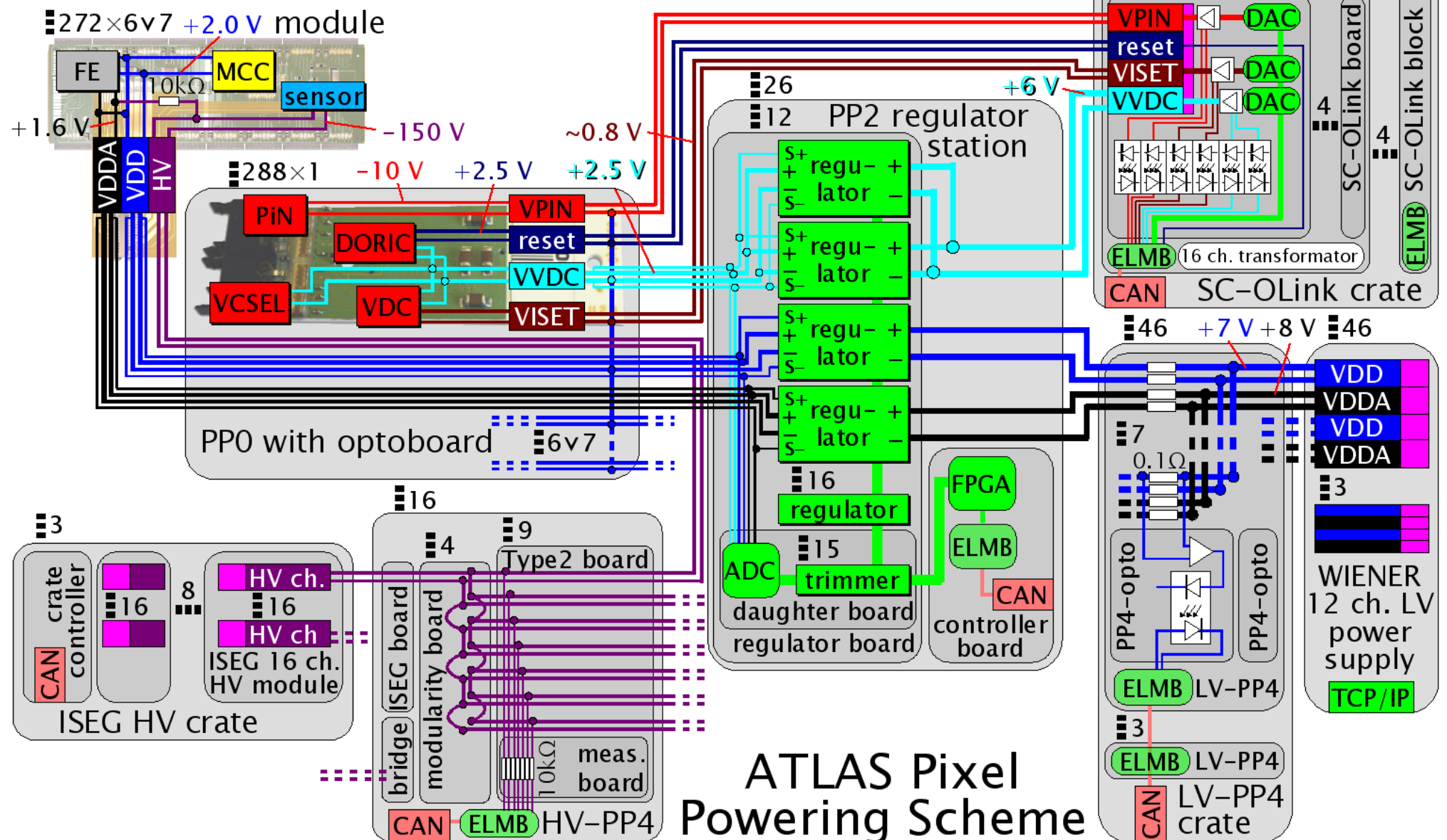
Patch Panel Layout



E IV

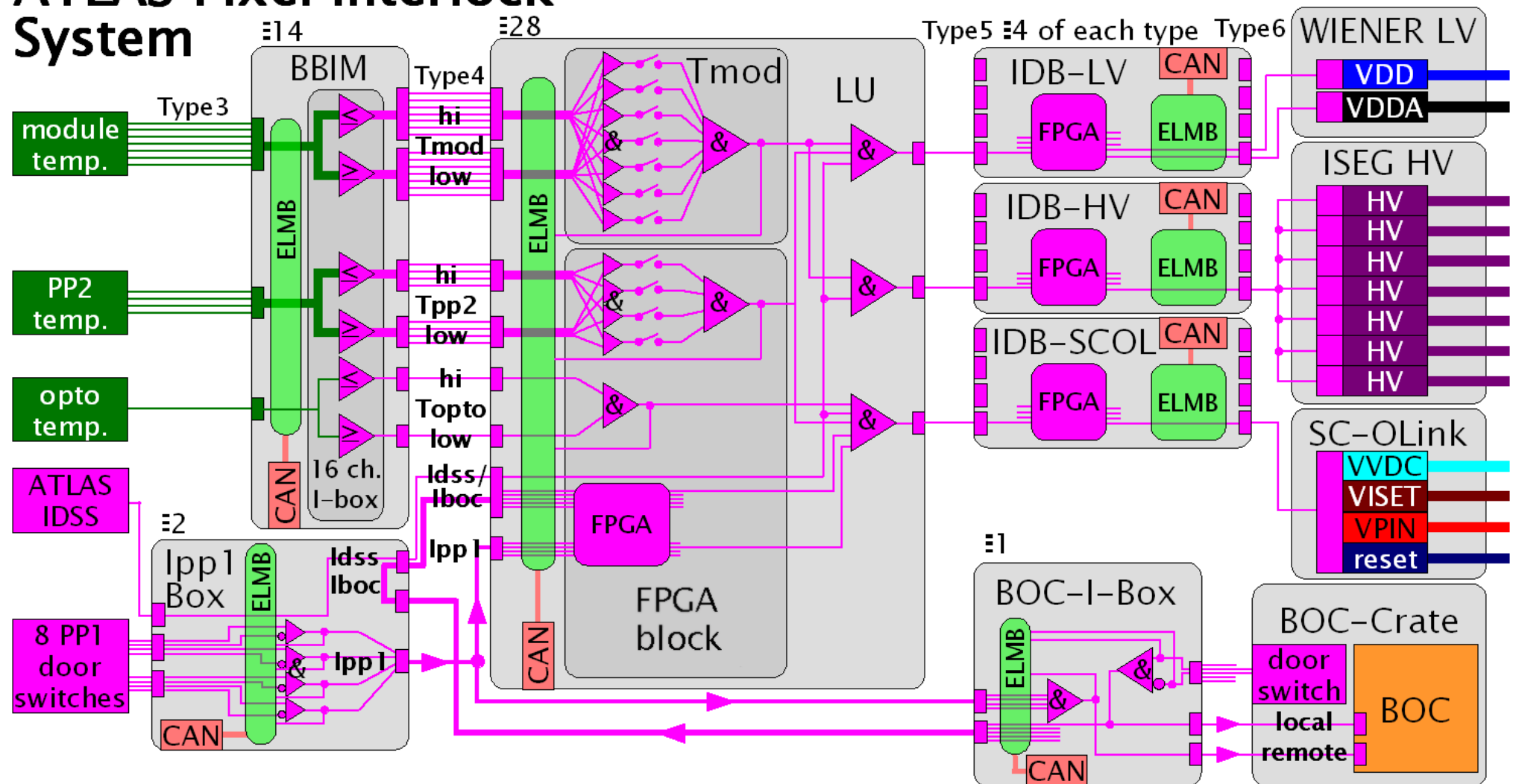


Powering Scheme

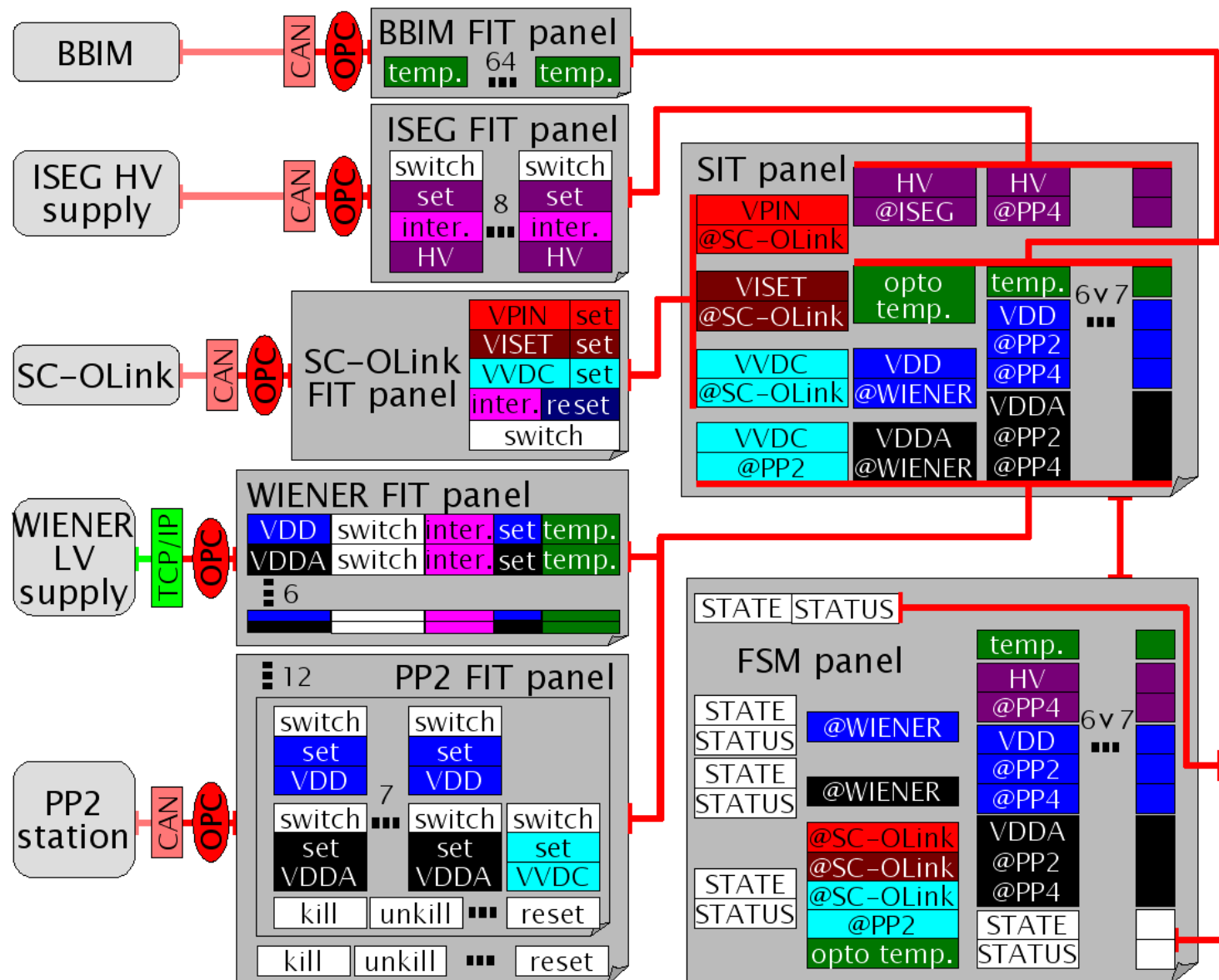


Interlock System

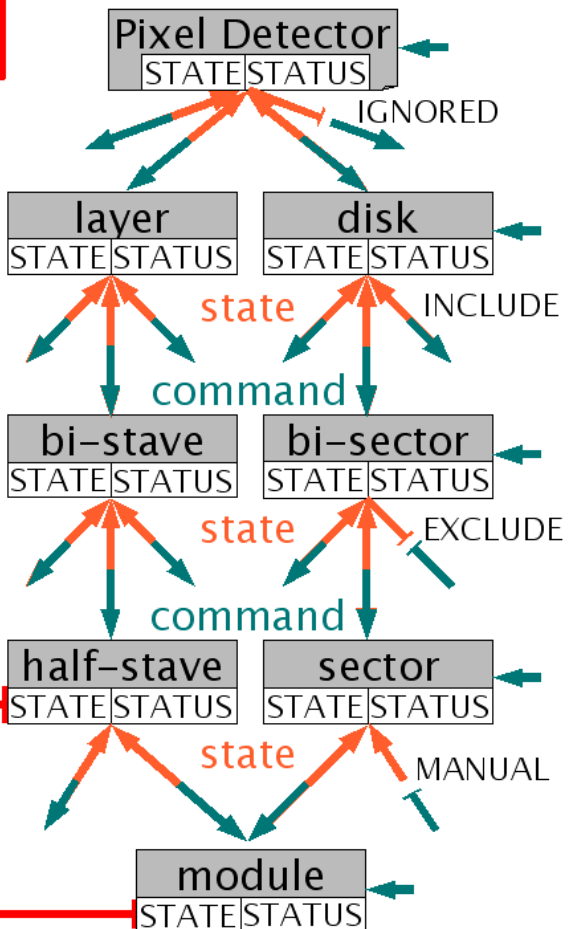
ATLAS Pixel Interlock System



Detector Control System



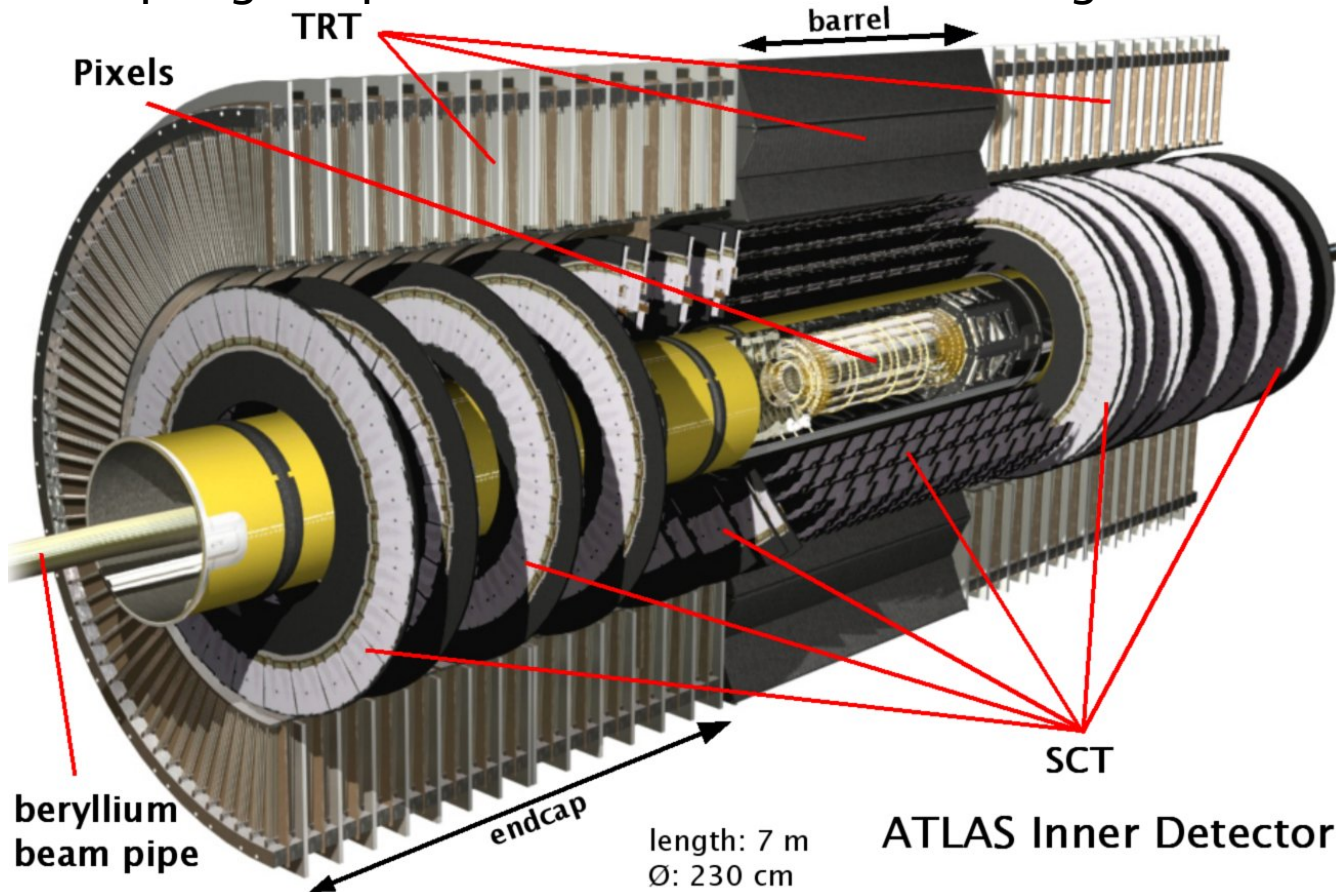
ATLAS Pixel Detector Control System



ATLAS Inner Detector

E IV

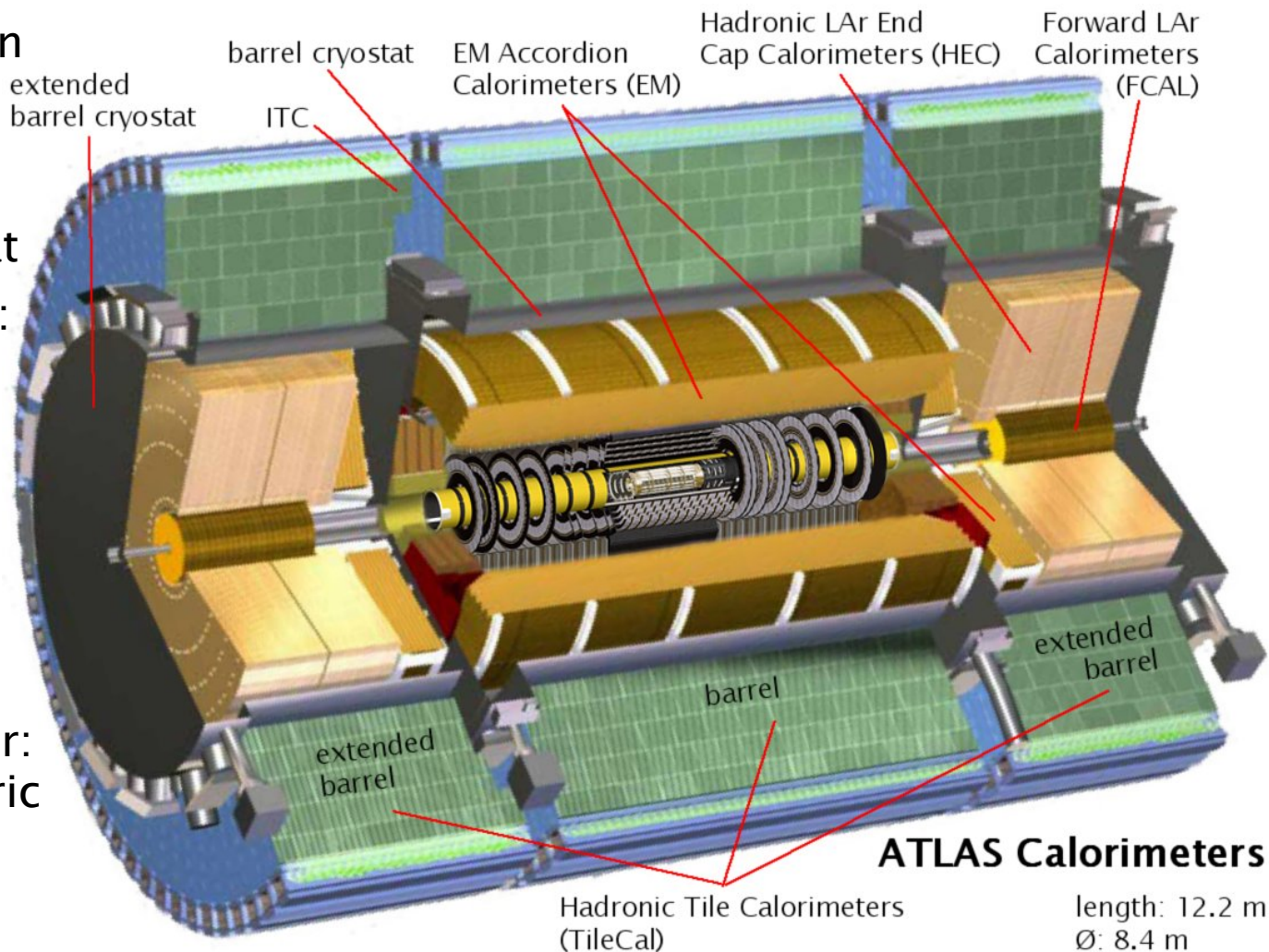
- high-resolution tracking sub-detectors closest to the interaction point & continuous tracking sub-detectors at the outer radii
- Transition Radiation Tracker: straw detectors can cope with high particle rates & occupancy; 36 space points; charged particle passing through dielectric constant boundary \Rightarrow mirror charge \Rightarrow electric dipole \Rightarrow time dependent dipole field \Rightarrow transition radiation; Xenon, CO₂, CF₄ gas mixture \Rightarrow detecting transition-radiation photons, created in a radiator between the straws, with Xenon \Rightarrow identification of e⁻; 30 μ m gold-plated W-Re wires \Rightarrow straw lengths < 144 cm; drift-time measurement \Rightarrow track resolution of 50 μ m



- Semiconductor Tracker: eight high-precision space points per track with Silicon microstrip detectors with 80 μ m pitch and 40 mrad stereo angle \Rightarrow 6.2 million channels; front-end amplifier followed by discriminator; track resolution of 16 μ m in R ϕ direction and 580 μ m in z direction
- Pixel Detector ...

ATLAS Calorimeters

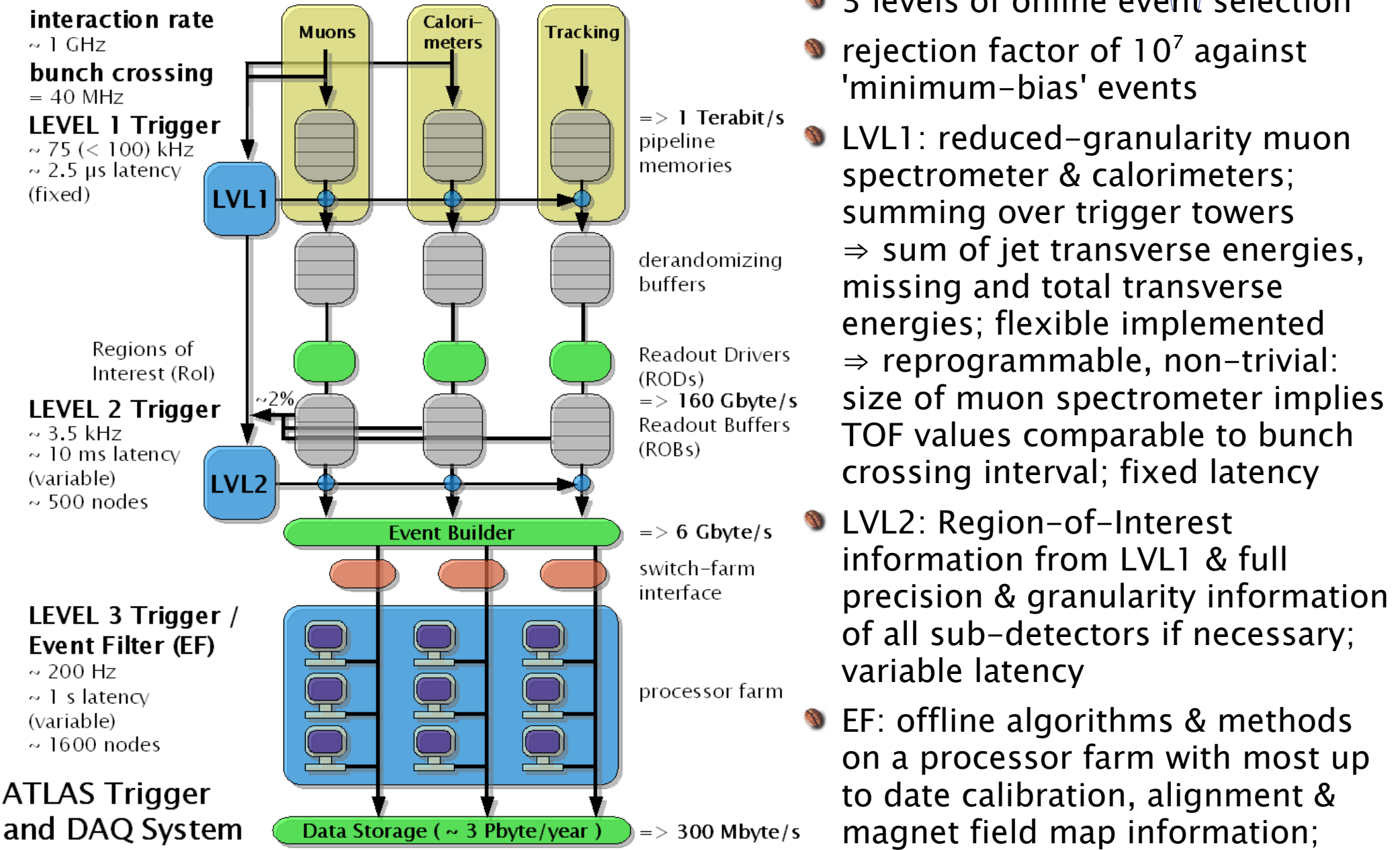
- sampling technique to measure particle- and jet-energies: alternating layers of passive absorber & active detector materials
- TileCal: absorber: Fe; detector: scintillating tiles \Rightarrow wavelength shifting fibres \Rightarrow PMT
- EM calorimeter: absorber: lead; detector: liquid Argon with accordion-shaped Kapton electrodes \Rightarrow preamplifier & bipolar shaper outside the cryostat
- HEC calorimeter: absorber: copper; detector: liquid Argon with 3 parallel electrodes: central one for readout – two carry 4 kV HV \Rightarrow preamplifier boards at wheel periphery
- FCAL: absorber: copper & sintered tungsten; detector: liquid Argon with concentric rods at a positive HV & grounded tube electrodes



ATLAS Trigger



E IV



The ATLAS Experiment



E IV

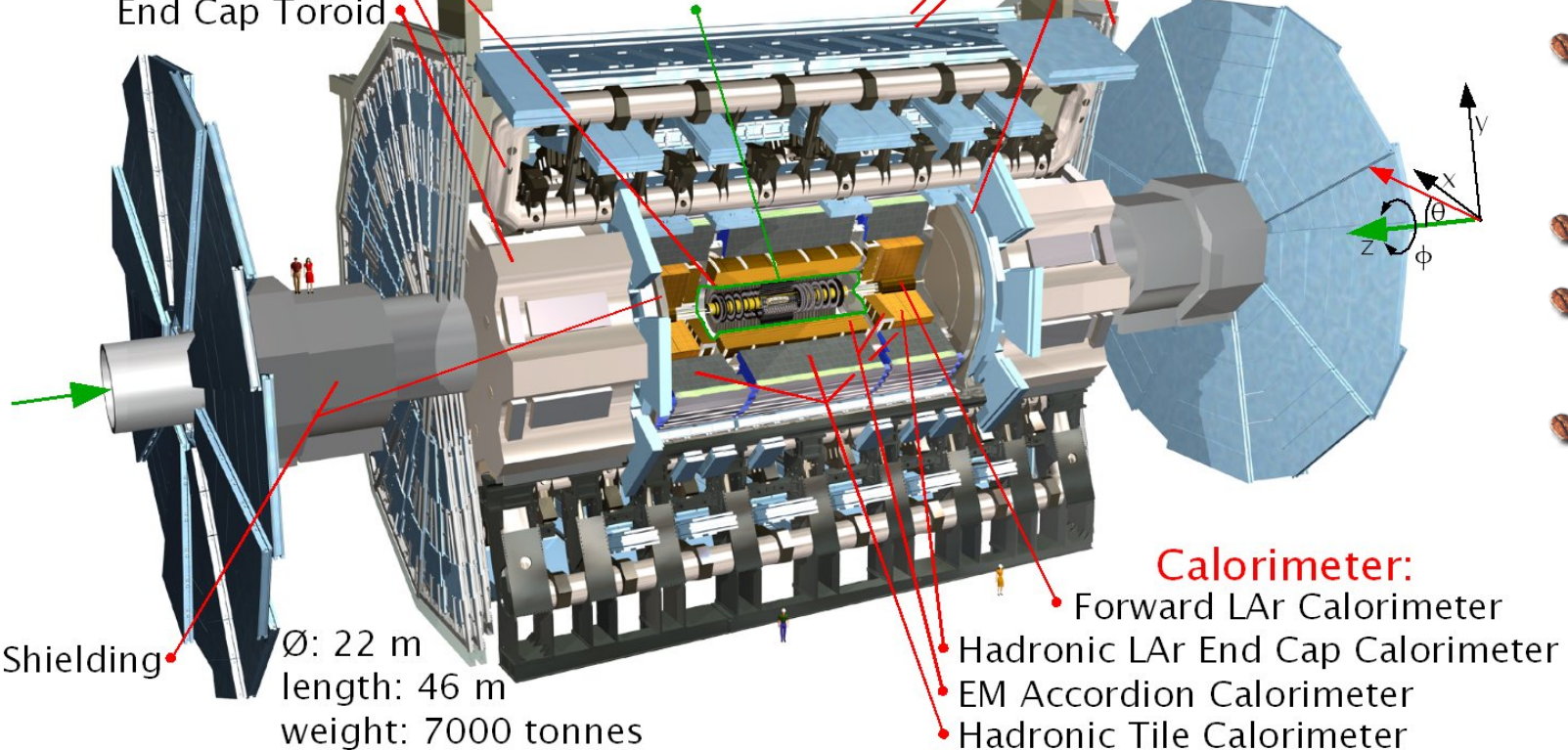
- diameter: 22 m; length: 46 m; weight 7000 tons
- air-core (\Rightarrow to avoid multiple scattering) barrel toroid magnetic field: 4 T
- central solenoid magnetic field for inner detector: 2 T

ATLAS Layout Overview

Magnet system:
Central Solenoid
Air-core Barrel Toroid
End Cap Toroid

Inner Detector:
Transition Radiation Tracker
Semi-Conductor Tracker
Pixel Detector

Muon Spectrometer:
Monitored Drift Tubes
Resistive Plate Chamber
Cathode Strip Chamber
Thin Gap Chamber



basic design criteria:

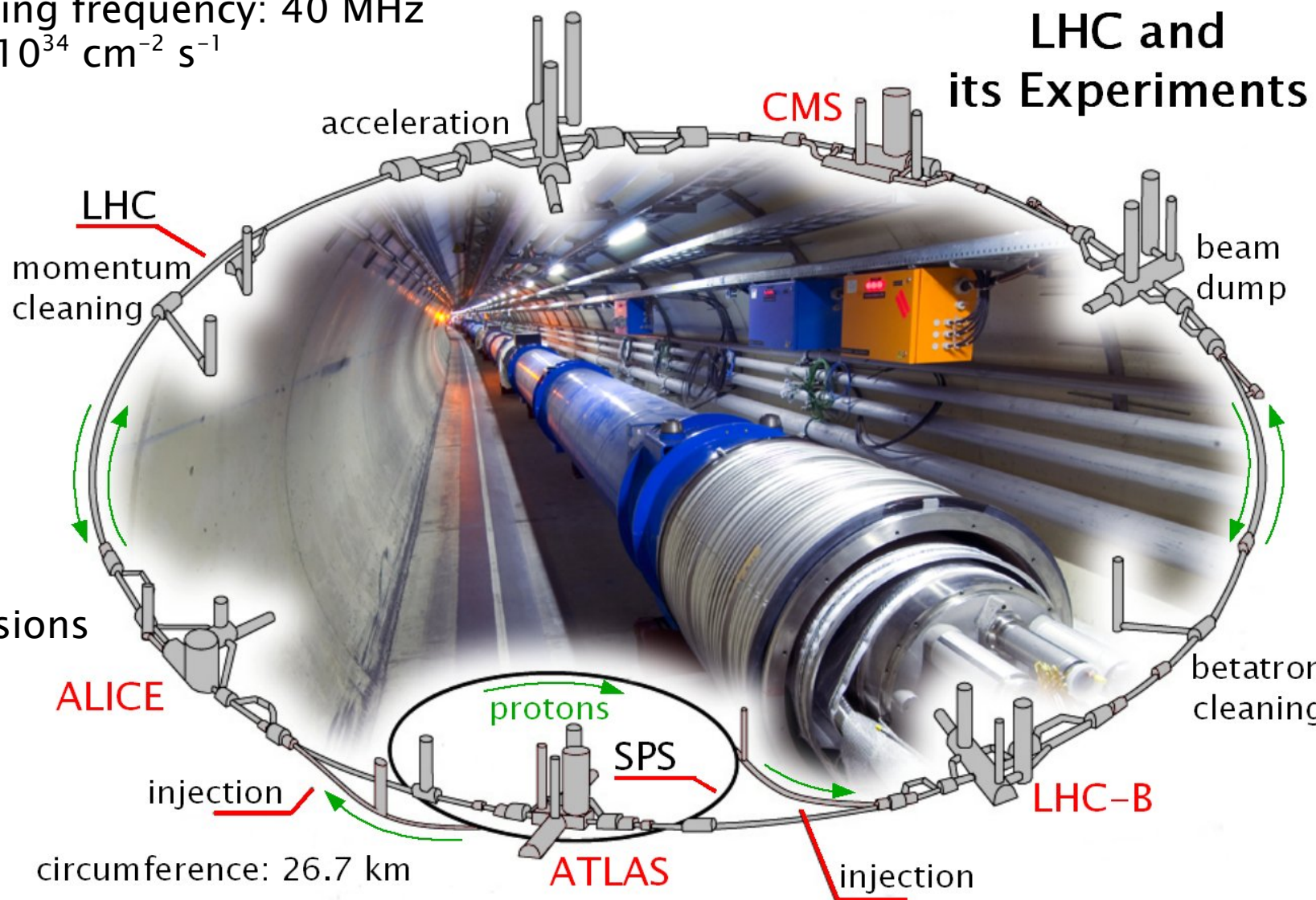
- very good electromagnetic calorimetry
- high-precision muon momentum measurement
- efficient tracking
- large acceptance in η
- triggering and measurement of particles with low transverse momentum thresholds

SPS, LHC and the LHC experiments



E IV

- SPS: 450 GeV
- LHC: 26.7 km circumference; 2·7 TeV; 2835 bunches with 10^{11} protons each
 - ⇒ beam current: 0.53 A ⇒ beam energy: 668 MJ
 - ⇒ bunch crossing frequency: 40 MHz
 - ⇒ luminosity: $10^{34} \text{ cm}^{-2} \text{ s}^{-1}$



LHC and its Experiments

- ATLAS & CMS: p-p collisions
- LHC-b: b-physics
- ALICE: heavy ion collisions